UAB
Universitat Autònoma de Barcelona

The *S. cerevisiae* protein phosphatase Ppz1: unraveling the molecular basis of its toxicity and its connection with intracellular localization

Doctoral thesis presented by

MARCEL ALBACAR CAROT

graduated in Biology

for the degree of PhD in Biochemistry, Molecular Biology and Biomedicine from the Universitat Autònoma de Barcelona

Departament de Bioquímica i Biologia Molecular and Institut de Biotecnologia i Biomedicina of the Universitat Autònoma de Barcelona

Thesis supervised by **Dr. Antonio Casamayor Gracia** and **Dr. Joaquín Ariño Carmona**

Dr. Antonio Casamayor Gracia   Dr. Joaquín Ariño Carmona   Marcel Albacar Carot

Cerdanyola del Vallès, Desembre 2021

AGRAÏMENTS

Bé, sembla que ja ho tindríem. Des d'octubre de 2016, passant per una pandèmia global, un ciberatac a la UAB i algun que altre dia de mal d'esquena, ha arribat el dia de deixar per escrit els resultats d'aquests anys de feina. Abans d'això, però, necessito agrair a totes les persones que d'una manera o d'una altra han contribuït a que aquest treball tirés endavant. Començaré per donar les gràcies als meus directors, al Dr. Joaquín Ariño i al Dr. Antonio Casamayor, per l'oportunitat de fer el doctorat al seu grup. Recordo com si fos ahir el moment en què vaig saber que m'havien escollit, portava temps buscant feina i ja començava a donar per perduda la possibilitat de dedicar-me a la recerca... Moltíssimes gràcies, Joaquín, per les hores de feina, la paciència i la dedicació invertides en la direcció d'aquest treball. D'igual manera, moltíssimes gràcies, Antonio, per l'esforç de resoldre cada dubte/problema/consulta que et portava al despatx i moltes gràcies també per les hores dedicades a la meva formació com a investigador. El dia que marxi del laboratori, em podrà anar millor o pitjor, però l'important és tot el que he après de vosaltres: constància, rigor i pensament crític al laboratori. A més, crec que soc dels pocs privilegiats que poden dir que han fet poiata amb els dos!

Vull donar les gràcies ara a la gent de Llevats que ja no està físicament al laboratori. Començaré per Maria, un sol de persona carregada de paciència que em va ensenyar com funcionaven moltes coses del laboratori. A vore si en una mica de sort en no molt de temps coincidim tots més a propet i podem fer arrossets sovint (o com a mínim mirar com el fa Guillem...). Moltíssimes gràcies per tot, i, per fer un petit incís, diu la llegenda que quan sona al laboratori "Esbarzers" de la Gossa Sorda, es poden sentir crits de "*Maria, Teléfono*!". És automàtic, no puc evitar-ho...

Mil gràcies també a Ana, Chunyi, perquè sempre estava disposada a donar un cop de mà quan alguna cosa no acabava de sortir bé. Els noms de les teves soques encara avui ens donen problemes, ja he perdut el compte de les vegades que la ZCZ01 li hem dit CZC01... Espero que vagi tot molt bé i tant de bo ens puguem tornar a trobar.

Infinites gràcies per a Diego, no sé ni per on començar sincerament. Intentaré no passar-me de voltes fent el *flashback* o no sortim d'aquí. Podria començar per un dels meus primers dies per Llevats, quan ensenyant-me com preparar un gel de poliacrilamida vas acabar sense pantalons, coses que passen. Però sobretot em quedo amb les tardes llargues de poiata preparant mostres per a algun dels múltiples western que hem fet *mano a mano* o purificant proteïnes. Tardes durant les que podia sonar "La ventanita" i "La bilirubina" entre altres *temazos* per no defallir. Encara conservo al meu calaix un *post-it* on es pot llegir "*Me quiero morir*" que porta el teu autògraf, crec que hauria d'afegir "*No me extraña*" i passar-li a Santo... Estic bastant segur de

que ets la persona que conec que més ganes té de fer ciència i més preparada està per fer-ne. Per no parlar de la teva capacitat de transmetre la teva passió per la investigació a la gent que t'envolta. Només espero que aviat puguis tornar cap aquí i, investigant o no, puguem quedar per fer unes cerveses o un vermut torero i parlar de la vida.

Moltíssimes gràcies a Carlos, també conegut com a *Carlas* si pregunteu a un estudiant de pràctiques en particular, per les infinites hores de comentar experiments i resultats (i alguna que altra cosa *friki*). Que consti en acta que lo de infinites no ho dic en segones, ni té a veure amb la capacitat d'enrotllar-te com una persiana... Mil gràcies per les batalles compartides contra el pH-metre, i per la calma que transmets fent poiata, si arriba a ser per mi, el pH-metre estaria avui fora de l'atmosfera terrestre. Et vull donar les gràcies també per haver expandit, encara que a la força, els meus gustos musicals. Espero que tinguis sort per Sevilla, i a veure si ens veiem aviat.

Moltes gràcies a Elisa pel molt bon cop de mà amb múltiples PCR i *clonings* diversos, però sobretot, pel bon rotllo que va portar al laboratori. Encara tenim guardat el "dramómetro", l'únic que no conservem és allò dels dijous de Oreja de Van Gogh, sempre es diu que els bons costums són els primers que es perden...

De la multitud que som ara mateix a Llevats, infinites gràcies a Montse, la nostra tècnic, que de veritat no sé que faríem sense ella... Moltes gràcies per les hores de feina invertides, la dedicació i l'interès que poses darrere de cada experiment que fem. Gràcies pel bon rotllo i per no treure la vena de Rubí, que hi ha dies que no sé com aguantes sense fotre'ns un clatellot a cadascú...

Un quintar de gràcies per a Santo, a qui per variar una mica li recomano que vagi escrivint. Gràcies pel suport moral i l'assistència tècnica durant l'etapa final de la tesi. Una milla cúbica de gràcies també per no haver marcat el 2525 quan he fet algun acudit dolentíssim, fruit de l'estrès d'escriure per suposat... Molta força per a l'etapa final, que ja la tens aquí, si fa falta que cada cap de setmana anéssim a dinar *a bolsillo roto* per agafar energia, s'hi va i punt.

Moltíssimes gràcies també a Abdel, possiblement l'estudiant de màster amb més curiositat i ganes d'investigar que hem tingut a Llevats. Me n'alegro molt de que et quedis a fer el doctorat amb nosaltres i que no t'haguem espantat. Estic convençut de que t'anirà molt bé, i no perquè el projecte sigui molt interessant, sinó per les ganes i les hores que li estàs posant des del primer dia que vas posar els peus a Llevats.

Ara sortint del grup, però tampoc anant gaire lluny, vull donar les gràcies a la gent del Servei de Genòmica, en especial a Roger, per vindre cada matí, i alguna que altra tarda, a

amenitzar una mica el laboratori. Moltes gràcies també a Manuela, de l'SCAC, pel suport tècnic amb la citometria de flux.

De fora de la UAB vull agrair a Javier Torres i Ramon Martí del grup de Patologia neuromuscular i mitocondrial del VHIR la seva feina determinant dNTPs. Moltes gràcies també a Olga Zimmermannova, perquè el segon capítol d'aquest treball és en bona part fruit de la col·laboració amb el seu grup.

No vull oblidar-me de mencionar que no podré estar mai prou agraït a tots els involucrats amb el Col·lectiu de Doctorands de la UAB, de tot cor moltes gràcies a tots.

Moltíssimes gràcies a Jaime, Lucía i Patri pels bons moments de *Wimpis* i vermuts, i de tant en tant alguna excursió per a dissimular una mica. Moltes gràcies a Jordi, per les birres compartides (en poca freqüència per al meu gust) i les xerrades científiques.

Moltes gràcies als amics i amigues de Tortosa, la família *Jeenjony*, que els he vist poc però de forma molt intensa des de que va començar la pandèmia. Les celebracions dels 30 han sigut de lo millor de l'any 2021, i, per cert, potser hauríem d'anar posant-li data al famós viatge a Cuba... #estiuet

I, ja arribant al final, moltes gràcies als meus pares per donar-me l'oportunitat d'anar a estudiar "fora", amb tot l'esforç econòmic que això suposa. Moltes gràcies també pel suport moral, i, per lo bé que me cuideu quan baixo de visita. Les temporades de restriccions de mobilitat per la pandèmia ens han mantingut separats massa dies per al meu gust, espero que puguem recuperar el temps i gaudir més sovint dels dinars a la Muntanya. Moltes gràcies al meu germà Sergi, pel suport moral i per les xorrades que m'envies pràcticament a diari, que vulgues que no sempre n'hi ha alguna que em fa riure. No seria qui soc si no fos per vatros.

Ja per acabar, gràcies, Raquel, gràcies per tot. Moltes gràcies pel suport moral durant aquests anys i per aguantar totes les parides que puc arribar a dir en un dia sense tirar-me per la finestra. Gràcies per riure-te'n de la majoria, per dolentes que siguin. Però, sobretot, gràcies per haver portat al Nino al pis.

TABLE OF CONTENTS

TABLE OF CONTENTS

1. ABBREVIATIONS

AMP	Adenosine monophosphate
AMPK	AMP-activated protein kinase
ATP	Adenosine triphosphate
BSA	Bovine serum albumin
CDK	Cyclin dependent kinase
CWI	Cell wall integrity
C-Terminal	Carboxyl terminal
dNTP	deoxyribonucleotide triphosphate
DNA	Deoxyribonucleic acid
DTT	Dithiothreitol
EDTA	Ethylenediaminetetraacetic acid
eIF	eukaryotic initiation factor
ER	Endoplasmic reticulum
FACS	Fluorescence-activated cell sorting
GDP	Guanosine diphosphate
GFP	Green fluorescent protein
GST	Glutathione S-transferase
GTP	Guanosine triphosphate
HA	Human influenza hemagglutinin
IgG	Immunoglobulin G
kDa	kilodaltons
LB	Lysogeny broth
MAP	Mitogen-activated protein
MAPK	Mitogen-activated protein kinase
MEK	Mitogen-activated protein kinase kinase

17

ABBREVIATIONS

mRNA	messenger ribonucleic acid
N-Terminal	Amino terminal
OD	Optical density
ORF	Open reading frame
PBS	Phosphate Saline Buffer
PCR	Polymerase chain reaction
PPCDC	Phosphopantothenoylcysteine decarboxylase
PPM	Metal-dependent phosphatases
PPP	Phosphoprotein phosphatases
PVDF	Polyvinylidene difluoride
RNA	Ribonucleic acid
ROS	Reactive oxygen species
SDS	Sodium dodecyl sulfate
SDS-PAGE	Sodium dodecyl sulphate–polyacrylamide gel electrophoresis
SEM	Standard error of the mean
tRNA	transfer ribonucleic acid
TCA	Trichloroacetic acid
UPR	Unfolded protein response
WT	Wild-type
YNB	Yeast nitrogen base
YP	Yeast extract peptone
YPD	Yeast extract peptone dextrose

2. SUMMARIES

The *PPZ1* and *PPZ2* genes of *Saccharomyces cerevisiae* code for two Ser/Thr phosphatases that are only found in fungi. These Ppz enzymes have a highly conserved C-terminal catalytic domain, related to the PP1c phosphatase. One interesting feature of the Ppz phosphatases is the presence of a more divergent and unstructured N-terminal region, which is not found in PP1c enzymes. Remarkably, this N-terminal region has a Gly-2 that is suitable for N-myristoylation, a modification known to anchor proteins to the plasma membrane. Ppz1 is more biologically relevant than the Ppz2, and it is a crucial determinant of cation homeostasis, since it: a) negatively regulates high-affinity K^+ import by inhibiting the Trk system, the major K^+ import system in yeast cells, and b) represses the expression of the *ENA1* gene, a P-type ATPase sodium pump. Ppz1 has two negative regulatory subunits, Vhs3 and Hal3, being the latter the major inhibitor. These regulatory subunits bind to the catalytic domain of the phosphatase and inhibit its enzymatic activity. Remarkably, Ppz1 has been described to be the most toxic protein for yeast cells when overexpressed and its toxicity was shown to be dependent on the enzymatic activity. In this work we aimed to elucidate the mechanism behind the toxicity of this phosphatase.

Firstly, we present several experiments that support and extend data recently obtained by transcriptomic and phosphoproteomic assays of cells overexpressing Ppz1. We demonstrate here that Ppz1 overexpression results in the accumulation of reactive oxygen species, causes DNA damage, and provokes alterations in the phosphorylation state and intracellular localization of several proteins required for adaptation to low glucose.

Second, we describe that part of the toxic effect of an excess of Ppz1 activity is caused by alteration in monovalent cation homeostasis. However, this effect would not derive from the known role in the regulation of Trk1/Trk2 K^+ transporters, but from the hyperactivation of Nha1, a Na^+/H^+ antiporter found in the plasma membrane and perhaps from the inhibition of the Pma1 H^+-ATPase.

Lastly, we studied the subcellular localization of Ppz1-GFP in different overexpressing conditions. Ppz1 is essentially located at the plasma membrane, while Hal3 shows a cytosolic localization. Remarkably, we found that the overexpression of the native phosphatase and Hal3 induced the internalization of both proteins to the vacuolar membrane. We also present evidence that the disruption of this internalization blocks the beneficial effect of overexpressing Hal3 in cells where Ppz1 is overexpressed.

Els gens *PPZ1* i *PPZ2* de *Saccharomyces cerevisiae* codifiquen dues Ser/Thr fosfatases que només es troben en fongs. Els enzims Ppz tenen un domini catalític C-terminal molt conservat, relacionat amb el de la fosfatasa PP1c. Un tret característic de les fosfatases Ppz és la presència d'una regió N-terminal més divergent i desestructurada que no té relació amb l'enzim PP1c. Notablement, aquesta regió presenta una Gly-2 adequada per ser N-miristilada, una modificació que associa les proteïnes a la membrana plasmàtica. Ppz1 és més rellevant biològicament que Ppz2, i és un factor determinant de la homeòstasi catiònica, ja que: a) regula negativament l'import d'alta afinitat de K^+ inhibint els transportadors Trk, el principal sistema d'import de K^+ en llevats, i b) reprimeix l'expressió del gen *ENA1*, una Na^+/K^+-ATPasa. Ppz1 té dues subunitats reguladores negatives, Vhs3 i Hal3, essent l'últim el principal inhibidor. Aquestes subunitats reguladores s'uneixen al domini catalític de la fosfatasa i inhibeixen la seva activitat enzimàtica. Curiosament, la Ppz1 s'ha descrit com a la proteïna més tòxica per a les cèl·lules de llevat quan se sobre-expressa i la seva toxicitat s'ha demostrat que depèn de l'activitat enzimàtica. En aquest treball hem volgut contribuir a elucidar els mecanismes darrere de la toxicitat d'aquesta fosfatasa.

Primerament, presentem diversos experiments que donen suport i expandeixen els assajos de transcriptòmica i fosfoproteòmica de cèl·lules que sobre-expressen Ppz1. En aquest treball mostrem com la sobre-expressió de Ppz1 comporta una acumulació d'espècies reactives d'oxigen, causa danys en el DNA i provoca alteracions en l'estat de fosforilació d'algunes proteïnes requerides per l'adaptació a baixa glucosa.

En segon lloc, hem descrit que part de la toxicitat deguda a l'excés d'activitat Ppz1 està causada per una alteració de la homeòstasi de cations monovalents. No obstant, aquest efecte no derivaria del seu rol com a regulador negatiu dels transportadors de K^+ Trk1/Trk2, sinó que seria degut a una hiperactivació de Nha1, un antiportador de Na^+/H^+ que es troba a la membrana plasmàtica, i, potser a la inhibició de la H^+-ATPasa Pma1.

Per últim, hem estudiat la localització cel·lular de Ppz1 en diferents condicions de sobre-expressió. Ppz1 es troba essencialment a la membrana plasmàtica, mentre que Hal3 mostra una localització citosòlica. Sorprenentment, hem descobert que la sobre-expressió de la fosfatasa nativa i de Hal3 alhora indueix la internalització d'ambdues proteïnes a la membrana vacuolar. També mostrem evidències de com la disrupció d'aquesta internalització bloca l'efecte beneficiós de sobre-expressar Hal3 en cèl·lules en les que se sobre-expresa Ppz1.

3. INTRODUCTION

3.1. *Saccharomyces cerevisiae* as a model organism

The budding yeast *Saccharomyces cerevisiae* is a unicellular fungus that belongs to the Saccharomycetacea family, included in the Ascomycota phylum. For millennia human beings have been taking advantage of the ability of the *S. cerevisiae* to ferment bread dough and beverages. Remarkably, some wine remains are 7000 years old, albeit it still is unclear if back then humans accidentally bumped across these fermented beverages, or its production was intended (Maicas, 2020). Nowadays, besides its major role in food industry, *S. cerevisiae* is widely used in the field of biotechnology as a system for producing different compounds of commercial interest (biomass, organoleptic compounds, etc.) and for heterologous protein expression.

In nature *S. cerevisiae* can be found in the skin of ripe fruits such as grapes and has an optimum growth temperature of around 30 °C. Laboratory strains of *S. cerevisiae* can survive and proliferate as haploid or diploid cells. When in the first form, cells proliferate through mitosis and are sexually differentiated as mating type ***a*** or ***α***. Two haploid cells of opposite mating types can conjugate to generate a diploid cell, which can either a) proliferate via mitosis, or b) in nutrient scarcity conditions, undergo meiosis to produce four haploid spores.

S. cerevisiae began to be used as a model in genetic and metabolic studies due to its easy cultivation and manipulation. In 1996, it became the first eukaryotic organism whose genome was fully sequenced (Goffeau *et al*, 1996). Its genome is formed by 12.1 Mbp arranged across 16 chromosomes, encoding around 6000 genes of which 85% has a described biological role (Botstein & Fink, 2011). *S. cerevisiae* has been widely used as a model organism in molecular and genetic research because of the conservation between yeast and higher eukaryotes of those mechanisms that determine basic cellular functions, such as cell division. All these features make *S. cerevisiae* an outstanding research model for studying eukaryotic cell processes.

3.2. Protein phospho-dephosphorylation as a regulatory mechanism of cell function

The reversible phosphorylation of proteins is crucial to the regulation of most aspects of cell function, such as metabolism, cell cycle and stress response. The phosphorylation state of any given protein depends on the balance between the protein kinases and the protein phosphatases. By phosphorylating a protein, a phosphate will be incorporated, changing the net charge of the protein. This alteration can result in changes of the functional properties of the protein, for example, it can modify its subcellular localization, impede the interaction with other proteins, or even increase or decrease its biologic activity (Cohen, 2002). Recent analyses pointed out that 50% of the *S. cerevisiae* proteome can be phosphorylated (Vlastaridis *et al*, 2017;

Oughtred *et al*, 2019). Because of this, reversible protein phosphorylation is considered as the most common post-translational modification.

Protein phosphorylation can take place only in nine residues: serine, threonine, tyrosine, cysteine, arginine, lysine, aspartate, glutamate and histidine. In eukaryotic cells, however, the prevailing amino acids that undergo phosphorylation are serine, threonine and tyrosine (Moorhead *et al*, 2009). Typically, between 2 to 4% of the genome of a eukaryotic organism encodes phosphatases and kinases (Manning *et al*, 2002), and commonly the number of kinases is much higher than that of phosphatases. In *S. cerevisiae*, 127 kinases exist while only 43 phosphatases have been identified (Offley & Schmidt, 2019), a ratio that is conserved in higher eukaryotes. For example the human genome is thought to encode for 518 potential protein kinases (Johnson & Hunter, 2005), but it would only contain 150 genes encoding for protein phosphatases.

Depending on the residue that a phosphatase can dephosphorylate, phosphatases can be included into one of the three main families: Serine/Threonine Phosphatases, Protein Tyrosine Phosphatases or Dual Phosphatases (dephosphorylate Ser/Thr and Tyr).

3.2.1. Ser/Thr phosphatases in *S. cerevisiae*

The family of Ser/Thr phosphatases is the most abundant among the three main groups of phosphatases. These phosphatases were originally classified as type 1 (PP1) or type 2 (PP2), based on biochemical assays. A later classification, based on both biochemical and functional features of the phosphatases divided them into four major classes: PP1, PP2A, PP2B and PP2C (Cohen, 1989). Nowadays, Ser/Thr phosphatases are divided into three families: phosphoprotein phosphatases (PPPs), metal-dependent phosphatases (PPMs) and aspartate-based phosphatases (Shi, 2009a). In the Figure 1 a tree alignment of the PPMs and PPPs families in *S. cerevisiae* is shown.
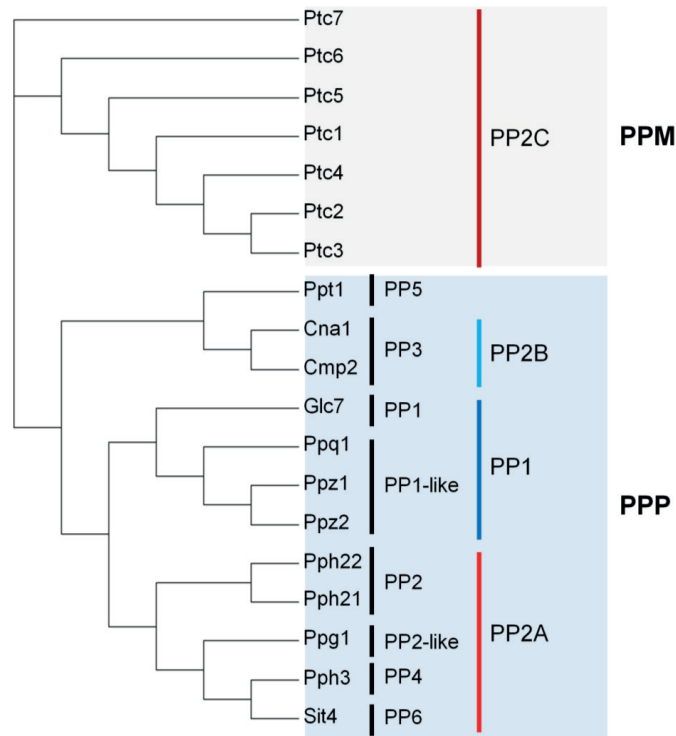
Figure 1. Ser/Thr phosphatases classification. Tree alignment of the Ser/Thr phosphatases of *S. cerevisiae* included in the Metal-dependent Protein Phosphatases (PPM) family, and in the Phosphoprotein Phosphatases (PPP) family. From (Ariño *et al.*, 2019).

3.2.1.1. Phosphoprotein phosphatases (PPPs)

The PPP family is formed by the following phosphatases: PP1, PP2A, PP2B, PP4, PP5, PP6 and PP7. Structurally, all PPP share a high level of similarity, especially in the catalytic core (150 residues) (Cohen, 1991). After a biochemical characterization it was determined that PP1 preferably dephosphorylates the β-subunit of the phosphorylase kinase, whereas PP2A acts on its α-subunit. PPP members have different regulatory subunits that modulate their function in the cell. For example, PP1 activity can be regulated by interacting with the polypeptides Inhibitor-1 and -2, which show no effect on PP2 activity. PP1 depends on Mn^{2+} ions to catalyze the dephosphorylation reaction *in vitro*, while PP2A does not depend on them. PP2B requires Ca^{2+}, instead (Ingebritsen & Cohen, 1983). The PPP family also contains a group of enzymes which are structurally related to type 1 and type 2A protein phosphatases, but functionally different. In *S. cerevisiae*, examples for PP4 (Pph3), PP5 (Ppt1) and PP6 (Sit4) have been identified (Stark, 1996), however, there is no equivalent for PP7.

3.2.1.2. Metal-dependent phosphatases (PPMs)

This Ser/Thr protein phosphatase family is formed by PP2C and pyruvate dehydrogenase phosphatases. PP2C shares the common features of PP2 (it acts on the α-subunit of the phosphorylase kinase and does not respond to Inhibitor-1 and -2), but it is not related in its

sequence to the PPP enzymes. PP2C needs Mg^{2+} and Mn^{2+} to catalyze the dephosphorylation reaction. In contrast to the PPP family, PPMs do not have any known regulatory subunit, as they function as monomeric enzymes. In fact, the ability of PP2C to perform different functions is probably due to the existence of numerous isoforms of the enzyme. In *S. cerevisiae*, seven PPM isoforms exist, being Ptc1 the most studied (Ariño *et al*, 2011).

3.2.1.3. Aspartate-based phosphatases

This last group is formed by FCP/SCP proteins (TFIIF-associating component of RNA polymerase II CTD phosphatase/small CTD phosphatase), which use the aspartate-based catalysis mechanism and their function depends on the presence of Mg^{2+}. The only substrate described for the members of this family of phosphatases is the C-terminal domain (CTD) of RNA polymerase II, which contains diverse tandems repeats of a serine-rich heptapeptide (Shi, 2009a).

3.3. The type 1 Ser/Thr phosphatase

The protein phosphatase 1 (PP1) was one of the first members of the PPPs family to be biochemically characterized, and nowadays it still is the most widely studied. In eukaryotic organisms PP1 needs to interact with different regulatory subunits to perform its physiological functions, among which there are glycogen metabolism, muscle contraction, RNA processing, protein synthesis, apoptosis induction and control of multiple checkpoints throughout the cell cycle (Cannon, 2010; Verbinnen *et al*, 2017). So, each functional PP1 enzyme is formed by the evolutionary conserved catalytic subunit (PP1c) associated to one or more specific regulatory subunits, which can regulate PP1c function by governing its substrate specificity and subcellular localization.

In mammalian genomes there are three genes encoding for PP1c enzymes: PP1α, PP1β/δ and PP1γ. The last one, however, can produce two different isoforms (PP1γ$_1$ and PP1γ$_2$) of the enzyme as a result of alternative splicing. In the genome of *S. cerevisiae* instead, only 1 gene (*GLC7*), which is essential, has been found to encode PP1c (Ohkura *et al*, 1989; Clotet *et al*, 1991; Feng *et al*, 1991). *GLC7*, as the other *GLC* genes, was identified in a mutant screen after isolation of a mutant that showed a reduced amount of glycogen (Feng *et al*, 1991; Cannon *et al*, 1994). A complementation study confirmed Glc7 orthology with the human PP1, since every human isoenzyme was able to complement the *glc7* deletion in yeast cells (Gibbons *et al*, 2007).

GLC7 encodes a protein formed by 312 residues (36 kDa) that shares 85% of identity with the four human PP1 proteins. The Glc7 protein also has a central section that is similar to the yeast protein phosphatases PP2A, PP2B and PPZ. Nowadays, multiple 3D-structures of several mammalian PP1c have been resolved. Structure-wise, the PP1 catalytic subunit adopts a compact

α/β fold (Figure 2), with a β sandwich wedged in the middle of two α-helical domains, which are the C- and N-terminus of the protein (Egloff *et al*, 1995). The β-sandwich and the two α-helical domains establish a "Y"-shaped cleft, which defines three grooves: the hydrophobic, the acidic and the C-terminal. In the center of the "Y"-shaped cleft, the active site of the phosphatase can be found. In this site, three histidines, two aspartates and one asparagine coordinate two metal ions (Mn^{2+} and Fe^{2+}) that are essential for the catalytic activity. Among all members of the PPP family, the residues mentioned are highly conserved, a fact that suggests a common mechanism of metal-catalyzed reaction (Shi, 2009b).

Figure 2. Crystal structure of the PP1c. Structure of the PP1 catalytic subunit (blue) bound to okadaic acid (yellow). The Y-shaped surface groove (pink) is established by the three domains of PP1c. The Fe 2+ and Mg 2+ ions (red spheres) are represented in the active site of the enzyme (Shi, 2009b).
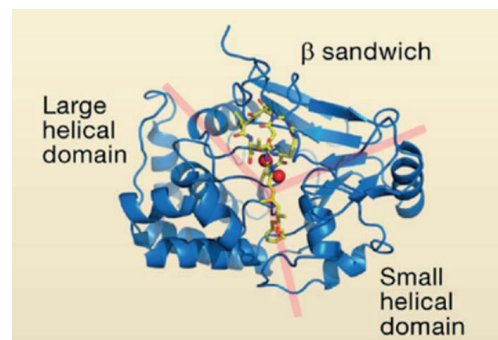
3.3.1. Functions

The many different functions that Glc7 can accomplish in *S. cerevisiae* depend on the cellular compartment where the phosphatase is found. When in the cytosol, Glc7 functions are related to carbohydrate metabolism, chitin synthesis, regulation of septin assembly, endocytosis and bud site selection. In the nucleus, Glc7 is responsible for transcriptional regulation, microtubule attachment to kinetochore and cell cycle checkpoints (Cannon, 2010). In carbohydrate metabolism, the PP1 enzyme dephosphorylates and activates glycogen synthase in mammals and yeast. In *S. cerevisiae* it seems that Gac1 is the subunit that regulates this Glc7 function, as Gac1 contains an RVxF motif plus a glycogen synthase binding region (Wu & Tatchell, 2001).

Glc7 also plays a crucial role in the phenomenon of repression by glucose. The two paralog subunits Reg1 and Reg2, assisted by Sip5, regulate the Glc7-mediated dephosphorylation of Snf1 (SNF1/AMPK protein kinase family) in high-glucose conditions (Sanz *et al*, 2000; Maziarz *et al*, 2016). Snf1 kinase is part of the SNF1 complex, which is formed by: i) Snf1 α-catalytic subunit, ii) three β-regulatory subunits (Sip1, Sip2 and Gal83), and iii) the γ-subunit Snf4. The main regulatory element of Snf1 catalytic activity is the phosphorylation of Thr210, by one of these kinases: Sak1, Elm1 and Tos3 (McCartney & Schmidt, 2001). The subcellular localization of the SNF1 complex depends on which β-subunit is bound to the complex. In a glucose scarcity situation

these subunits translocate to different cellular compartments, directing the kinase activity to specific substrates (Vincent *et al*, 2001). Gal83 is the most abundant β-subunit and the only subunit that can direct the complex to the nucleus (Hedbacker & Carlson, 2006). It is also the responsible of the SNF1 complex response to glucose limiting conditions (Hedbacker *et al*, 2004). The Reg1-Glc7 holoenzyme preferentially dephosphorylates Snf1 when it forms a complex with the Gal83 subunit. This dephosphorylation results in Snf1 inactivation. Other phosphatases as Ptc1 and Sit4 contribute in maintaining Snf1 in a dephosphorylated state while cells grow in the presence of glucose (Ruiz *et al*, 2011, 2013). One of the main targets of Snf1 is Mig1, a transcription factor that represses the expression of genes needed to obtain glucose from alternative carbon sources. When *S. cerevisiae* cells are growing in the presence of glucose, Mig1 remains inside the nucleus. However, when glucose is exhausted, Snf1 phosphorylates Mig1, promoting the nuclear export of the transcription factor (Hedbacker & Carlson, 2006). A schematic representation of the yeast cell response to glucose scarcity is depicted in Figure 3.
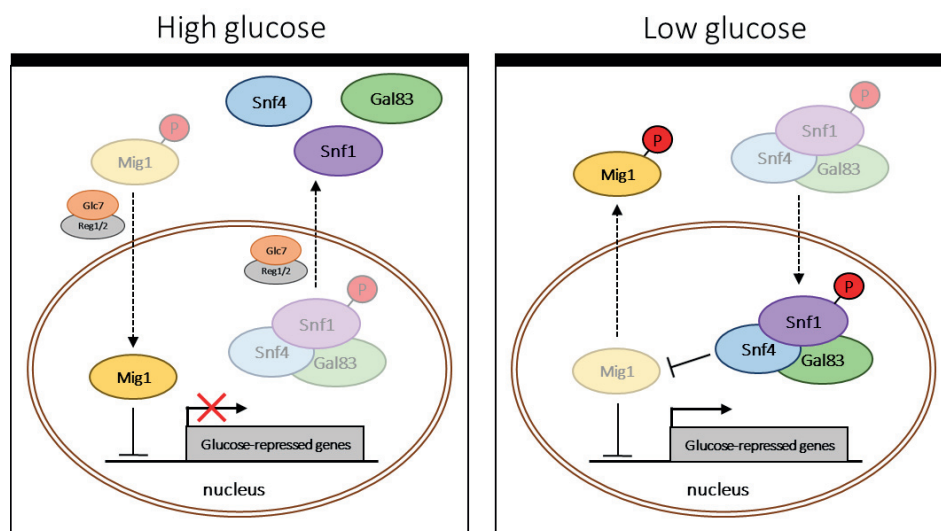
Figure 3. Schematic depiction of the low-glucose response in yeast cells. In high glucose conditions (left panel), Snf1 remains inactive in the cytosol. However, when yeast cells detect that glucose is scarce in their surroundings (right panel), Snf1 is activated by phosphorylation and translocated to the nucleus, where it dephosphorylates the transcriptional repressor Mig1, causing its eviction from the nucleus. If glucose becomes again available in the cellular environment (left panel), the complex Glc7-Reg1 dephosphorylates Snf1, inactivating the kinase and ejecting it from the nucleus (Adapted from (Velázquez, 2019)).

Glc7 is also related to the unfolded protein response (UPR). The lack of Reg1 promotes hypersensitivity to UPR-inducing factors as well as an augmented UPR-element dependent transcriptional response. These effects take place due to an inappropriate Snf1 activation (Ferrer-Dalmau *et al*, 2015).

Another essential cellular function where Glc7 plays an important role is cell division, by participating in several cell cycle checkpoints. The absence of the essential regulatory subunit Ypi1, the yeast homologue of mammalian Inhibitor-3, promotes the morphogenetic checkpoint. Ypi1, together with Sds22, binds to Glc7 forming a trimeric complex, which is responsible for Glc7 translocation to the nucleus (Pedelini *et al*, 2007). After Ypi1 depletion, the securin Pds1 is stabilized, pointing to the activation of the G2/M checkpoint (Marquina *et al*, 2012). Because in normal conditions the majority of Glc7 localizes in the nucleus, the effects observed could be due to an alteration of Glc7 nuclear localization, as previously reported for Ypi1-depleted cells (Pedelini *et al*, 2007). Another regulator of Glc7 could be the Shp1 protein, which is involved in shmoo formation and bud site selection. This protein could be working in a complex with Cdc48 and promote cell cycle progression (Böhm & Buchberger, 2013). Glc7 nuclear localization requires the Cdc48-Sph1 complex, which probably would promote the assembly of the Glc7-Sds22-Ypi1 complex (Cheng & Chen, 2015).

Glc7 also mediates septin regulation by interacting with the subunits Bni4, Afr1 and Gip1. The Glc7-Bni4 holoenzyme is responsible for targeting Chs3 (chitin synthase III) to the incipient bud sites when Pho85-Pcl1,2 phosphorylates Bni4 (Zou *et al*, 2009). Recently, Ref2 has been proposed as a regulatory subunit of Glc7. Ref2 would be needed to dephosphorylate the formin Bni1, determining its subcellular localization during cytokinesis (Orii *et al*, 2016).

Glc7 has also been described to participate in monovalent cation homeostasis (Williams-Hart *et al*, 2002). The absence of Ref2 induces saline stress hypersensitivity, which can be explained by the inability of the *ref2* mutant to properly induce the expression of the *ENA1* gene, encoding a P-type ATPase sodium pump (Ferrer-Dalmau *et al*, 2010).

One last function of Glc7 is translation regulation. The eukaryotic transcription factor eIF2 is a crucial element for the initiation of protein translation. Three subunits form the eIF2 complex: eIF2α, eIF2β and eIF2γ. For translation to take place, Ser51 of eIF2α subunit must be dephosphorylated. In *S. cerevisiae*, Glc7 dephosphorylates eIF2α by interacting with an RVxF-like motif present in eIF2γ (KKVAF) (Rojas *et al*, 2014). A schematic representation of Glc7 functions and regulatory subunits can be found in Figure 4.
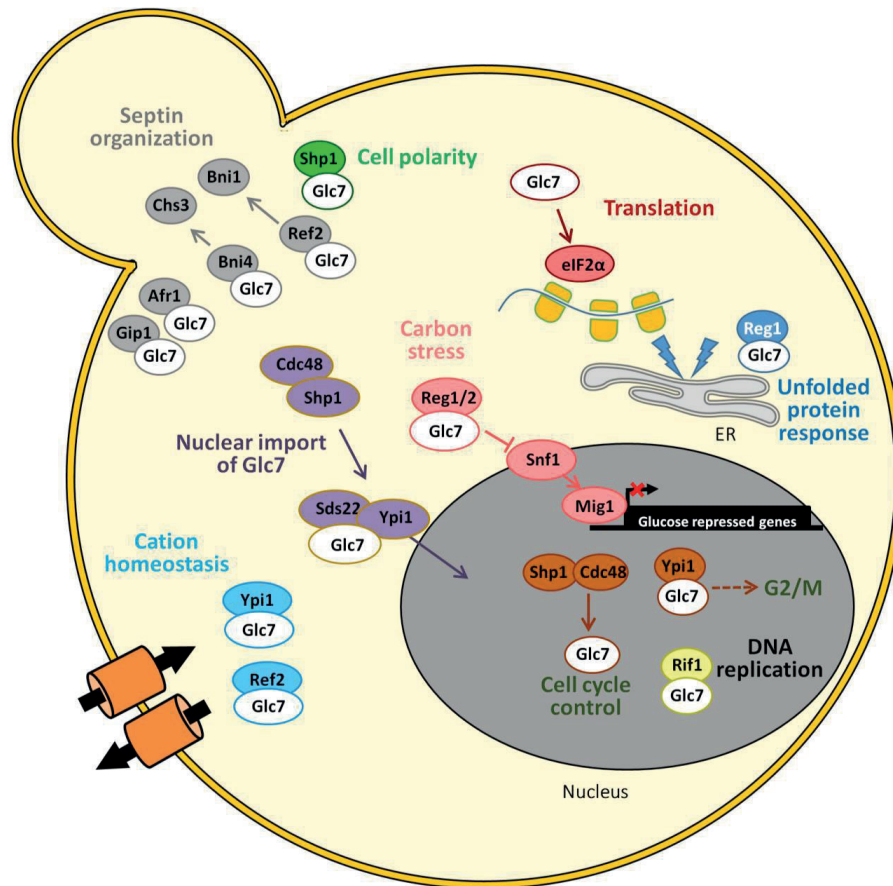
Figure 4. Cartoon depicting the diverse cellular processes where Glc7 plays a role, in addition to the diverse regulatory subunits needed to accomplish each function. From (Ariño *et al.*, 2019).

It has been reported that the overexpression of *GLC7* gene is deleterious for yeast cells (Liu *et al*, 1992) as it promotes chromosome missegregation, similar to that observed for *ipl1* mutants (Francisco *et al*, 1994). The lethality caused by an excess of Glc7 activity appears to be dependent on Glc8, Reg2 and Sds22 functions, suggesting a relationship between Glc7 toxicity and its nuclear localization (Ghosh & Cannon, 2013).

3.3.2. Glc7 regulation and binding motifs

The catalytic subunit of the PP1 enzyme does not exist freely in the cell, it must be associated to one of its regulatory subunits to fulfill a precise function. The number of different regulatory subunits can vary among eukaryotes. For instance, in mammals there are more than 100 putative regulatory subunits (Moorhead *et al*, 2007), whereas in *S. cerevisiae*, at least 30 are present (Cannon, 2010; Offley & Schmidt, 2019). These regulatory subunits define PP1c function, subcellular localization, activity and substrate affinity.

Even though PP1c regulatory subunits are not structurally related, most of these subunits bind PP1c in the same manner. They all contain short sequences of about 4 to 8 residues that

provide a surface to interact with PP1c. These short sequences are known as SLiMs (Short Linear Motifs) and despite of their conservation throughout evolution, they are somewhat degenerated. In mammalian, 10 different PP1-SLiMs have been described, whereas in the yeast *S. cerevisiae* most of the regulatory subunits interact with the hydrophobic groove of Glc7 by the RVxF consensus sequence. Some examples are: Afr1, Bni4, Bud14, Gac1, Gip2, Ref2, Reg1, Reg2, and Sla1. On the contrary, Sds22 and Pti1 bind to Glc7 but do not contain an RVxF motif. The first one interacts with a region close to the catalytic core of Glc7 by means of its characteristic leucine-rich repeats (Ceulemans & Bollen, 2004), while for Pti1, an essential component of the cleavage and polyadenylation complex, there is no interaction motif known (He & Moore, 2005).

3.4. PPZ phosphatases in *S. cerevisiae*: Ppz1 and Ppz2

Whereas PP1 is ubiquitous, PPZ phosphatases are restricted to fungi. These phosphatases were first identified in *S. cerevisiae* and are encoded by the *PPZ1* and *PPZ2* genes (Lee *et al*, 1993; Posas *et al*, 1992). They contain a C-terminal catalytic domain (≈350 residues), which is well conserved and similar to that of PP1, and a structurally disordered N-terminal extension. This N-terminal domain is rich in Ser, Thr and Asn and it is highly variable in sequence and length among fungi. *PPZ1* and *PPZ2* genes encode proteins of 690 and 710 residues, respectively, which share an 85.9% identity in their C-terminal catalytic domains and a 32.2% identity in their N-terminal regions (Calafí *et al*, 2020a). When comparing PPZs catalytic domains to Glc7, Ppz1 shares a 57.1% identity and, Ppz2, a 60.4%. However, unlike *GLC7*, *PPZ1* and *PPZ2* genes are not essential (even the double mutant *ppz1 ppz2* is still viable), which suggests that PPZs from *S. cerevisiae* do not completely share Glc7 functions.

A remarkable feature of PPZ phosphatases N-terminal extension is the presence of a Gly in position 2, which is conserved among other fungi and suitable for N-myristoylation. Ppz1 myristoylation has been proved to take place *in vivo* (Clotet *et al*, 1996) and it has also been described the N-myristoylation *in vitro* of the initial octapeptides from Ppz1 and Ppz2 by the N-myristoyl transferase Nmt1 (Johnson *et al*, 1994). The myristoylation of any protein is a determinant for its subcellular localization, as it mediates the interaction with the membrane and it also increases the stability of the protein (Yonemoto *et al*, 1993). Recently, the Gly-2 of Ppz1 has been described as a crucial feature for the phosphatase to localize in the peripheral membrane (Lee *et al*, 2019). Besides the Gly-2, the N-terminal extension of the Ppz phosphatases contains a relatively conserved short sequence, which can be found in many fungi in the form of SxRSxRxxS consensus (Minhas *et al*, 2012). This short sequence has a functional role, regulating cationic homeostasis.

INTRODUCTION

In addition to *S. cerevisiae*, to this date several Ppz from different fungi have been studied: Pzh1 (*Schizosaccharomyces pombe)* (Balcells *et al*, 1997), Pz1-1 (*Neurospora crassa*) (Vissi *et al*, 2001), PpzA (*Aspergillus nidulans*) (Leiter *et al*, 2012), CaPpz1 (*Candida albicans*) (Ádám *et al*, 2012), UmPpz1 (*Ustilago maydis*) (Zhang *et al*, 2019b) and CnPpz1 (*Cryptococcus neoformans*) (Zhang *et al*, 2019a).

3.4.1. Cellular roles of Ppz1 in *S. cerevisiae*

Ppz1 enzymatic activity is essential for its normal function in the cell. A sole mutation in the Arg-451, a conserved residue in many Ser/Thr phosphatases from eukaryotic organisms that corresponds to Arg-95 in the catalytic subunit of PP1, renders Ppz1 inactive and disturbs its proper cellular functions (Clotet *et al*, 1996). Ppz1 was first identified as a phosphatase involved in the maintenance of cell wall integrity (Posas *et al*, 1993). Nevertheless, Ppz1 activity was soon determined as a crucial factor in cation homeostasis (Posas *et al*, 1995; Yenush *et al*, 2002). The deletion of the *PPZ1* gene renders *S. cerevisiae* cells hypertolerant to toxic cations and sensitive to caffeine-induced stress, among other phenotypes, whereas the deletion of *PPZ2* shows no observable phenotype. This fact suggested that Ppz1 has a more relevant biological role. However, deleting *PPZ2* on a *ppz1* mutant strain strengthens its phenotypes.

3.4.1.1. The role of Ppz1 in cation homeostasis regulation

The maintenance of ionic homeostasis is a crucial task for all living cells, as many physiological parameters depend on it: cellular size, turgor, intracellular cation concentration, internal pH and membrane potential. In yeast cells, major changes in the intracellular concentration of the primary monovalent cations (H^+, K^+ and Na^+) can lead to cell damage (Serrano, 1996). Despite the fact that Na^+ is able to enter yeast cells through several low-affinity cation import systems, *S. cerevisiae* can keep an appropriate concentration of Na^+, even in environments with high concentrations of the cation. Yeast cells rely on a tight coordination between their uptake and efflux systems to achieve a solid adaptation to changes in their surroundings. In *S. cerevisiae* two major transporters are responsible of the extrusion of Na^+: Nha1 (a Na^+/H^+ antiporter) and Ena1 (a P-type ATPase Na^+ pump).

NHA1 was identified as a gene that improved the growth of a salt sensitive strain when overexpressed (Prior *et al*, 1996). This gene encodes a protein of 985 residues, with 12 predicted transmembrane domains and a long C-terminal cytosolic region (550 residues). The deletion of *NHA1* in a wild-type background results in higher sensitivity to K^+ and Na^+ at acidic pH (Bañuelos *et al*, 1998). The Nha1 protein is localized in the peripheral membrane, where it displays its major role as a proton antiporter with similar affinity for Na^+ and K^+, but it can also export Rb^+ and Li^+

(Bañuelos *et al*, 1998; Ohgaki *et al*, 2005). Even though its importance for cation homeostasis, *NHA1* expression is not increased by the addition of NaCl to the medium but it is constitutive, because of this, it is considered as a housekeeping gene (Bañuelos *et al*, 1998). Several residues of Nha1 have been found to modulate its activity and substrate specificity (Ariño *et al*, 2010). A functional study of the long Nha1 C-terminus region revealed that this domain is not necessary for its proper localization in the plasma membrane or the transport of its substrates, but it is involved in the cellular response to sudden changes in environmental osmolarity (Kinclová *et al*, 2001). However, a more recent study from Papouskova and coworkers demonstrated that the amino acids 761-841 (C5 conserved domain) of Nha1 are essential for the plasma membrane localization of the antiporter (Papouskova *et al*, 2021).

At acidic pH, Nha1 is the major system for Na^+ extrusion, whereas at higher pH levels, the transporter Ena1 is the main responsible for Na^+ removal (Bañuelos *et al*, 1998). In many yeast genomes there are 3 to 5 *ENA* copies that encode very similar proteins (Ariño *et al*, 2010). These proteins are formed by 1091 amino acids and their predicted structure has 10 transmembrane domains. The Ena transporters localize in the plasma membrane and they actively extrude Na^+, K^+ and Li^+, in reactions coupled to the hydrolysis of ATP molecules (Haro *et al*, 1991; Benito *et al*, 1997). Deleting the whole *ENA* cluster leads to a strong sensitivity to salt and alkaline pH (Haro *et al*, 1991). *ENA1* was the first identified member of the tandem and it is described to be the most functionally relevant (Haro *et al*, 1991). The expression of the *ENA* genes is very low in normal growth conditions, but that of *ENA1* greatly increases after exposing yeast cells to high sodium (and/or lithium) levels and alkaline pH (Haro *et al*, 1991). *ENA1* transcriptional regulation requires the participation of many different pathways that will result in the activation or inhibition of its transcription. The promoter of *ENA1* contains diverse regulatory elements that can be recognized by specific transcription factors, such as: Crz1, Sko1, Mig1 and Nrg1, among others (Ruiz & Ariño, 2007). Interestingly, the presence of glucose has been described to repress *ENA1* expression (Alepuz *et al*, 1997).

In *S. cerevisiae*, PPZ phosphatases are important determinants of salt tolerance, as they are involved in the *ENA1* gene repression (Figure 5) (Posas *et al*, 1995; Ariño, 2002). Yeast cells lacking both phosphatases display increased levels of *ENA1* mRNA. Deleting only the *PPZ1* gene already renders the cells tolerant to high Li^+ and Na^+ concentrations, and this is exaggerated by the deletion of both *PPZ1* and *PPZ2* genes (Posas *et al*, 1995).
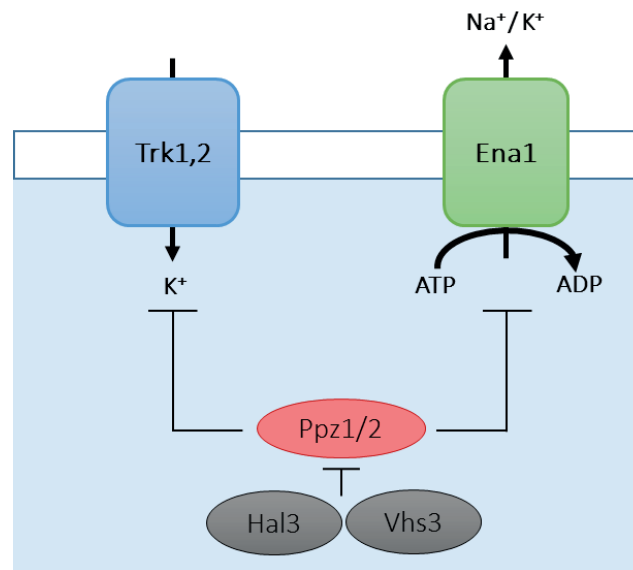
Figure 5. The role of Ppz1 in the regulation of Ena1 and Trk1,2 transporters. The impact of Ppz1 in monovalent cation homeostasis can be explained by its negative regulatory role on Trk1,2 and Ena1. In the case of the high-affinity potassium import system Trk1,2, Ppz1 is thought to inhibit the activity of the transporter, whereas, for Ena1, the negative regulation takes place at a transcriptional level, since the presence of Ppz1 represses the expression of the *ENA1* gene.

The other major role that PPZ phosphatases play in *S. cerevisiae* is regulating the intracellular concentration of K^+ (Figure 5). Maintaining a proper internal concentration of this cation is crucial for cell survival as it is the determinant for cell volume, turgor, membrane potential and ionic strength. A proper K^+ uptake is needed to reduce the membrane potential, preventing the entry of toxic cations as Na^+ or Li^+. In the yeast *S. cerevisiae*, there are two major mechanisms that mediate the K^+ uptake, the high-affinity and the low-affinity K^+ transporters (Rodríguez-Navarro & Ramos, 1984). The high-affinity potassium transporters are Trk1 and Trk2 (Gaber *et al*, 1988; Ko *et al*, 1990; Ko & Gaber, 1991), being Trk1 the most biologically relevant. Trk1 is a membrane protein with a predicted structure of 12 transmembrane domains and it is localized in the lipid rafts present in the plasma membrane (Yenush *et al*, 2005). The deletion of both components of the high-affinity system results in a strong defect in potassium transport and a slow or null growth phenotype when potassium cations are scarce. This is easily restored by media supplementation with K^+.

Several kinases and phosphatases control the activity and stability of the Trk transporters. For instance, the protein kinases Hal4 and Hal5 are essential for the stabilization of Trk1 and Trk2 at the plasma membrane. However, there is no evidence of a direct phosphorylation of Trk by Hal4 and Hal5. PPZ phosphatases are involved in the regulation of the activity of the Trk transporters. Even though the details of this mechanism remain unclear, it has been described

that Ppz1 physically interacts with Trk1, and that Trk1 phosphorylation increases in cells lacking the *PPZ1* gene (Yenush *et al*, 2005). Nevertheless, the direct dephosphorylation of Trk1 by Ppz1 has not been confirmed neither *in vitro* nor *in vivo*. Even so, there is the case of HvHak1 (a K$^+$ transporter found in some fungi but not in the yeast *S. cerevisiae*), which, when expressed heterologously in *S. cerevisiae*, displayed an increased K$^+$ influx in the absence of *PPZ1* (Fulgenzi *et al*, 2008). This fact raised the possibility that HvHak1 could be regulated by a Ppz-like protein controlling K$^+$ influx in those fungi where this transporter is present.

As mentioned above, originally, PPZ phosphatases were associated to the maintenance of the cell wall integrity in *S. cerevisiae*, since Lee and coworkers identified *PPZ2* as a dosage dependent suppressor of the lytic phenotype of cells lacking *SLT2* (Lee *et al*, 1993). Some of the phenotypes described for strains that lack some members of the pathway (*bck1*, *mkk1/mkk2* or *slt2*) match some *ppz1 ppz2* phenotype, such as increased size (elongated morphology), or caffeine and temperature sensitivity. These defects result in cell lysis in *ppz1 ppz2* strains, which can be suppressed by media supplementation with 1 M sorbitol. Furthermore, the mutation of *slt2* in a *ppz1 ppz2* background has an additive effect. The Slt2/Mpk1 pathway and the PPZ phosphatases are related by the connection between the phosphatases and the potassium uptake regulation. Thus, the augment of cellular turgor due to a higher K$^+$ uptake of cells lacking both *PPZ1* and *PPZ2* genes would result in an increase of cell wall pressure, leading to an activation of Slt2 pathway. In fact, the double mutant *ppz1 ppz2* displays a higher Slt2 activity (Yenush *et al*, 2002; Merchan *et al*, 2004). Therefore, Ppz1 proposed role in the maintenance of cell wall integrity is, indeed, a consequence of its function in cation homeostasis.

3.4.1.2. Ppz1 and cell cycle progression

For every eukaryotic cell, as in the case of *S. cerevisiae*, cell cycle is a process that can be divided in these four phases: G$_1$, S (DNA replication), G$_2$ and M (Mitosis). Cell cycle is a complex and tightly regulated process, and it involves three major control points, known as checkpoints. Before being able to enter this process, *S. cerevisiae* cells must accomplish a few requirements. This is regulated by the Start checkpoint, which decides if cells enter to the cycle or not. Cells must have enough levels of G$_1$ cyclin/Cdc28 protein kinase activity for the DNA synthesis, bud formation and replication of the spindle body to overcome this checkpoint. As the entrance to cell cycle is an irreversible process, this process must be subjected to tight regulation. Once entering the cell cycle process, the next checkpoint occurs at the G$_1$/S transition and it determines DNA replication by controlling that all conditions are suitable to carry out a new division cycle, such as proper cell size and absence of DNA damage. The last checkpoint takes place at the G$_2$/M

transition, where it regulates the entry into mitosis after verifying that the DNA was properly duplicated during phase S (Tyson *et al*, 2002).

Even though in mammals there are several CDK that regulate the cell cycle, in *S. cerevisiae* only one CDK, Cdc28, is present (Mendenhall & Hodge, 1998; Miller & Cross, 2001). By the end of mitosis, the complex formed by Cdc28 and Cln3 is the responsible for sensing the required cell size to proceed through another Start checkpoint (Nasmyth, 1993). When the cell achieved the proper size, Cdc28-Cln3 activates the transcriptional complexes that induce genes needed for G_1, such as *CLN1, CLN2, CLB5* and *CLB6* (Koch *et al*, 1996). Some phosphatases, such as Glc7 and Sit4, are needed to ensure the transcription of several genes essential for the G_1/S transition (Fernandez-Sarabia *et al*, 1992; Hisamoto *et al*, 1994).

Sit4 is a type 2A-related protein phosphatase encoded by the gene *SIT4* in *S. cerevisiae* that was originally identified in a screen as a suppressor of a transcriptional defect in *HIS4* (Arndt *et al*, 1989). A few years later, it was described its function in the G_1/S progression (Sutton *et al*, 1991) as it was needed to ensure the expression of the Cln1 and Cln2 cyclins and the transcription factor Swi4.

The fact that Hal3 (see section 5), a negative regulatory subunit of Ppz1, was identified as able to rescue the growth defect of a *sit4* mutant when overexpressed (Di Como *et al*, 1995), prompted the proposal of Ppz1 as a regulatory component of the cell cycle. In agreement with this, the overexpression of Ppz1 provokes a halt in the cell growth, decreased levels of *CLN2* and *CLB5*, and the accumulation of cells in G_1 in an exponentially growing culture, all pointing to a delay in the G_1/S transition (Figure 6) (Clotet *et al*, 1999). On the contrary, the deletion of the *PPZ1* gene attenuates the slow growth defect of a *sit4* mutant, in addition to promoting an earlier expression of both *CLN2* and *CLB5*, thus facilitating the entry in S phase. Then, Ppz1 has a relevant role in cell cycle opposite to that of Sit4. Besides, Ppz1 negatively regulates several processes that affect the bud formation through a mechanism that would not be mediated by Sit4, Bck2 or Cln3 (Clotet *et al*, 1999).
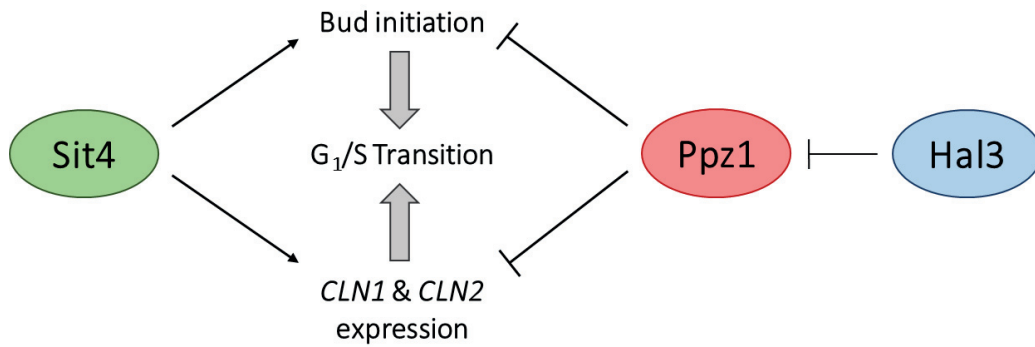
Figure 6. Ppz1 and Sit4 display opposite roles in cell cycle progression. Adapted from (Clotet et al., 1999)

3.4.1.3. Ppz1 role in protein translation

Protein translation is a crucial biological process by which the information carried by the mRNA is decoded by the ribosomes, resulting in specific polypeptide production. The process of translation can be divided into three different phases: initiation, elongation and termination. Ppz1 phosphatases have been shown to interact *in vivo* with EF1Bα (Tef5), which is the GTP/GDP exchange factor for translation elongation factor 1 (De Nadal *et al*, 2001). Moreover, the conserved Ser86 of Tef5 was found hyperphosphorylated in the double mutant *ppz1 ppz2* strain. De Nadal and coworkers suggested that Ppz1 was involved in translational fidelity, as the *ppz1 ppz2* strain showed an enhanced read-through at all three nonsense codons (De Nadal *et al*, 2001). The fact that Ppz1 was shown to participate in the read-through efficiency and manifestation of non-Mendelian anti-suppressor determinant [ISP⁺] reinforced the idea of Ppz1 being involved in the translation process (Aksenova *et al*, 2007). Moreover, recent findings showed that Ppz1 was bound to ribosomes engaged in translation and it could be co-purified with several ribosomal proteins and translation factors (Calafí *et al*, 2020b).

3.4.1.4. Other functions

Recent work from Lee and coworkers pointed out a role for Ppz1 in ubiquitin homeostasis. A double mutant *ppz1 ppz2* displays a defect in ubiquitin levels that could be attributed, at least in part, to an increased level of phosphorylation of ubiquitin at Ser57 (Lee *et al*, 2017). Two years later, they described that Ppz1 mediates the endocytosis of the methionine transporter Mup1 (Lee *et al*, 2019). The presence of methionine in the environment triggers Mup1 endocytosis mediated by Art1, a ubiquitin ligase adaptor for Rsp5. Ppz1 dephosphorylates Art1, promoting cargo recognition at the plasma membrane. Even though Ppz1 is not essential for Art1 translocation, it is crucial for the Art1-Mup1 interaction. It must be noted that both functions, ubiquitin and endocytosis, are unrelated since a Ppz1-G2A variant , a cytosolic version of the phosphatase, was able to fully complement the ubiquitin defect in a *ppz1 ppz2* double

mutant background, but it did not complement the endocytic traffic defects observed in this background (Lee *et al*, 2019). This fact indicated that plasma membrane localization is essential for Ppz1 endocytic function but dispensable for its role in ubiquitin homeostasis.

3.5. Regulatory subunits of Ppz phosphatases: Hal3 and Vhs3

Whereas more than 30 regulatory subunits of the PP1c enzyme were described for *S. cerevisiae*, only two have been found for the PPZ phosphatases. These subunits are Hal3 and Vhs3, both acting as negative regulatory subunits.

In 1995, the gene *HAL3* was identified in two different laboratories independently. As mentioned above, it was identified as a multicopy suppressor of the growth defect displayed by a *sit4* mutant, and it was named *SIS2* (as in Sit4 suppressor) (Di Como *et al*, 1995). On the other hand, Ferrando and coworkers described that a wild-type strain showed an enhanced salt tolerance when Hal3 (from *hal*otolerance) was overexpressed (Ferrando *et al*, 1995). The protein encoded by the gene *HAL3/SIS2* (from now on Hal3), is formed by 562 amino acids and it is localized in the cytoplasm (Ferrando *et al*, 1995). This protein has a C-terminal tail, of around 80 amino acids, which is very rich in acidic residues, particularly in aspartic.

The role of Hal3 has been studied in living cells and diverse phenotypes caused by its overexpression have been described. Firstly, the expression levels of *ENA1* are higher in cells that overexpress the *HAL3* gene, which was suggested as the mechanism behind the tolerance to high salt concentrations of wild-type cells that overexpress Hal3 (Ferrando *et al*, 1995; De Nadal *et al*, 1998; Ruiz *et al*, 2003). Secondly, wild-type cells that overexpresses Hal3 display an increased K^+ uptake via Trk transporters and it allows cell growth at limiting K^+ conditions (Ferrando *et al*, 1995; Yenush *et al*, 2002). More phenotypes of Hal3 overexpression are the induction of the lytic phenotype on the *slt2* mutant (De Nadal *et al*, 1998) and the increase of Tef5 phosphorylation levels in wild-type strains (De Nadal *et al*, 2001). In fact, some of the phenotypes seen upon Hal3 overexpression are very similar to those found in a *ppz1* mutant, whereas the phenotypes seen in a *hal3* mutant are completely opposite to those of a *ppz1* mutant (De Nadal *et al*, 1998). Such behavior would be compatible with Hal3 being a negative regulator for Ppz1 in most of Ppz1 major cellular functions.

Indeed, the Hal3 was reported to act as a Ppz1 negative regulatory subunit, able to bind to the catalytic C-terminal of Ppz1, thus inhibiting its enzymatic activity (De Nadal *et al*, 1998). This binding is much stronger when the N-terminal region of the phosphatase is absent (De Nadal *et al*, 1998). At a structural level, Hal3 has no resemblance with any of the PP1c regulatory subunits and it is not able to interact with Glc7 (De Nadal *et al*, 1998; García-Gimeno *et al*, 2003),

even though Hal3 contains a sequence ([263]KLHVLF[268]) that it is similar to the RVxF motif present in most of PP1c subunits (Bollen *et al*, 2010). Further work aimed to clarify if the RVxF-like motif was needed to the Hal3-Ppz1 interaction showed that mutation of His265 or Phe268 did not affect the ability of Hal3 to interact with and to inhibit the phosphatase. This fact suggested that the mechanism of the Ppz1-Hal3 interaction could be different from that of PP1c and its regulatory subunits (Muñoz *et al*, 2004). A random mutagenesis study disclosed two residues of Hal3 (Glu-460 and Val-462) that, when mutated, generated Hal3 versions that were unable to inhibit the phosphatase, albeit they were still able to bind to Ppz1 (Muñoz *et al*, 2004).

Vhs3, which is structurally related to Hal3, was identified as a multicopy suppressor of the *hal3 sit4* mutant conditional lethality (Muñoz *et al*, 2003), and its name derives from *viable in hal3 sit4* mutant. The protein Vhs3 consists of 674 residues that shares a 49% of identity with Hal3, and also presents the characteristic acidic C-terminal tail (Ruiz *et al*, 2004). The overexpression of *VHS3* results in phenotypes very similar to those of *HAL3* overexpression, such as: a) improvement of the salt tolerance of a wild-type strain by an increase of *ENA1* expression levels, b) accentuation of the lytic phenotype of a *slt2* mutant, and c) rescue of the G_1/S transition blockade displayed by a *sit4* mutant (Ruiz *et al*, 2004). It must be noted that only in the case of the rescue of cell cycle blockade the effect of overexpressing *VHS3* can compare in potency to that of *HAL3* overexpression. For the other two phenotypes, the overexpression of *HAL3* has a predominant effect. All the phenotypes listed above could be explained by a regulation of Ppz1 phosphatase activity by Vhs3. This protein interacts with the catalytic domain of Ppz1 and, as observed for Hal3, the binding is more intense when the N-terminal region of the phosphatase is missing (Ruiz *et al*, 2004). However, the deletion of *VHS3* does not reduce cell tolerance to salt, unlike the case of deleting *HAL3*. This fact, together with the very mild phenotypes of a *vhs3* mutant, suggested that Vhs3 had a less relevant biological role than Hal3, which could be explained by its lower expression levels (Ruiz *et al*, 2004).

Interestingly, the double mutant *hal3 vhs3* is synthetically lethal and this could not be rescued by deleting *PPZ1*, *PPZ2* or even both genes. This indicated that Hal3 and Vhs3 could have, in addition to Ppz1 inhibition, a novel function that was crucial for cell survival (Ruiz *et al*, 2004). In *S. cerevisiae* there is an essential protein, Cab3, which is structurally related to Hal3 and it shares a 28% of identity with it. Moreover, Cab3 has an acidic tail with a length similar to that of Hal3. Even though these similarities between both proteins, Cab3 does not inhibit the phosphatase activity of Ppz1 (Ruiz *et al*, 2009).

INTRODUCTION

The synthetically lethal phenotype of the double mutant *hal3 vhs3* was understood when it was found that Hal3 and Vhs3 can associate with Cab3 to form a heterotrimeric phosphopantothenoylcysteine decarboxylase (PPCDC) enzyme, which meant that Hal3 and Vhs3 were actually moonlighting proteins (Ruiz *et al*, 2009). In this case *S. cerevisiae* would be an exception as in most organisms the PPCDC enzyme consists of a homotrimer with three catalytic sites, each formed at the interface of two monomers. In yeast, there is only a single catalytic site, which is formed at the interface of Cab3 and either Hal3 or Vhs3. In keeping with this role, *CAB3* is an essential gene (Ruiz *et al*, 2009). Abrie and coworkers propose that Vhs3 could be more frequently found as part of a PPCDC complex than Hal3, meaning that the latter would be more frequently found in a monomeric form and function as a negative regulatory subunit of Ppz1 (Abrie *et al*, 2015).

3.6. The toxic effects of Ppz1 overexpression

As in the case of Glc7, Ppz1 overexpression is deleterious for yeast cells (Clotet *et al*, 1996; De Nadal *et al*, 1998), and because of this, its activity must be tightly regulated. Transforming cells with an episomal vector containing the *PPZ1* gene under the control of its own promoter results in cells with a slow growth phenotype when compared to wild-type cells. Moreover, when the gene is expressed from a strong promoter, like the *GAL1-10*, the deleterious effect is exacerbated leading to a virtually total halt in cell growth. Further work showed that the overexpression of the C-terminal domain alone caused a similar phenotype to that of overexpressing the whole phosphatase, whereas the N-terminal half of the phosphatase alone did not show any negative effect to cell growth (Clotet *et al*, 1996). Even in the case of strong Ppz1 overexpression, the harmful effects could be countered by the overexpression of *HAL3* (De Nadal *et al*, 1998).

Makanae and coworkers, in a genome-wide analysis, described that in *S. cerevisiae PPZ1* was the gene for which yeast cells could harbor a lesser number of copies (Makanae *et al*, 2013), suggesting that Ppz1 was the most toxic protein in overexpression. Recent work from our laboratory showed that the overexpression of a catalytically inactive mutant (R451L) has no negative effects on cell growth (Calafí *et al*, 2020b), suggesting that the toxicity of Ppz1 is due to an excess of its phosphatase activity. This mutation does not affect the ability of Hal3 to bind to the phosphatase (De Nadal *et al*, 1998). However, it was found that overexpression human PPCDC did not alleviate the growth defect of Ppz1-overexpressing cells. Therefore, the plausible hypothesis that Ppz1 overexpression could led to the sequestering of Hal3 and Vhs3, causing a deficit of the essential PPCDC activity that might contribute to Ppz1 toxicity could be ruled out. Furthermore, overexpressing Ppz1 results in Gcn2-dependent increased phosphorylation of eIF2α at Ser-51, a modification that results in a global inhibition of protein synthesis (Calafí *et al*,

2020b). In consonance with this result, deleting the *GCN2* gene attenuated the growth defect of a Ppz1-overexpressing strain. Thus, the deleterious effect seen on Ppz1-overexpressing cells could be in part attributed to a disturbance in normal protein synthesis.

Overexpression of Ppz2 has no deleterious effect (Calafí *et al*, 2020a), in spite of the fact that its C-terminal catalytic domain is very similar to that of Ppz1 (85.9% identity). Therefore, chimeric versions of Ppz1 and Ppz2 were recently created in our laboratory to study the actual structural determinants behind Ppz1 toxicity. Interestingly, the version containing the N-terminal of Ppz2 and the C-terminal of Ppz1 (Ppz2:1) had no negative effects on cell growth. However, a Ppz1:2 version (Ppz1 N-terminal and Ppz2 C-terminal) had a very similar effect to that of the native Ppz1 version, even though it was expressed at lower levels (Calafí *et al*, 2020a). Thus, the N-terminal unstructured region of Ppz1 is indeed a further determinant for its toxicity. Moreover, mutating Ppz1 Gly-2 to Ala, a change that renders Ppz1 cytosolic (see section 4) resulted in a less toxic version of the phosphatase, suggesting that Ppz1 substrates related with its toxicity are attached to the membrane (Calafí *et al*, 2020a).

4. MATERIALS AND METHODS

4.1. Yeast strains and media

Saccharomyces cerevisiae cells were grown at 28 °C in YP (1% yeast extract, 2% peptone and 2% dextrose) or synthetic medium with the appropriate drop-out mix of amino-acids for plasmid selection when needed. The synthetic medium is composed of 0.17% yeast nitrogen base (YNB) without ammonium sulfate nor amino acids, 0.5% ammonium sulfate, 2% glucose and 0.13% drop-out mix (Adams *et al*, 1998). To culture yeast cells carrying constructs under a *GAL1-10* promoter, glucose was replaced by 2% raffinose.

Translucent medium (Navarrete *et al*, 2010) at pH 5.8 supplemented with 50 mM KCl (with the appropriate drop-out mix) was used to wash and resuspend cells, prior to flow cytometry analysis. For growing yeast cells to be used in assays involving fluorescence detection, media were prepared sterilizing the corresponding carbon source separately in order to reduce background signal.

All yeast strains used in this work are listed in Table 1.

Table 1. Yeast strains used in this work

Strain	Genotype	Source of reference
BY4741	*MAT**a**, his3Δ1, leu2Δ0, met15Δ0, ura3Δ0*	(Brachmann *et al*, 1998)
ZCZ01	BY4741 *PPZ1* promoter::KanMX6-p*GAL*	(Calafí *et al*, 2020b)
ZCZ06	ZCZ01 *nha1::LEU2*	Chunyi Zhang, laboratory stock
DCS32	BY4741 *trk2::nat1 trk1::LEU2*	(Canadell *et al*, 2015)
CCP011	BY4741 *nha1::LEU2*	Carlos Calafí, laboratory stock
MAC001	ZCZ01 with *pIU-ADGEV* integrated	This work
MAC003	ZCZ01 *PPZ1-GFP:HIS3MX6*	This work
MLM04	BY4741 promoter *PPZ1*::tetO$_7$	(Calafí *et al*, 2020b)
DBY746	*MAT**α**, trp1, leu2-3, ura3*	David Botstein
DBY746 *vps27*	DBY746 *vps27*::KanMX4	Lina Barreto, laboratory stock

4.2. Recombinant DNA techniques

Escherichia coli DH5α cells were used as plasmid DNA host and were grown at 37 °C in LB medium (10 g/l tryptone, 5g/l yeast extract and 5g/l NaCl) supplemented with 100 µg/mL ampicillin for plasmid selection. DNA recombinant techniques such as restrictions and DNA ligations were performed using Fast Digest restrictions enzymes and the Fast T4 DNA Ligase from Thermo Fisher. Purification of DNA fragments from PCR products or restriction enzyme digestions

was done using the NucleoSpin Gel and PCR Clean-Up kit (Macherey-Nagel), after isolating the fragments by agarose gel electrophoresis.

To perform a point substitution in the *PPZ1* gene, a Quickchange site-directed mutagenesis method was used (Liu & Naismith, 2008). Two complementary primers that contained the change of interest were designed and used to amplify a whole plasmid. To this end the Q5 High-Fidelity DNA polymerase (New England Biolabs) was used to amplify the construct. The PCR product was purified with NucleoSpin Gel and PCR Clean-Up kit (Macherey-Nagel) and digested with a Fast Digest DpnI enzyme (Thermo Scientific). After the digestion, the product was used to transform *E. coli*.

E. coli and *S. cerevisiae* cells were transformed following the CaCl$_2$ (Sambrook *et al*, 1989) and lithium acetate method, respectively (Ito *et al*, 1983).

Strain MAC001 was constructed by transforming the ZCZ01 (*GAL1:PPZ1*) strain (Calafí *et al*, 2020b) with a cassette containing the "ADGEV" hybrid transcription factor (Takahashi & Pryciak, 2008) which allows induction of *GAL1-10* promoters by adding β-estradiol to the medium. Strain MAC003 (*GAL1:PPZ1-GFP*) was constructed by transforming strain ZCZ01 with the cassette GFP-HIS3MX6, following the methodology described in (Janke *et al*, 2004). Strain ZCZ06 was constructed by transforming strain ZCZ01 with a *NHA1::LEU*2 cassette obtained by SacI/XbaI enzymatic digestion from plasmid pcRII - *NHA1::LEU2*, a kind gift of Dr. Alonso Rodríguez-Navarro.

To ensure the correct insertion of cassettes, colony PCRs were performed by heating a small fraction of a colony resuspended in 20 µL of MiliQ water at 95 °C for 5 minutes. One µL was used as a template for the PCR reaction.

Plasmids

- YEp195 Hal3: *URA3*-marked episomal expression vector containing *HAL3* under its endogenous promoter (De Nadal *et al*, 1998).
- YEp181 Hal3: *LEU2*-marked episomal expression vector containing *HAL3* under its endogenous promoter cloned at EcoRI/HindIII sites.
- YEp195 Ppz1: *URA3*-marked episomal expression vector containing *PPZ1* under its own promoter (Clotet *et al*, 1999).
- YEp181 Hal3-GFP: *HAL3-GFP* was PCR-amplified from DVS004 (*HAL3-GFP*) genomic DNA using the oligonucleotides HAL3_Fw_-500_EcoRI and EGFP_mCherry_Rv_HindIII. It was subcloned in YEp181 by restriction with EcoRI and HindIII.

- YEp181 Hal3-mCherry: the *HAL3-mCherry* fragment was PCR-amplified from DVS008 (*HAL3-mCherry*) genomic DNA using the oligonucleotides HAL3_Fw_-500_EcoRI and GFP_mCherry_Rv_HindIII. It was subcloned in an empty YEp181 by restriction with EcoRI and HindIII.

- YEp195 Ppz1-GFP: the *PPZ1-GFP* fragment was PCR-amplified from strain DVS001 using the oligonucleotides PPZ1_Fw_-470_KpnI and EGFP_mCherry_Rv_HindIII and the fragment was subcloned (KpnI and HindIII) in YEp195.

- YEp195 Ppz1-mCherry: the *PPZ1-mCherry* fragment was PCR-amplified from strain DVS007 using the oligonucleotides PPZ1_Fw_-470_KpnI and EGFP_mCherry_Rv_HindIII. It was subcloned in YEp195 by restriction (KpnI and HindIII).

- YEp195 Ppz1-G2A-GFP: taking as template YEp195 Ppz1-GFP, a Quickchange PCR was performed with the oligonucleotides Ppz1 G2A_Fw and Ppz1 G2A_Rv to mutate the Gly-2 codon to an Ala-2 codon.

- YEp195 Ppz1-R451L-GFP: YEp195 Ppz1-GFP C-terminal was digested with PacI and Kpn2I and the fragment was replaced by the equivalent one from the pCM189 Ppz1 R451L construct (Carlos Calafí, laboratory stock).

- pWJ1344: pRS415-based vector (*LEU2*) containing Rad52-YFP under *RAD52* promoter (Alvaro *et al*, 2006).

- YEp195 MIG1-GFP: multicopy plasmid containing a GFP-tagged version of Mig1 (Velázquez *et al*, 2020).

- P4964: YCp50 (*URA3*) empty vector.

- P79: P4694 with *BAS1* under its own promoter (Pinson *et al*, 2000b).

- P1924: YCp50-based (*URA3*) carrying a fusion *BAS1-BAS2* (*PHO2*) under the control of *BAS1* endogenous promoter (Pinson *et al*, 2000b).

- pREG1-HA[1-443]: pWS93-based (*URA3*) multicopy plasmid that carries a 3xHA-fusion with the N-terminal region, residues 1-443, of Reg1 (Sanz *et al*, 2000).

- pRS316-SNF1-3HA: centromeric vector with *URA3* marker expressing a 3xHA-fusion with Snf1 (Pessina *et al*, 2010).

- pRS316-SNF1-T210A-3HA: centromeric *URA3*-marked vector expressing a 3xHA-fusion with a non-phosphorylatable version of Snf1 at Thr210 (Pessina *et al*, 2010).

- pRS316-SNF1-T210E-3HA: *URA3*-marked centromeric vector expressing a 3xHA-fusion with a phosphomimetic version of Snf1 at Thr210 (Pessina *et al*, 2010).

- pIU-ADGEV: vector that contains the hybrid transcription factor "GEV" (Gal4 DNA-binding domain, human estrogen receptor, VP16 activation domain) (Takahashi & Pryciak, 2008).

- pCM190-PPZ1: *URA3*-marked episomal expression vector containing the tetO$_7$-promoter where expression of *PPZ1* is repressed in the presence of doxycycline (Calafí *et al*, 2020b).

- pcRII - *NHA1::LEU2*: vector that contains the disruption cassette *nha1*::*LEU2*, obtained from Dr. Alonso Rodríguez-Navarro.

- pRS315 mCherry-HDEL: *LEU2*-marked centromeric plasmid containing the ER localization signal tagged with m-Cherry, obtained from Dr. Oriol Gallego.

The oligonucleotides used in this work can be found in Table 2.

Table 2. Oligonucleotides used in this work

Primer	Sequence
HAL3_Fw_-500_EcoRI	ATGAATTCATTATCCGTAGGATGACCTA
EGFP_mCherry_Rv_HindIII	ATAAGCTTCTGTTATCCCTAGCGGATCT
PPZ1_Fw_-470_KpnI	ATGGTACCAACTCAAGGAGAAGGGCA
Ppz1 G2A_Fw	CTTTCCTTCCTTTTCAAAATGGCTAATTCAAGTTCAAAATCTTCGAAA
Ppz1 G2A_Rv	TTTCGAAGATTTTGAACTTGAATTAGCCATTTTGAAAAGGAAGGAAAG

4.3. Yeast growth tests

Drop test in agar plates was used to evaluate the sensitivity of yeast strains and mutants to several stresses. Plates with synthetic medium supplemented with different concentrations of LiCl and caffeine were prepared as described in (Posas *et al*, 1995). Cultures were grown overnight in YPD until saturation. Then, they were diluted to OD$_{600}$ = 0.05 and two extra 5-fold dilutions were further prepared. Three µl of each dilution were deposited on the plate. Plates were incubated at 28 °C and cell growth was monitored for 3 to 6 days.

To study the toxicity of Ppz1 overexpression in the ZCZ01, ZCZ06 and MAC001 strains, cultures were processed as described above, but different plates were used. For the ZCZ01 strain, plates were prepared with YP (or selective media when needed) with 2% raffinose and increasing concentrations of galactose. In the case of strain MAC001, plates contained YPD supplemented with β-estradiol. In all cases, one plate without the expression inductor was prepared.

To study cell growth in liquid conditions, each culture was grown overnight to saturation. Dilutions were made to OD$_{600}$ = 0.004, unless otherwise indicated, in fresh medium and distributed by triplicate in honeycomb plates (Thermo Fisher). A Bioscreen C apparatus (Thermo Fisher) was used for monitoring cell growth at 28 °C by reading the OD$_{600}$ every 30 minutes for 2

to 3 days. Plates were shaken at the maximum amplitude setting for 7 minutes before each measure.

4.4. Fluorescence microscopy and flow cytometry techniques

4.4.1. ROS formation evaluation

Assessment of reactive oxygen species formation was performed by growing BY4741 and ZCZ01 cells on YP with 2% raffinose at 28 °C with shaking until $OD_{600} = 0.6$ was reached. After this, galactose was added to the medium so that its final concentration was 2% to induce *PPZ1* transcription. Dihydrorhodamine 123 (Sigma), a compound that becomes fluorescent upon oxidation, was added at the same time at a final concentration of 2.5 µg/ml. Samples of one ml of culture were taken after 2, 4 and 6 hours and fixed with formaldehyde (2%) for 5 min, washed twice and resuspended in Phosphate Saline Buffer (PBS). Cells were observed under an inverted fluorescence microscope (Nikon Eclipse TE2000-E) using a FITC filter. For the flow cytometry-based analysis, ten µl of each sample were diluted in one ml of PBS and were run through the FACSCanto (Benton & Dickinson) cytometer at the Servei de Cultius Cel·lulars i Anticossos (IBB facility).

4.4.2. Rad52 foci formation

BY4741 and ZCZ01 cells were transformed with the PJ1344 plasmid, which express Rad52-YFP under the *RAD52* promoter. Cultures were carried out on synthetic medium lacking leucine with 2% raffinose as carbon source. When $OD_{600} = 0.6$ was reached, galactose was added to a final concentration of 2%. Samples of one ml were taken at 0, 2, 4, 6 and 20 hours after induction and cells fixed as above before observation using a custom filter (excitation: 500 nm, emission: 535 nm) of the Nikon Eclipse TE2000-E microscope.

4.4.3. Determination of Mig1-GFP intracellular localization

BY4741 and MLM04 cells were transformed with the YEp195-Mig1-GFP plasmid. Transformants were grown overnight in synthetic media lacking uracil and supplemented with 100 µg/ml doxycycline to repress expression of the *PPZ1* gene. Cells were then washed twice and diluted until $OD_{600} = 0.08$ in the same media without doxycycline and growth was resumed for 24 hours. At this point, cultures were diluted again in fresh media to an $OD_{600} = 0.2$ and split in two aliquots that were resuspended in the same medium but containing either 2% or 0.05% of glucose. After 4.5 h of growth, cells were fixed by incubation with 2% formaldehyde and treated as above. Mig1-GFP cellular localization was determined as described above using the FITC filter of the Nikon Eclipse TE2000-E microscope.

4.4.4. *In vivo* fluorescent microscopy

Fluorescence microscopy observation of living cells was performed as follows. Cells were grown overnight to saturation in synthetic media, prepared as described in the Yeast Strains and Media section. At this point, cells were diluted to $OD_{600} = 0.2$ in fresh media and growth was resumed at 28 °C until $OD_{600} = 0.6$ was reached. Then, one ml dilutions at $OD_{600} = 0.12$ were prepared and 300 µl loaded to a well of a µ-Slide 8 Well (Ibidi), previously coated with 10 µL Concanavalin A (1 mg/mL) (Sigma-Aldrich). The µ-Slide 8 Well was incubated for 30 min at 28 °C to let cells settle to the bottom of the wells. Pictures were taken using a Nikon Eclipse TE2000-E microscope. The FITC filter of the apparatus was used to detect the GFP tags, whereas for the mCherry and DsRed tags, the TXRED filter was used.

For the MAC003 strain, the medium contained 2 % raffinose instead of glucose. When cells reached $OD_{600} = 0.6$, galactose was added to the culture at a final concentration of 2 %, to induce Ppz1-overexpression.

4.4.5. Vacuolar staining by FM4-64

DBY746 cells transformed with the plasmids of interest were grown until saturation in synthetic medium with the proper composition for plasmid selection and then diluted to $OD_{600} = 0.2$ in fresh media. Growth was resumed at 28 °C until $OD_{600} = 0.6$ was reached. At this point one ml aliquots of each culture were collected by centrifugation and resuspended in 100 µl of the same medium. Vacuole staining with FM4-64 was performed as described in (González *et al*, 2006) except that instead of YPD, synthetic medium was used. The incubation time with the FM4-64 was 30 min. Cells were then deposited in a µ-Slide 8 Well (Ibidi) as above and observed under the Nikon Eclipse TE2000-E inverted microscope or under a Leica TCS SP5 confocal microscope.

4.4.6. Ppz1-GFP quantification by Flow Cytometry

Starting from a saturated overnight culture, 10 mL fresh synthetic media lacking uracil and leucine were inoculated at $OD_{600} = 0.2$ and cells were grown at 28 °C with shaking until $OD_{600} = 0.8$ was achieved. After this, cells were collected by centrifugation in 10 mL tubes and washed twice with 1 ml of Translucent medium without uracil and leucine. Cells were finally resuspended in 500 µL of the same medium and kept at RT with shaking while the experiment was performed. Cytometry tubes were prepared by adding 1 mL of fresh Translucent medium + 10 µL of cells ($\approx$4 x 10^6 cells) and cultures were run immediately through the FACSCanto (Benton & Dickinson) cytometer at the Servei de Cultius Cel·lulars i Anticossos (IBB facility). For each measure 20000 events were counted at a medium flow rate. GFP was excited at 488 nm and its emission was

captured by coupling the GFP detector with a 502 longpass dichroic mirror and a 530/30 bandpass filter.

4.5. dNTP quantification

Sample preparation to evaluate dNTP levels of BY4741 and ZCZ01 strains was as follows. Cells were grown in YP with 2% raffinose at 28 °C with shaking until $OD_{600} = 0.6$ was reached. At this point, samples equivalent to five OD_{600} of cells ($\approx 10^8$ cells) were collected by filtration on GN-6 Metricel (47 mm, 0.45 μm, Gelman Sciences) membranes. Samples were then processed as described in (Chabes *et al*, 2003) and dNTP levels were determined by a polymerase-based method. These determinations were performed as described in (González-Vioque *et al*, 2011), in collaboration with the Neuromuscular and Mitochondrial Diseases Research Group from Vall d'Hebron Research Institute.

4.6. Protein immunodetection

4.6.1. Sample collection and extract preparation

Yeast protein extracts were prepared as follows. To detect the expression of Ppz1 and Hal3 expressed from YEp-based plasmids, cultures were grown overnight until saturation. Cells were diluted in 10 ml of fresh media at $OD_{600} = 0.2$ and growth was resumed until $OD_{600} = 0.8$. Cells were collected by centrifugation (5 min at 1,000xg), supernatants were discarded, and pellets were resuspended in 100 μL of Lysis Buffer (50 mM Tris-HCl pH 7.5, 150 mM NaCl, 10% Glycerol, 0.1% Triton X-100) supplemented with 1 mM fresh dithiothreitol (DTT) and EDTA-free Protease Inhibitor Cocktail (Roche). Cell lysis was performed by adding 125 μL of Zirconia 0.5 mm beads (BioSpec) and vigorously shaking the samples in a FastPrep (MP Biomedicals) at 5.5 m/s for 45 seconds (3 cycles, cooling the tubes on ice for two minutes between repeats). Then, 25 μL of Lysis Buffer were added to the samples and these were centrifuged for 10 minutes at 650xg at 4 °C. After this, supernatants were recovered and the total protein was quantified by the Bradford method (Sigma-Aldrich).

For monitoring Ppz1 levels in the MAC003 strain, cells were grown at 28°C in synthetic medium supplemented with raffinose (2%) until $OD_{600} = 0.6$. At this time, a non-induced sample of 10 mL was collected by centrifugation and then galactose was added up to 2% to the remaining culture. Samples at different time-points after Ppz1 induction were collected and cells were treated as above.

To detect Pma1 protein, the phosphorylated form of Snf1, total Snf1 protein, and the phospho-induced mobility shift of Reg1, cells were treated as it follows. BY4741 and ZCZ01 cultures were grown overnight in YPD until saturation and diluted in fresh YP-raffinose at $OD_{600} =$

0.2. Growth was resumed and when cultures reached OD_{600} = 0.6, galactose was added to the medium at 2% final concentration. The proper volume corresponding to 4.5 OD_{600} of cells (5 to 10 ml) was taken prior to the addition of galactose (t = 0), and subsequent aliquots were taken at the indicated times. Protein extracts were obtained by precipitating yeast proteins from the cultures with 6% trichloroacetic acid (TCA). For detecting the phosphorylated form of Snf1, total Snf1 protein, and the phospho-induced mobility shift of Reg1, samples were treated as described in (Orlova *et al*, 2008) and finally resuspended in 135 μL of 1x SDS-PAGE loading buffer (30 μL/1 OD_{600}). From this last resuspension, 10 μL were loaded in the gel. In the case of Pma1 detection, after the addition of TCA, cells were kept on ice for 15 minutes and then centrifuged. Two washes with cold water were performed and precipitated protein were stored at -80 °C. The same procedure was performed for 1-, 2- and 4-hours samples. Prior running the gel, protein samples were resuspended with 120 μL of 2x Laemmli buffer (preincubated at 37 °C). Five μL of each sample were loaded in the gel.

4.6.2. SDS-PAGE and immunoblotting

For culture aliquots that were not treated with TCA, protein extracts containing 40 μg of proteins were mixed with 4x SDS–PAGE loading buffer so that the final concentration was 1x. Samples were then heated at 95 °C for 5 minutes, except for those used to Pma1 immunodetection. Proteins resolved by SDS-PAGE at a concentration of 10% acrylamide/Bis-acrylamide (37.5:1 ratio), unless otherwise indicated. Proteins were transferred to a polyvinylidene difluoride (PVDF) membrane (Immobilon-P, Millipore) by semi-dry transference using a TE77XP apparatus (Hoefer).

Ppz1 was detected using anti-GST-Ppz1 antiserum (Posas *et al*, 1992), at a 1:250 dilution in TBST (Tris-buffered saline plus 0.1% Tween 20) supplemented with 5% fat-free powdered milk (Régilait). Hal3 was detected using anti-Hal3 antibody (Ferrando *et al*, 1995) at a 1:500 dilution as above. Phosphorylated Snf1 was evaluated with anti-phospho-Thr172-AMPK (Cell Signaling Technology) at 1:1,000 dilution in TBST supplemented with 5% BSA. Pma1 was detected using anti-Pma1 (a kind gift from R. Serrano) at a 1:5,000 dilution in TBST. Incubation with secondary antibody was done with a 1:20,000 dilution of anti-rabbit IgG-horseradish peroxidase antibodies (GE Healthcare) except for Pma1 where a 1:15,000 of the same secondary antibody was used.

Total Snf1 was determined using a 1:1,000 dilution of anti-polyHis (Merck, #H1029) antibodies. HA-tagged Reg-1 proteins were detected using anti-HA antibodies (Biolegend, #901502), at 1:1000 dilution. For these two cases, an incubation with 1:10,000 dilution of secondary anti-mouse IgG-horseradish peroxidase antibodies (GE Healthcare) was performed.

4.7. H$^+$ pumping evaluation

To analyze the H$^+$ pumping ability of BY4741, ZCZ01 and ZCZ06 cells, cultures were grown on YPD until saturation. Then, cultures were diluted at OD$_{600}$ = 0.2 with fresh YP plus 2% raffinose, and growth was resumed for 4 - 5 hours until cultures reached OD$_{600}$ = 0.6. At this point, an aliquot was taken (t=0), and the rest of the culture was made 2% galactose to induce *PPZ1* expression. Further samples were taken at 1, 2 and 4 hours after galactose addition, by centrifuging the proper volume to ensure that, once resuspended in 20 ml of YPD, OD$_{600}$ would be 0.6. Then, KOH was added to cell suspension so that its final concentration was 20 mM and the pH rose to ≈ 8.0. Culture pH was recorded each 10 seconds for approximately 30 minutes, using a Crison GLP21 pH-meter and the GLP21 data acquisition software. Acidification values were calculated from the slope (nM H$^+$/min) of the linear segment of the curve (usually starting at min 8 up to min 30). During the data collection there were no significant differences of cell growth between the strains tested.

5. OBJECTIVES

In the context of the study of the cellular alterations that undergo yeast cells upon an excess of Ppz1 enzymatic activity, the purpose of this work has been:

1. To get insight into biological processes uncovered by the transcriptomic and phosphoproteomic data obtained in our laboratory, as a way to understand the precise molecular basis of Ppz1 toxicity.

2. To investigate an unforeseen link between Ppz1 overexpression and cation homeostasis.

3. To examine Ppz1 subcellular localization in overexpressing conditions and how overexpression of Hal3 could affect the distribution of the phosphatase.

6. RESULTS

6.1. Overexpression of Ppz1 affects multiple cellular targets

Overexpression of Ppz1 is deleterious for yeast cells, and recent work from our laboratory demonstrated that this toxicity depends on its phosphatase activity, as overexpression of the catalytically inactive version Ppz1-R451L has little effect on cell growth (Calafí *et al*, 2020b). Phosphoproteomic and transcriptomic analyses of yeast cells overexpressing the native version of Ppz1 showed that a plethora of cellular targets did change their expression levels and/or phosphorylation state (Calafí *et al*, 2020b; Velázquez *et al*, 2020). Both phosphoproteomic and transcriptomic assays were performed using a BY4741-derivative strain in which *PPZ1* gene is placed under the control of a *GAL1-10* promoter. In this experimental setting, addition of galactose (to 2%) to cells grown in YP with 2% raffinose triggered a fast and strong increase in Ppz1 levels (Calafí *et al*, 2020b). This chapter compiles a set of experiments performed to test diverse hypotheses arising from transcriptomics and proteomics data, to get further insights into the molecular basis of Ppz1 toxicity.

6.1.1. Ppz1 overexpression causes ROS accumulation and Rad52 foci formation

Detoxification of reactive oxygen species (ROS) is crucial for yeast cells survival, and proper balance between ROS formation and their removal must be tightly maintained. As a response to oxidative stress, yeast cells up-regulate the expression of those genes related with the antioxidant defense (Farrugia & Balzan, 2012). Several of those genes are consistently up-regulated in the transcriptomic profile of cells overexpressing Ppz1 (Velázquez *et al*, 2020). To determine the presence of ROS under Ppz1-overexpressing conditions, cells from strains BY4741 and ZCZ01 were incubated, in the presence of 2% galactose, with dihydrorhodamine 123, a compound that becomes fluorescent when oxidized. We analyzed the fluorescent signal of the cells using fluorescent microscopy and flow cytometry approaches. As shown in Figure 7A, the fluorescence signal increased with time only in cells overexpressing Ppz1, pointing out that an excess of Ppz1 activity increased the presence of ROS in cells.

As it is well known, prolonged exposure to ROS leads to DNA damage. To test if Ppz1-overexpressing cells exhibited a DNA damage response we used BY4741 and ZCZ01 cells harboring a plasmid expressing Rad52, an endonuclease required to repair double-stranded breaks, tagged with YFP. Rad52 is recruited, among other proteins, to the sites where DNA needs to be repaired. As Rad52 accumulates in these DNA breaks, it appears as a very intense signal, known as focus. Rad52 foci were already detected after 4 hours of induction in Ppz1-overexpressing cells and their number greatly increased after 20 hours (Fig. 7B, left panel), when 35% of ZCZ01 cells were Rad52 foci positive, whereas only 10% of the wild-type were. The right

panel of Figure 7B shows a representative micrograph taken 20 hours after Ppz1 overexpression induction.
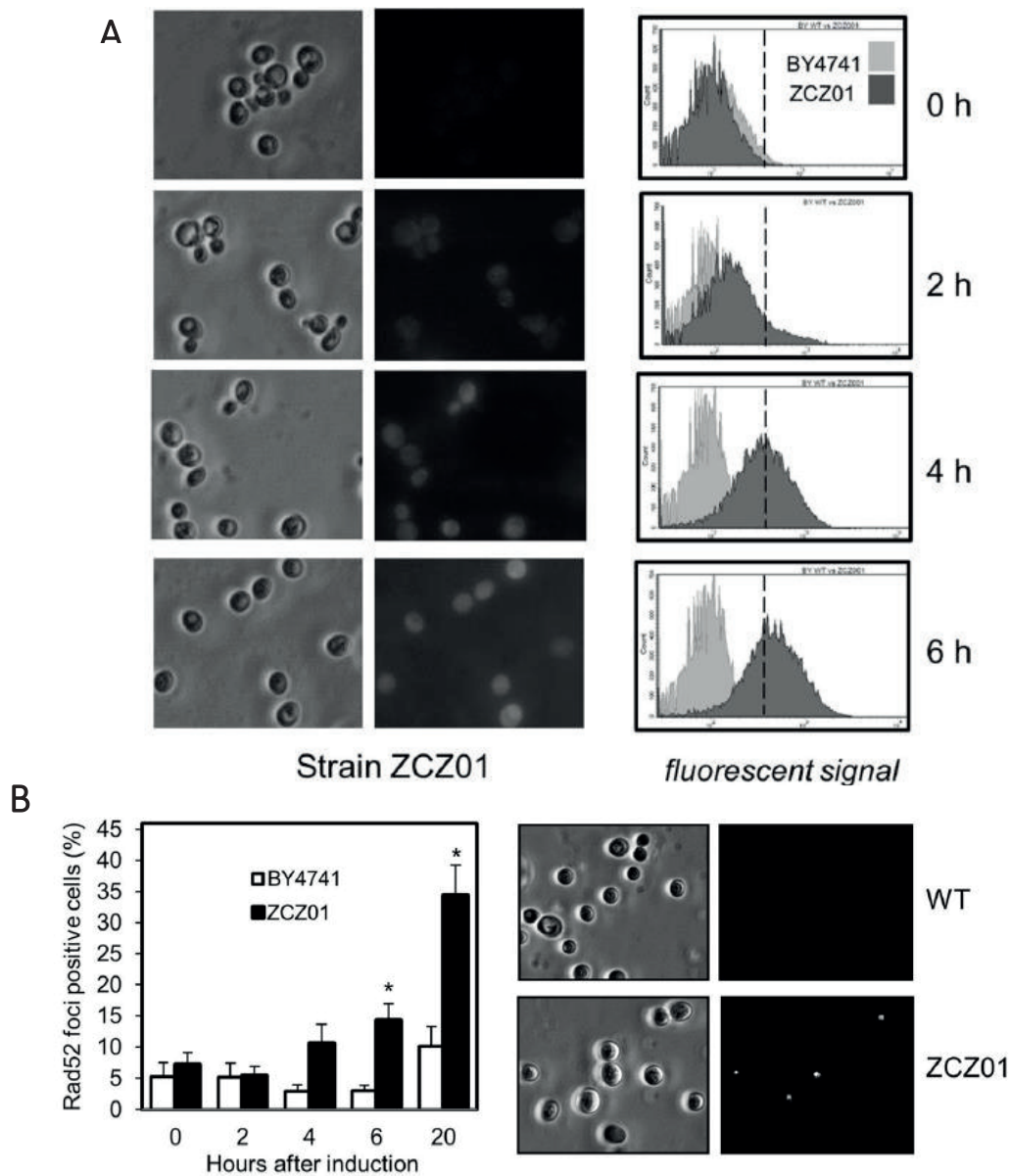
Figure 7. Overexpression of Ppz1 causes oxidative stress and DNA damage. A) BY4741 and ZCZ01 cells were growing on YP with 2% raffinose and galactose was added at 2% final concentration to induce Ppz1 expression. At the same time, cultures were loaded with dihydrorhodamine 123. At the given times, samples were taken and subjected to fluorescence microscopy (left panel) or analyzed by flow cytometry (right panel). Left panel does not show wild-type cells as they did not produce any fluorescence at any time tested. B) Wild-type and ZCZ01 cells were transformed with plasmid pWJ1344, a vector that contains an YFP-tagged version of Rad52 under the control of its own promoter. Cells were grown in synthetic medium lacking leucine, and galactose was added to induce Ppz1 expression at a 2% final concentration. Samples were taken at 0, 2, 4, 6 and 20 hours after induction. The percentage of cells positive for Rad52 foci was estimated. Data is presented as the mean ± SEM from four experiments. *$p < 0.05$, calculated by the Student's t-test. For time 20 hours a representative micrograph is shown.

6.1.2. Repression of the *ADE* pathway in Ppz1-overexpressing cells is not mediated by Bas1/Bas2

Transcriptomic results suggested that many genes involved in the *ADE* pathway were repressed after 2 and 4 hours of Ppz1 overexpression (Velázquez *et al*, 2020). We considered that such repression might lead to impaired purine biosynthesis, thus limiting DNA synthesis capacity and hence leading to arrest of cell growth. The expression of most genes in the ADE pathway is under the positive control of the Bas1 and Bas2 transcription factors, and previous studies had pointed out that oxidative stress leads to down-regulation of the *ADE* pathway by impairing the necessary Bas1/Bas2 interaction (Pinson *et al*, 2000a). In this study, Bertrand Daignan-Fornier's group also demonstrated how a Bas1-Bas2 fusion protein was able to restore *ADE* genes expression when cells suffer from oxidative stress. We considered that if Ppz1-overexpressing cells would have the *ADE* pathway repressed due to the loss of Bas1-Bas2 interaction under oxidative stress, ZCZ01 cells containing a plasmid with the Bas1-Bas2 fusion should improve growth under Ppz1-overexpressing conditions. To test this, ZCZ01 cells were transformed with the following plasmids: P4964 (YCp50 empty vector), P79 (YCp50-based with *BAS1* under its own promoter) and P1924 (YCp50-based with *BAS1-BAS2* fusion under *BAS1* endogenous promoter) (Pinson *et al*, 2000a). As shown in Figure 8, none of the tested vectors improved ZCZ01 cell growth under Ppz1-overexpressing conditions.
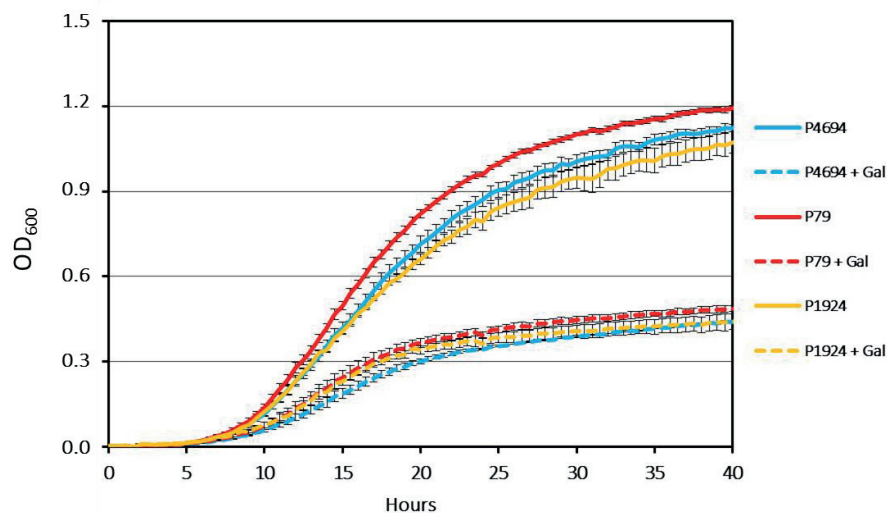
Figure 8. Expression of a constitutively active version of Bas1/Bas2 does not improve ZCZ01 growth. ZCZ01 cells were transformed with the following vectors: P4964 (empty vector), P79 (P4964 with *BAS1* under its own promoter) and P1924 (P4964 with *BAS1-BAS2* (*PHO2*) under the *BAS1* promoter). Media without galactose and media with 0.5% galactose (+ Gal) were used to dilute the cultures, which were processed as described in section 4.3. The mean ± SEM for four independent experiments is shown.

RESULTS

6.1.3. Cell cycle arrest of cells overexpressing Ppz1 is not caused by nucleotide shortage

      To further test our hypothesis, we decided to determine dNTP levels in BY4741 and ZCZ01 cells under Ppz1-overexpressing conditions. In collaboration with the Research Group on Neuromuscular and Mitochondrial Diseases from Vall d'Hebron Research Institute, we quantified the levels of each dNTP at 0, 2 and 4 hours of Ppz1 overexpression. As it can be seen in Figure 9, dNTP levels in ZCZ01 cells are actually higher than in the BY4741 wild-type strain. Therefore, cell cycle arrest caused by Ppz1 overexpression cannot be explained by scarcity of DNA biosynthetic precursors.
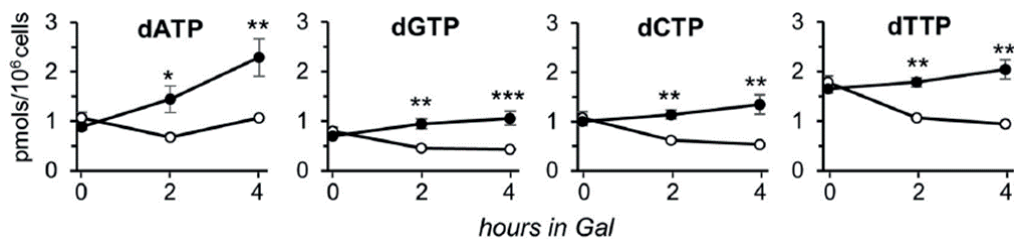
Figure 9. dNTP levels are not scarce in Ppz1-overexpressing cells. BY4741 (open circle) and ZCZ01 (filled circle) cells were grown on YP-Raff until they achieved an OD_{600} = 0.6. Then, 2% galactose was added and samples were taken at 0, 2 and 4 hours after the induction. Samples were processed as described in section 4.5. dNTP analysis was made in collaboration with the Research Group on Neuromuscular and Mitochondrial Diseases from Vall d'Hebron Research Institute as described in section 4.5. Data presented corresponds to the mean ± SEM from 3 to 5 independent experiments. *p<0.05; **p<0.01; ***p<0.001, calculated by the Student's t-test.

6.1.4. Ppz1 overexpression alters the normal cellular response to a low glucose-induced stress

      During the course of this thesis, and with the aim of getting a deeper knowledge about the alterations produced by the overexpression of *PPZ1*, an exploratory mRNA-Seq experiment was performed in low glucose conditions. The expression profiles of wild-type cells were analyzed in 2% glucose and 60 min after shifting to 0.25% glucose (low glucose conditions). Likewise, the profiles in the same conditions were determined in cells overexpressing the *PPZ1* gene (containing the pCM190-PPZ1 plasmid). In the case of wild-type cells, the shift to low glucose significantly induced the up-regulation (change log(2)≥ 1) of a set of 85 genes mostly involved, as expected, in carbohydrate metabolism (p-value: 1.02E-11). In cells overexpressing Ppz1, the shift to low glucose triggered the up-regulation of a higher number of genes (204). However, only 29 were in common with the genes upregulated in wild-type cells (Fig. 10A).

Figure 10. Effect of Ppz1 overexpression in the transcriptional response to low glucose. Yeast cells containing the empty pCM190 or the pCM190-PPZ1 plasmid, where *PPZ1* gene is down-regulated in the presence of doxycycli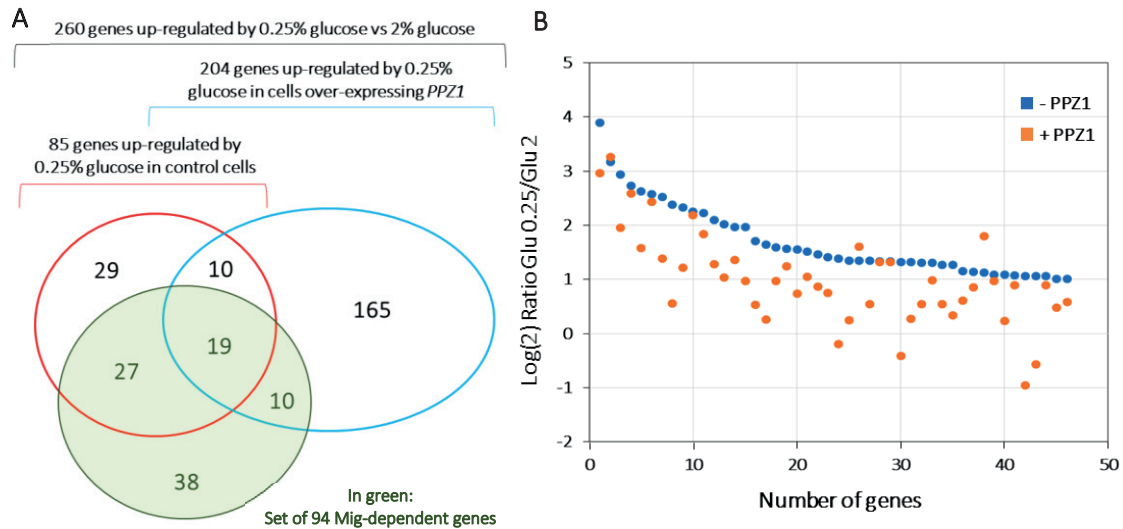ne, were incubated in the absence of the antibiotic for 3h, reaching a OD$_{600}$=0.55. At this point cells were washed and split in two cultures containing fresh YP-2% glucose or 0.25% glucose and cultured for 1 hour. Total RNA was prepared and the mRNA sequenced. **A**) Venn's Diagram showing the numbers for those genes found up-regulated in low glucose conditions in wild-type and Ppz1-overexpressing cells, plus the set of genes considered Mig-dependent. **B**) Expression changes (in log2) triggered by low-glucose in control (blue) and Ppz1-overexpressing cells (orange) for those 46 genes considered Mig-dependent that were up-regulated in control cells.

Since Mig1/Mig2 are transcription factors involved in the glucose-induced gene repression, we wondered if these genes found up-regulated by low glucose were under the control of Mig transcription factors. To this end, we considered the set of 94 genes previously found up-regulated in *mig* mutants (Westholm *et al*, 2008) as "Mig-dependent". From the 85 genes found up-regulated by low glucose in control cells, 46 genes (54.1%) were also found up-regulated in *mig* mutants, thus fitting as Mig-dependent genes. This set represents a 35-fold excess over the expected number assuming that low glucose conditions and Mig-dependence were independent events. Figure 10B shows a comparison of the transcriptional change of the 46 Mig-dependent genes up-regulated in the wild-type and that of the Ppz1-overexpressing cells. From this comparison it can be deduced that the expression level of many of these genes is substantially decreased in cells overexpressing Ppz1. Moreover, from the 204 genes found up-regulated in Ppz1-overexpressing cells, only 29 (14.2%) would fit in the Mig-dependent category, representing only a 9-fold excess over the expected number. Thus, the percentage of Mig-dependent genes induced in Ppz1-overexpressing cells upon shift to low glucose is 4 times lower than those found in the wild-type strain.

RESULTS

6.1.4.1. Ppz1 overexpression results in Snf1 dephosphorylation

A global phosphoproteomic analysis performed in the laboratory (Velázquez *et al*, 2020) suggested a fast dephosphorylation of Mig1 at Ser311 and 314, the physiological target residues for Snf1. This attracted our attention and encouraged us to study the phosphorylation state of Snf1 in control and Ppz1-overpressing cells. As shown in Figure 11 left panel addition of galactose rapidly increased the quantity of immunodetectable Ppz1 protein in ZCZ01 but not in wild-type cells. Phospho-Snf1 levels remained approximately constant in wild-type cells during the 4 hours of sampling. In contrast, when Ppz1 was over-expressed, the levels of phospho-Snf1 decreased progressively. A clear drop in phospho-Snf1/Snf1 ratio could be already observed after 1 hour of Ppz1 induction (Fig. 11, right panel). At this time point, even far from the peak in Ppz1 levels, the phospho-Snf1/Snf1 ratio is already reduced to 50%. Therefore, an excess of Ppz1 activity could be inactivating one of the major glucose sensor systems of yeast cells and thus might impede proper response to non-optimal carbon sources.
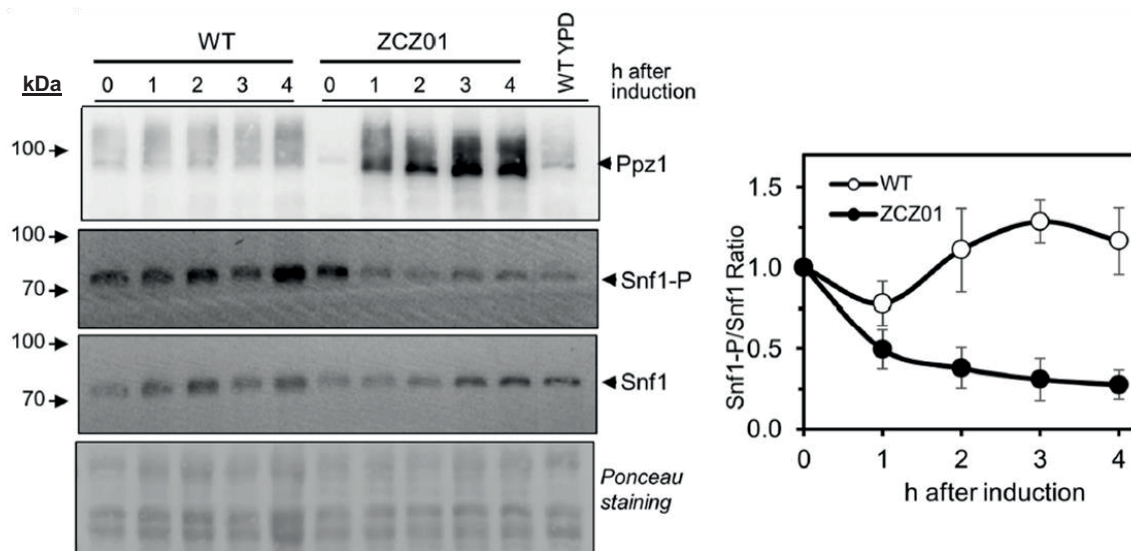
Figure 11. Ppz1 overexpression results in Snf1 dephosphorylation. The left panel shows a western blot assay for Ppz1, phosphorylated Snf1 (Snf1-P) and total Snf1 levels in BY4741 and ZCZ01 strains at the indicated times after the induction of Ppz1 expression. In the last lane a sample from BY4741 grown in glucose was loaded as a control for Snf1 dephosphorylation. Staining with Ponceau Red is shown as proof of proper sample loading and transfer efficiency. In the right panel the Snf1-P/Snf1 ratio was calculated from the integration of the signals of three independent experiments. The time = 0 values for the wild-type strain were defined as the unit and the mean ± SEM is represented.

6.1.4.2. Ppz1 overexpression induces Reg1 dephosphorylation

In glucose limiting conditions, Reg1 is phosphorylated in a Snf1-dependent manner, which promotes the release of Reg1-Glc7 from the kinase complex. When glucose is not scarce, Glc7 dephosphorylates Reg1, and Reg1-Glc7 is able to dephosphorylate Snf1 (Sanz *et al*, 2000). Our phosphoproteomic analysis revealed that Reg1 Ser346 and Ser349 were consistently

68

dephosphorylated in Ppz1-overexpressing cells (Velázquez *et al*, 2020). In addition, previous work from our laboratory proved that Ppz1 dephosphorylates *in vitro* a fragment of Reg1 comprising residues 1 to 443. All together suggests that Reg1 could be a target of Ppz1. In order to verify this hypothesis, we transformed BY4741 and ZCZ01 cells with a plasmid coding for a HA-tagged version of Reg1[1-443]. As shown in Figure 12, two forms of Reg1 can be detected in wild-type cells, the slow migrating one corresponding to the phosphorylated form of Reg1. When Ppz1 is overexpressed (ZCZ01 cells) a quick shift to the faster migrating specie was observed, indicating a decrease in the amounts of the phosphorylated form of Reg1[1-443]. As observed in Figure 12, after 4 hours of Ppz1 overexpression, the mobility pattern of Reg1[1-443] is identical to that of cells growing in the presence of glucose (rightmost lane).
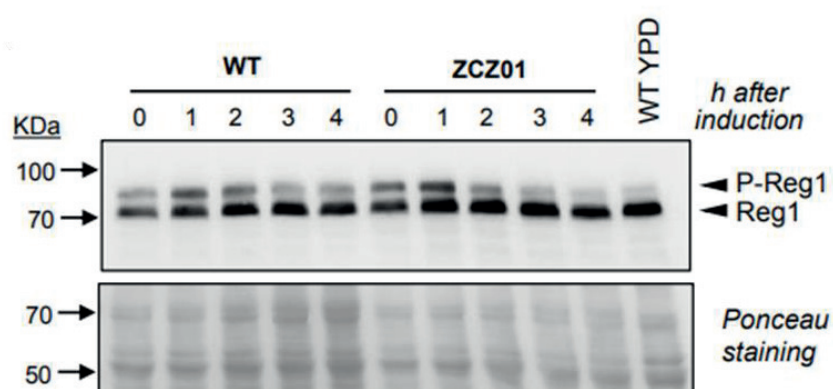
Figure 12. Overexpression of Ppz1 results in accumulation of the dephosphorylated form of Reg1. BY4741 and ZCZ01 strains were transformed with the plasmid pREG1-HA[1-443]. Transformants were grown in YP-Raff and galactose was added to induce Ppz1 overexpression. Samples were taken at different times and protein extraction and HA immunodetection were performed as described in section 4.6.

6.1.4.3. Mig1 is not properly evicted from the nucleus in low glucose conditions when Ppz1 is overexpressed

As described above, the transcription factor Mig1 is a target of Snf1 that needs to be dephosphorylated by the Glc7-Reg1 complex to be imported into the nucleus, where it exerts its transcriptional repression function (Schüller, 2003). In glucose limiting conditions Snf1 would be phosphorylated, thus active, and it would phosphorylate Mig1 at Ser311 and 314, evicting the transcription factor from the nucleus. We hypothesized that, in cells overexpressing Ppz1, Mig1 could not be properly translocated to the cytoplasm in low glucose conditions, since Snf1 should be less active in these cells.

As the *GAL1* promoter is strongly repressed by the presence of glucose in the medium, we decided to test the effect of Ppz1 overexpression on Mig1 localization in a galactose-free system. Wild-type (BY4741 strain) and MLM04 cells, in which the genomic *PPZ1* coding region is

controlled by the *tetO7* promoter (Calafí *et al*, 2020b), were transformed with the YEp195 multicopy vector coding for a Mig1-GFP fusion protein. With this galactose-free system, cells were grown with 2% glucose as described in section 4.4.3. At this point half of the culture was resuspended in a medium containing 0.05% glucose, while the other half was transferred to a fresh medium containing 2% glucose. As seen in Figure 13, the shift of wild-type cells (empty bars) to low glucose conditions resulted in a decrease of the nuclear localization of GFP-Mig1 (from about 20-25% to 5% of the cells). Under normal conditions (2% glucose), no significant differences in terms of localization of Mig1 were found when *PPZ1* was overexpressed (MLM04, full bars). However, when MLM04 cells were shifted to low glucose, there was no decrease in the percentage of cells having Mig1 localized in the nucleus, which was maintained around 30%. Therefore, we can conclude that overexpressing *PPZ1* does interfere with the normal removal of Mig1 from the nucleus under low glucose conditions, which could contribute to the defective transcriptomic response against a carbon stress situation.
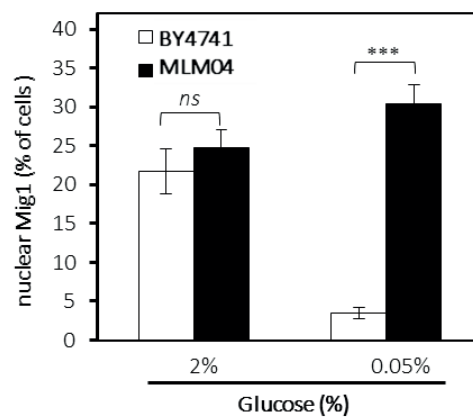
Figure 13. Mig1 remains in the nucleus in low glucose conditions in Ppz1-overexpressing cells. BY4741 and MLM04 strains were transformed with the YEp195 Mig1-GFP plasmid. Transformants were grown as described in section 4.4.3 and samples were fixed with formaldehyde (2%) for 5 min and then observed under a fluorescence microscope (Nikon Eclipse TE2000-E) using a FITC filter. Mean ± SEM from three independent experiments is shown in the graph (total cells counted 962 to 1174). ns, not significative (p>0.05); ***, p<0.0005.

6.1.4.4. Snf1 dephosphorylation is not at the base of the cell cycle arrest in Ppz1-overexpressing cells

It has been reported that yeast Snf1 must remain active to promote a normal G_1/S transition (Pessina *et al*, 2010). Since *PPZ1*-overexpresion causes a strong cell-cycle delay and in these cells Snf1 becomes dephosphorylated, we decided to test if this cell-cycle effect could be due to a deficient Snf1 activation. For this purpose, we transformed BY4741 and ZCZ01 cells with a centromeric pRS316 plasmid containing the native version of Snf1, a non-phosphorylatable Snf1 (Snf1-T210A) and a phospho-mimetic version of the kinase (Snf1-T210E). As the T210E version is

intrinsically active, if cell-cycle arrest of Ppz1-overexpressing cells were caused by lack of Snf1 activity, the Snf1-T210E version should improve cell growth. However, none of the tested versions of Snf1 affected growth of wild-type or ZCZ01 cells at different concentrations of the inductor (Fig. 14). Because the expression of a constitutively active Snf1 (Snf1-T210E) did not improve growth of ZCZ01 cells in Ppz1-overexpressing conditions, it can be concluded that the G_1/S cell-cycle delay observed in cells overexpressing *PPZ1* cannot be attributed to a deficient activation of Snf1.
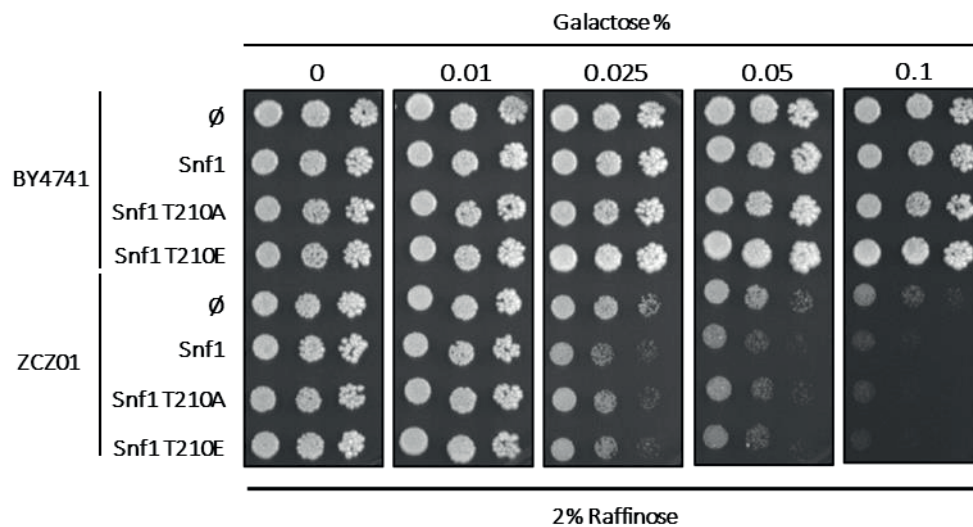
Figure 14. Hyperactive Snf1 versions do not improve ZCZ01 growth in Ppz1-overexpressing conditions. BY4741 and ZCZ01 cells were transformed with the following centromeric vectors: pRS316-SNF1-3HA (native Snf1), pRS316-SNF1-T210A-3HA (non phosphorylatable Snf1), pRS316-SNF1-T210E-3HA (phosphomimetic Snf1). Growth was tested in agar plates containing synthetic media lacking uracil supplemented with 2% raffinose and increasing concentrations of galactose. ∅, empty plasmid.

6.1.5. Generation of a new model to overexpresses Ppz1 in a β-estradiol-dependent manner (strain MAC001)

The use of a *GAL1-10*-based expression system involves cell growth in raffinose plus the addition of galactose to induce Ppz1 expression. We just presented evidence that high Ppz1 levels affect proteins that are important in carbon stress-related responses, and recent work from our laboratory has described that the presence of galactose worsens Ppz1 toxicity (Calafí *et al*, 2020b). We needed to rule out the possibility that the inability of Ppz1-overexpressing to adapt to a non-preferred carbon source cells could contribute to the growth blockage caused by Ppz1-overexpression using the *GAL1-10* system. Even though the MLM04 strain described above is a galactose-free system, it does not fully reproduce the strength and fast kinetics characteristics of the ZCZ01 strain. Because of this we decided to construct a yeast strain that provided a strong and fast expression of Ppz1 in a carbon source-independent manner. The MAC001 strain was

constructed by transforming ZCZ01 cells with the vector pIU-ADGEV (Takahashi & Pryciak, 2008). This vector contains the hybrid transcription factor "GEV" (Gal4 DNA-binding domain, human estrogen receptor, VP16 activation domain) and allows the regulation of the *GAL1-10* promoters by β-estradiol (Fig. 15A). We have monitored the quantity of Ppz1 in MAC001 cells growing in standard YPD medium (containing 2% glucose) after induction for 4h with different concentrations of β-estradiol ranging from 0.25 to 100 nM. As shown in Figure 15B, at 0.5-1 nM β-estradiol Ppz1 levels were similar to that of wild-type cells and from 5 nM upward, the levels were similar to those of ZCZ01 cells after 4 hours of induction with 2% galactose.

Figure 15. MAC001 strain provides fast and strong Ppz1 expression with glucose as carbon source. A) Since MAC001 cells contain the hybrid transcription factor "GEV" (Gal4 DNA-binding domain, human estrogen receptor and VP16 activation domain), gene expression from the *GAL1* promoter can be regulated by β-estradiol. B) Western blot assay showing Ppz1 levels in MAC001 cells after 4 hours of the addition of increasing concentrations of β-estradiol and ZCZ01 cells after 4 hours of induction with galactose (2% final concentration). Staining with Ponceau Red (bottom panel) is shown as proof of proper sample loading and transfer efficiency.

6.1.5.1. Over-expression of Ppz1 in MAC001 cells is also detrimental for cell growth in 2% glucose

We tested the ability of Ppz1-overexpressing MAC001 cells to grow in solid medium under different conditions. Since the MAC001 strain is a ZCZ01 derivative, and retains the control by galactose of *PPZ1* expression, we first tested growth in the presence of this inductor. As expected, growth of strain MAC001 in the presence of galactose was indistinguishable from that of ZCZ01 cells (Fig. 16A, upper panel). In addition, MAC001 cells grew very poorly in the presence of 5 nM β-estradiol, and they were unable to grow from 10 nM upward (Fig. 16A, lower panel). Wild-type and ZCZ01 cells growth were not negatively affected by the presence of β-estradiol, growing normally even at 100 nM (not shown). Liquid growth assays (Fig. 16B) show that 5 nM β-estradiol already causes an abrupt drop in the growth rate of MAC001 cells.
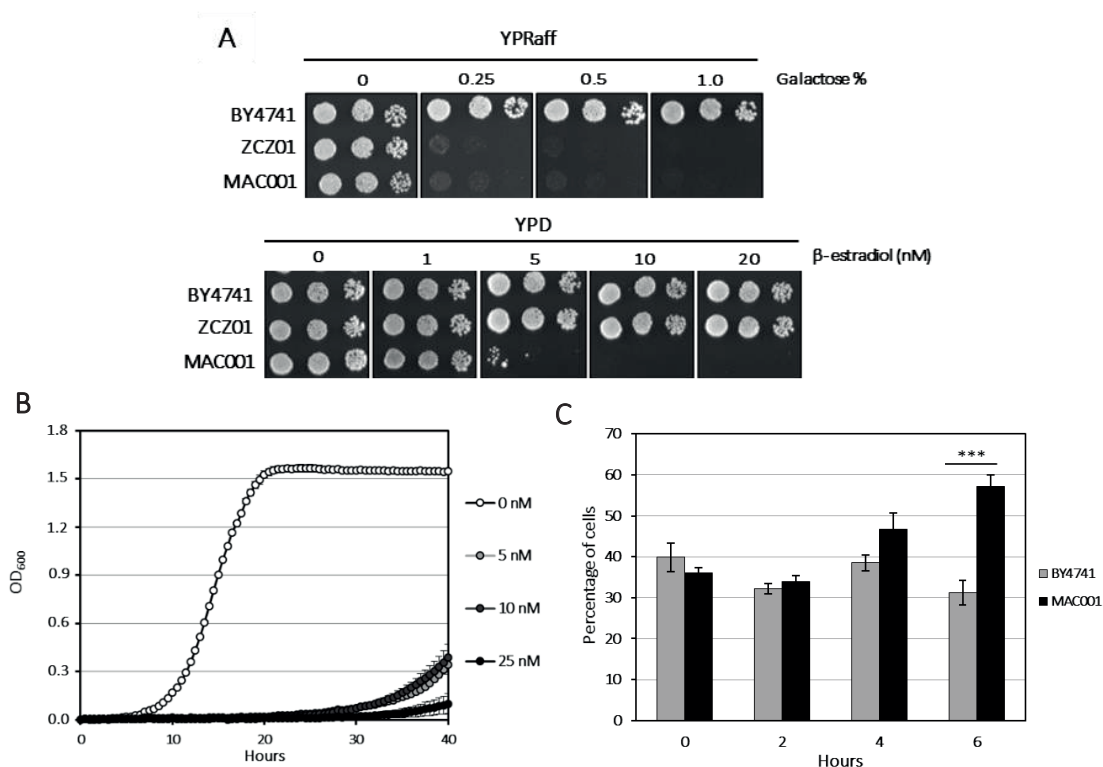

Figure 16. Overexpression of Ppz1 in the MAC001 strain leads to growth arrest and accumulation of unbudded cell. A) To study Ppz1 toxicity in MAC001 strain, BY4741, ZCZ01 and MAC001 were grown to saturation and diluted as described in section 4.3 to test their growth in Ppz1-overexpressing conditions. In the upper panel, YP-Raff with increasing galactose concentrations. In the lower panel, YPD with increasing concentrations of β-estradiol. Plates were incubated at 28 °C for 3 days. B) MAC001 cells were grown until saturation and dilutions in synthetic medium were prepared and cell growth monitored as described in section 4.3. The intensity of Ppz1 expression was modulated by supplementation of the medium with different concentrations of β-estradiol. C) The percentage of unbudded cells was determined as follows. BY4741 and MAC001 cells were grown in YPD up to $OD_{600} = 0.6$ and then 100 nM β-estradiol was added to the cultures. Samples were taken and at 0, 2, 4 and 6 hours. The percentage of unbudded cells for each strain at each time are represented as the mean ± SEMs from 4 to 6 independent experiments.

RESULTS

Ppz1 plays an important role in cell cycle, specifically in the G_1/S transition, since an excess of its phosphatase activity leads to a cell cycle arrest and an accumulation of cells in G_1 (Clotet *et al*, 1999).To this end, and as previously done in the *GAL1-10*-based system (Zhang, 2019), we wanted to verify if, in galactose-free conditions, overexpression of Ppz1 also caused an increase of unbudded cells. While BY4741 cells showed a 30-40% of unbudded cells during the whole time-course, a significant increase in the number of unbudded cells in Ppz1-overexpressing cells can be seen after 6 hours of the induction with 100 nM β-estradiol (Figure 16C). It seems reasonable that the increased percentage of unbudded cells could be responsible for the slow growth phenotype seen in the liquid growth assays from 5 nM upward, which confirms that Ppz1 overexpression is still detrimental for cells even when grown on YP plus 2% glucose.

6.2. The toxic effects of Ppz1 overexpression involve Nha1-mediated deregulation of K⁺ and H⁺ homeostasis

Ppz phosphatases are important determinants of salt tolerance. As described in the Introduction, Ppz1 regulates the influx of K⁺ by negatively regulating Trk1 and Trk2, the major potassium import system in *S. cerevisiae*, and the efflux of sodium by repressing the expression of the *ENA1* gene, coding for a Na⁺ pump. Therefore, it could be hypothesized that in a Ppz1-overexpressing situation, cells could be deprived of K⁺ cations due to a strong Trk1/2 inhibition.

6.2.1. The toxic effects of Ppz1 overexpression are rescued by the deletion of the *NHA1* antiporter gene, but not by potassium supplementation.

To test if potassium supplementation was enough to improve cell growth in Ppz1-overexpressing conditions we tested the ability of BY4741 and ZCZ01 (*PPZ1* gene under the *GAL1-10* promoter) cells to grow in plates with galactose and supplemented with increasing concentrations of KCl. As it can be seen in Figure 17A, ZCZ01 cells are not able to grow even when plates are supplemented with 100 mM KCl, while the double mutant *trk1 trk2* grows like the BY4741 strain at this same concentration of K⁺. This suggests that the growth defect induced by Ppz1 overexpression cannot be attributed to inhibition of the high-affinity K⁺ transport mediated by Trk1,2. Notably, during a screen in search of genes related to cation homeostasis that could influence growth of strain ZCZ01, we observed that deleting *NHA1* in the ZCZ01 background (strain ZCZ06) had a significant positive effect on cell growth (Figure 17A) and that this effect was still noticeable even when plates were supplemented with 2% galactose, which leads to very strong Ppz1 overexpression (Fig. 17B). As loss of toxicity could be explained by lower Ppz1 levels in the ZCZ06 background, we tested the amount of phosphatase by immunoblot analysis. As shown in Figure 17C, phosphatase levels are virtually identical in both ZCZ01 and ZCZ06 cells along the entire time-course. Therefore, the absence of Nha1 should be beneficial to Ppz1-overexpressing cells because it counteracts specific alterations of cellular processes induced by high levels of the phosphatase.
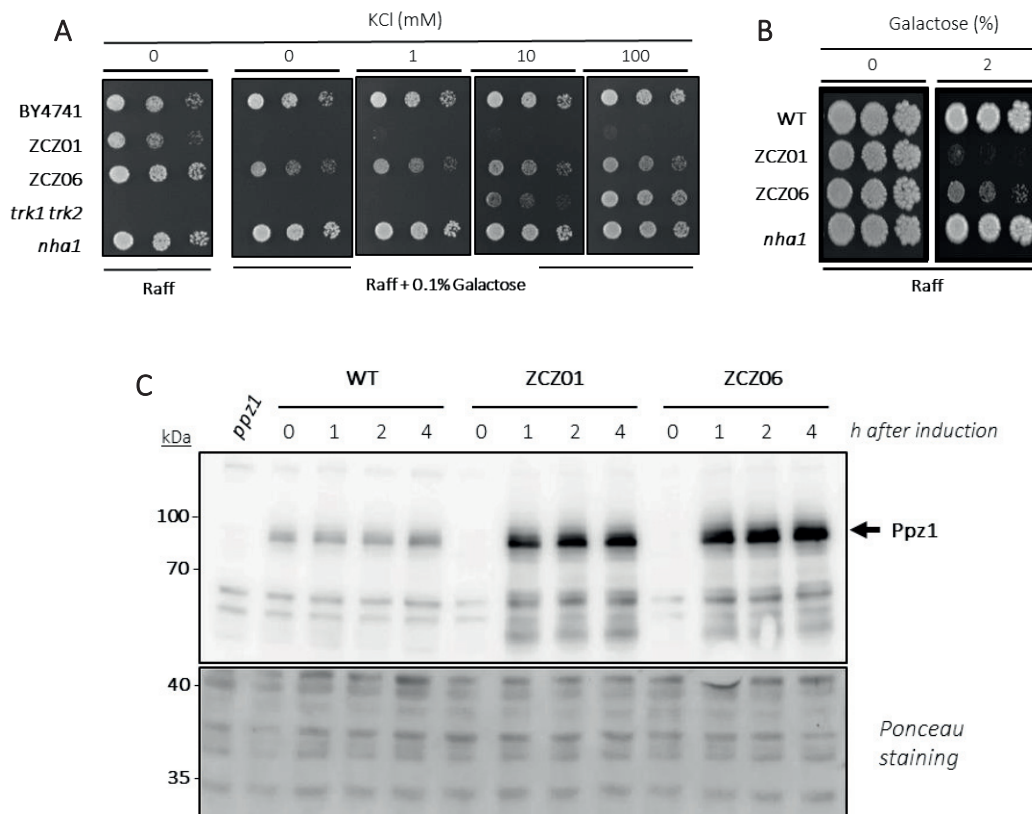
Figure 17. Deletion of NHA1 counteracts the toxicity derived from Ppz1 overexpression. A) Cells were spotted on K^+-free Translucent medium (Formedium™) including 2% raffinose (Raff) and 0.1% galactose (when indicated) and supplemented with various concentrations of KCl. Plates were incubated for 6 days at 28 °C. B) Cells were spotted as above in YP-Raff medium with or without 2% galactose. Growth was monitored after 6 days. C) Immunodetection of Ppz1 in strains BY4741 (WT), ZCZ01 (*GAL1:PPZ1*) and ZCZ06 (*GAL1:PPZ1*, *nha1*). Extracts from cells transferred to galactose-containing medium were prepared as indicated in section 4.6.2, subjected to SDS-PAGE (10% gels) and transferred to membranes. Ppz1 was detected with a polyclonal antibody. Membranes were subjected to Ponceau Red staining to monitor loading and transfer efficiency.

6.2.2. Nha1 attenuation of Ppz1 toxicity vanishes as pH approaches neutrality.

In collaboration with the Laboratory of Membrane Transport, Institute of Physiology of the Czech Academy of Sciences from Prague, intracellular K^+ and internal pH determination were performed for BY4741, ZCZ01 and ZCZ06 strains. Their result showed both intracellular pH and K^+ levels decreased dramatically in the ZCZ01 strain after 1 hour of Ppz1 induction. Deletion of *NHA1* (ZCZ06 strain) alleviated the rapid fall, albeit after three hours of Ppz1 induction pH and K^+ levels where closer to those of ZCZ01 than those of the wild-type strain. The drop in intracellular pH upon Ppz1 overexpression could be explained, at least in part, by a H^+ import process (likely coupled with K^+ efflux) mediated by Nha1. This would explain the attenuated intracellular acidification seen in ZCZ06, which lacks the *NHA1* gene. Such transport ought to be dependent of the H^+ gradient across the plasma membrane, and, consequently, the beneficial effect of the *nha1* mutation should weakens as the external concentration of H^+ decreased. To test this hypothesis,

we grew ZCZ01 and ZCZ06 in media buffered at different pH (from 5.5 to neutrality) under Ppz1-overexpressing conditions and determined the difference in growth between both strains. As documented in Figure 18, the progressive increase in external pH led to the parallel attenuation of the effect of the *nha1* mutation. This beneficial effect became virtually null when the external pH was 7.0.
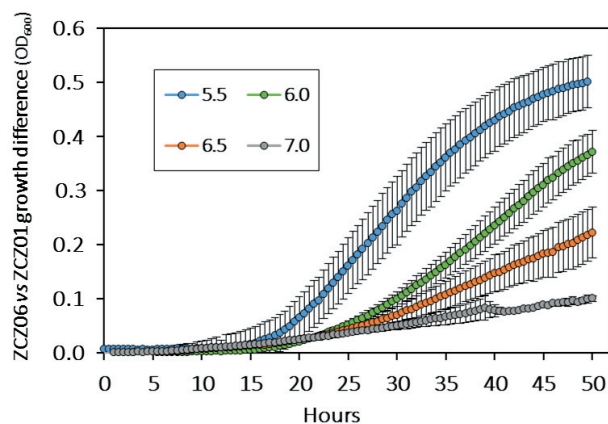

Figure 18. Effect of external pH on growth improvement caused by *NHA1* deletion. The growth rate of strains ZCZ01 and ZCZ06 was compared in liquid medium buffered at different pHs under conditions of Ppz1 overexpression (1% galactose), and the difference in growth (measured as OD_{600} values) calculated and plotted. Data are mean ± SEM from three independent experiments (with three technical triplicates each).

6.2.3. Overexpression of Ppz1 limits the capacity for acidification of the medium

To characterize further the basis for the observed intracellular acidification we tested the ability of wild-type, ZCZ01 and ZCZ06 strains to acidify the medium under standard growth conditions for Ppz1 overexpression. To this end, the pH of the culture was shifted to pH 8.0 and the rate of increase in H^+ concentration in the medium was followed for 30 min. We observed that at time zero, the acidification capacity of the wild-type and ZCZ01 strains were not significantly different (0.231 ± 0.030 vs 0.190 ± 0.025 nM H+/min). However, as seen in Figure 19A, the ability of strain ZCZ01 to acidify the medium was markedly lower than that of the wild-type strain, and the mutation of *NHA1* substantially normalized this behavior (the differences between strains ZCZ01 and ZCZ06 were significant at least at $p < 0.05$, except for t=1 h).

Because the H^+-ATPase Pma1 is a major contributor to the capacity of yeast cells to pump out protons, and overexpression of Ppz1 is known to induce a blockage in protein translation, we wondered whether the decrease in acidification capacity of the ZCZ01 strain could be due to lower-than-normal levels of the Pma1 protein, and if this could be affected by the *NHA1* deletion. To test this possibility, we prepared protein extracts from wild-type, ZCZ01 and ZCZ06 cells and monitored the presence of the Pma1 protein by immunoblot. As shown in Figure 19B, Pma1 levels are actually higher in ZCZ01 than in wild-type cells, and the amount of Pma1 in the ZCZ06 strain

does not differ from that of ZCZ01. Therefore, we must conclude that the acidification of the medium in ZCZ01 cells is not caused by a decrease in Pma1 protein levels.
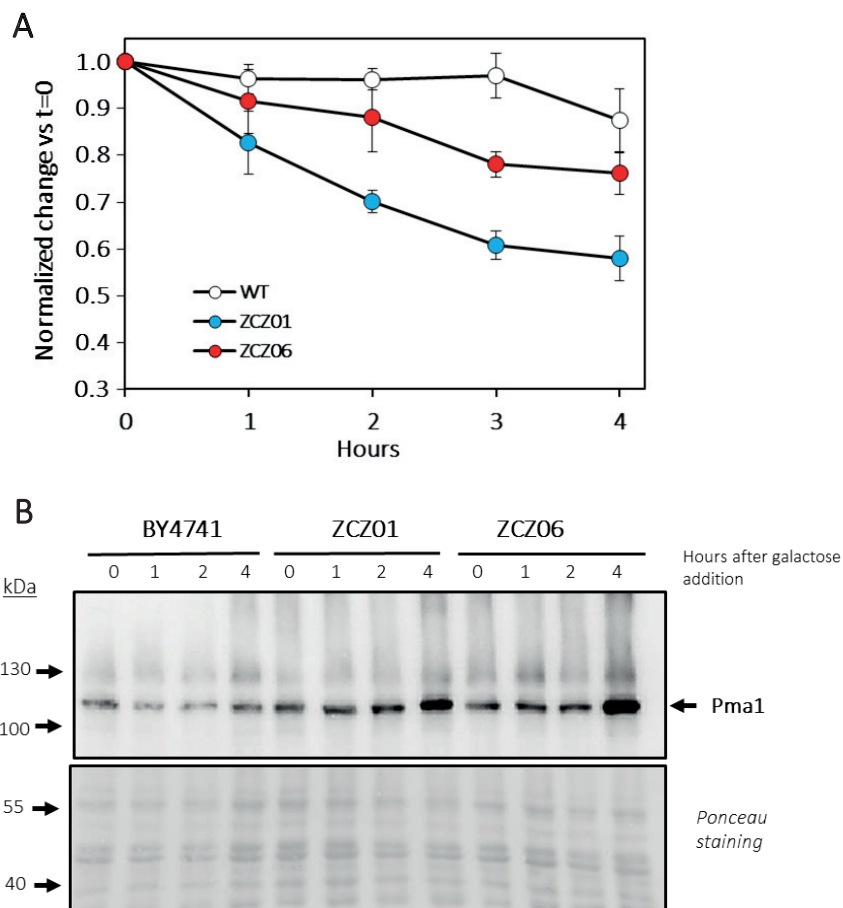
Figure 19. Overexpression of Ppz1 impairs the capacity for acidification of the medium. A) Cultures of the indicated strains were prepared as described in section 4.7 and made 2% galactose. Samples (20 ml, OD_{600}=0.6) were taken at the indicated times, pH raised to 8.0 by addition of KOH, and changes in pH were monitored for 30 min to calculate the acidification slope (nmols H^+/min). For plotting, data was adjusted to t=0 and represents the mean ± SEM from at least 5 independent experiments. *, $p< 0.05$; **, $p< 0.01$; ***, $p< 0.001$ with respect the BY4741 (WT) strain. B) Protein extracts from these strains were prepared at different times after Ppz1 induction, resolved by SDS-PAGE (8% gels), blotted and Pma1 detected with polyclonal antibodies. Ponceau staining of the membrane is shown at the bottom.

6.3. Analysis of the subcellular localization of Ppz1 and Hal3

As a first approach to study Ppz1 and Hal3 subcellular localization, a series of yeast strains containing fluorescent-tagged versions of the phosphatase were generated (Velázquez, 2019). However, chromosomic expression of Ppz1 under its endogenous promoter led to insufficient levels of protein, which complicated the analysis. Thus, we decided to amplify the tagged ORFs and clone them into YEp-based multicopy plasmids, as described in section 4.2.

6.3.1. Analysis of the subcellular localization of diverse full-length Ppz1 versions and Hal3

Previous evidence described that Ppz1 was mostly associated to the peripheral membrane while a fraction was also present in internal membranes (Venturi *et al*, 2000; Yenush *et al*, 2005), and that the ability to associate with membranes could be due to the myristoylable Gly at position 2 (Clotet *et al*, 1996). To get insights into the structural requirements for the localization of Ppz1 we included in this study two Ppz1 variants to examine how certain modifications could affect native Ppz1 localization. The first one was Ppz1-G2A, which has the myristoylable Gly-2 changed to Ala. A second variant included in this analysis was the inactive version of the phosphatase (Ppz1-R451L), so we could test if the lack of phosphatase activity alters the subcellular localization of the enzyme.

Strain DBY746 was transformed with plasmids carrying either native, G2A or R451L GFP-tagged versions of Ppz1. Cells were also transformed with an empty YEp181 vector, to allow growth in the synthetic medium lacking uracil and leucine. This was done to reproduce the growth conditions of the experiments including Hal3 described below. Transformants were prepared for *in vivo* fluorescent microscopy observation as described in section 4.4.4. As seen in panel A of Figure 20, the native version of the phosphatase mostly localizes at the peripheral membrane, although in can also be observed in some internal membranes, as previously described (Yenush *et al*, 2005; Venturi *et al*, 2000). The inactive version (Fig. 20B) shares the localization with the Ppz1-GFP version, but its presence in internal membranes is more accentuated. In contrast, when Gly-2 is changed to Ala, Ppz1 no longer localizes in peripheral or internal membranes but it becomes completely cytosolic (Fig. 20C).
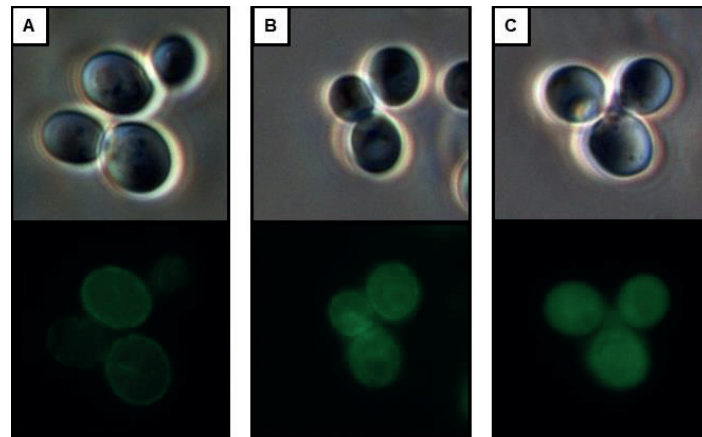
Figure 20. Both active and inactive Ppz1 localize mostly in peripheral membranes and the change Gly to Ala renders the phosphatase cytosolic. DBY746 cells carrying the following combinations of plasmids: **A**) empty vector + Ppz1-GFP, **B**) empty vector + Ppz1-R451L-GFP, and **C**) empty vector + Ppz1-G2A-GFP. Cultures were treated as described in section 4.4.4 and GFP signal was analyzed under a Nikon Eclipse TE2000-E inverted microscope using a FITC filter. Excitation was performed during 3000 ms.

It has been reported that overexpression of Hal3 from a multicopy plasmid eliminates the growth defect caused by an excess of Ppz1 (De Nadal *et al*, 1998). We decided to study if expressing *HAL3* from a multicopy plasmid could result in alterations on Ppz1 subcellular localization. Thus, DBY746 cells were co-transformed with the GFP-tagged Ppz1 versions and with the YEp181 Hal3 construct. As shown in Fig. 21A, when Hal3 is expressed from a multicopy plasmid, Ppz1-GFP is intensely detected in internal structures, while minimal amounts are found in the peripheral membrane. In contrast, the Ppz1-R451L version (Fig. 21B) does not modify substantially its localization, as it is detected in both peripheral and internal membranes. Lastly, the Ppz1-G2A version (Fig. 21C), which is still detected in the cytosol, displays an increase in signal intensity.

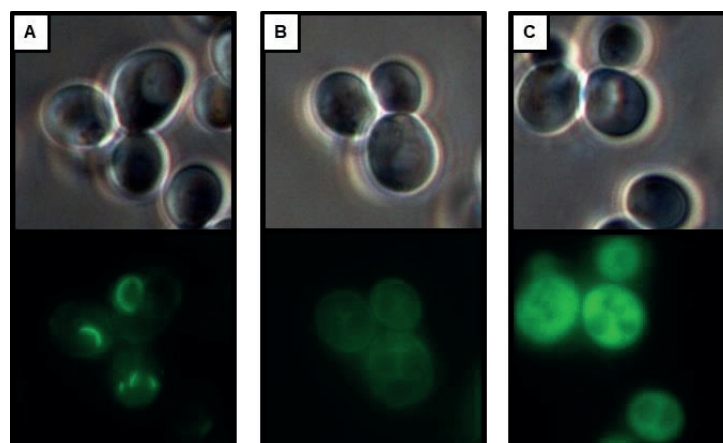Figure 21. Expression of Hal3 from a multicopy plasmid alters mainly the subcellular localization of the native version of Ppz1. DBY746 cells carrying the combinations of plasmids: Ppz1-GFP + Hal3 (A), R451L-GFP + Hal3 (B), G2A-GFP + Hal3 (C), Cultures were treated as described section 4.4.4 and the GFP signal was analyzed as in figure 20, although in this case excitation was performed during 1500 ms.

We know, from *in vitro* experiments, that Hal3 binds to the Ppz1 catalytic domain (De Nadal *et al*, 1998). The fact that the intracellular distribution of Ppz1 is altered when the cells carry a *HAL3* multicopy vector, prompted us to further investigate what was happening with Hal3 itself. To test if Hal3 could also localize in internal structures, DBY746 cells were transformed with two different combinations of plasmids, YEp195 plus YEp181 *HAL3-GFP* and YEp195 *PPZ1* (without tag) plus YEp181 *HAL3-GFP*. Analysis of the subcellular localization of Hal3-GFP in cells carrying the first combination of plasmids (Fig. 22A) shows that the signal is equally distributed around the cytosol of the cell. However, when Hal3-GFP is combined with YEp195 Ppz1, Hal3-GFP localizes in internal structures in addition to the cytosol (Fig. 22B).
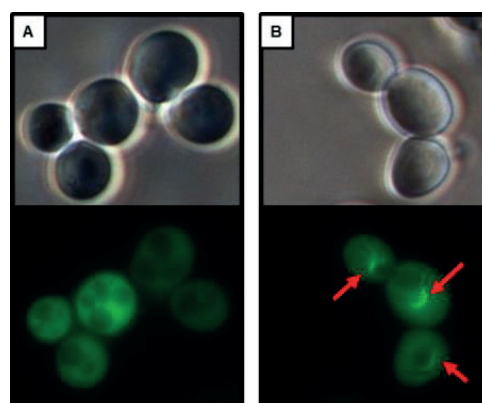
Figure 22. Hal3-GFP can be detected in internal structures when Ppz1 is expressed from a multicopy plasmid. DBY746 cells carrying the combinations: **A**) Hal3-GFP + empty vector, **B**) Hal3-GFP + Ppz1. In B, red arrows point the structures were Hal3-GFP is accumulating. Cultures were treated as described in section 4.4.4 and GFP signal was analyzed as above. Excitation was performed during 1000 ms.

Even though many efforts have been put in the study of the interaction of Ppz1 and Hal3 *in vitro*, very little is known about how it could take place *in vivo*. As of today, there is no evidence about what could trigger the need of inhibiting Ppz1 activity and/or how Hal3 is recruited to inhibit the phosphatase. To test if Ppz1 and Hal3 can colocalize when both are expressed from multicopy plasmids, we co-transformed DBY746 with two different combinations of vectors: a) YEp195 Ppz1-GFP plus YEp181 Hal3-mCherry, and b) YEp195 Ppz1-mCherry plus YEp181 Hal3-EGFP. As it can be seen in both Figure 23 (A and B) we can detect Hal3 in most of the internal membranes where we can detect Ppz1.

Figure 23. Ppz1 and Hal3 colocalize in internal structures *in vivo.* DBY746 cells carrying the combination of plasmids: (**A**) Ppz1-GFP + Hal3-mCherry and (**B**) Ppz1-mCherry + Hal3-GFP. Cultures were treated as described in section 4.4.4. GFP and mCherry signal were analyzed using a FITC and a TXRED filter, respectively. Excitation was performed during 1500 ms for GFP and 2000 ms for mCherry.
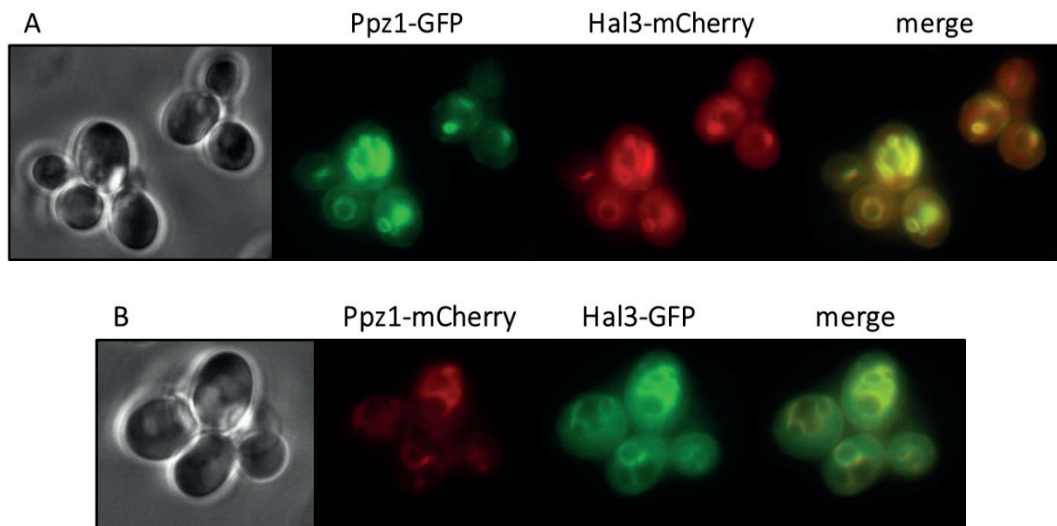
6.3.2. Studying the relationship between Ppz1 toxicity and subcellular localization

Our previous analysis of Ppz1 and Hal3 localization was carried out using multicopy vectors (YEp195/YEp181), which result in a mild to moderate overexpression of Ppz1. Cells carrying a multicopy vector containing *PPZ1* under its endogenous promoter will grow slower than those carrying an empty vector, but they will proliferate. However, expressing the phosphatase from a *GAL1-10* promoter results in a deleterious phenotype. So, to analyze the relationship between Ppz1 toxicity and subcellular localization we decided to generate a new ZCZ01-based strain, expressing Ppz1 with a GFP tag in its C-terminus from the *GAL1-10* promoter (strain MAC003). In this way, we could monitor Ppz1 localization in the same conditions that those used to obtain the transcriptomic and phosphoproteomic data.

6.3.2.1. The GFP-tagged version of Ppz1 maintain its high toxicity when expressed from the *GAL1* promoter.

To test if the GFP tag could have some attenuating effect on Ppz1 toxicity, strains BY4741, ZCZ01 and MAC003 were transformed with an empty vector and a multicopy vector carrying *HAL3*. Cultures were grown overnight until saturation and processed as described in section 4.3 for both drop test and liquid growth. As shown in Figure 24, cells expressing the GFP-tagged version of the phosphatase show the same behavior than those expressing the native Ppz1, both in drop test and liquid growth (A and B, respectively). Thus, the presence of the C-terminal tag does not alter Ppz1 toxicity. Moreover, the fact that expression of Hal3 recovers growth of the MAC003 strain in the same fashion that it does for the ZCZ01 background, points out that the GFP tag is not disturbing Ppz1-Hal3 interaction.
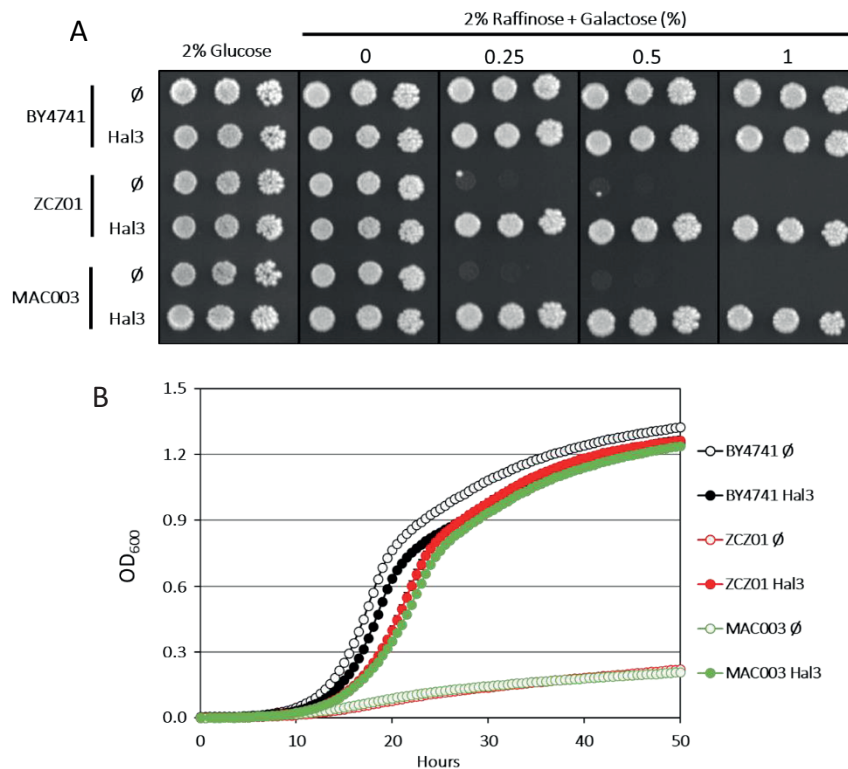
Figure 24. The MAC003 strain behaves like a ZCZ01 strain in Ppz1-overexpressing conditions. To perform these growth tests BY4741, ZCZ01 and MAC003 cells were transformed with a YEp195 empty vector (Ø) or with YEp195 Hal3. **A**) Transformants were grown until saturation and then the cultures were diluted as described in section 4.3 to perform a drop test in agar plates with increasing concentrations of galactose. **B**) From the same saturated cultures, a liquid growth test was prepared in synthetic medium lacking uracil plus 0.25% galactose as described in section 4.3. The mean ± SEM for 2 to 3 independent cultures is shown.

6.3.2.2. Ppz1 is anchored in the peripheral membrane and accumulates in very localized spots in the MAC003 strain

Because strain MAC003 shows a toxic phenotype similar to that from ZCZ01, we wanted to know the distribution of Ppz1 in this strong overexpression system. To test this, exponential cultures were grown overnight in synthetic medium with 2% raffinose, then galactose was added to the medium at 2% final concentration. Images were taken at the indicated times after the induction. As it can be seen in Figure 25 (upper panel), Ppz1 is distributed around the peripheral membrane of the cell, where some intense foci can be observed. The number and intensity of these foci increases with time, being clearly observable from 6 hours onward. Thus, as observed when the phosphatase was expressed from its own promoter from a multicopy plasmid, Ppz1 is mostly localized in the peripheral membrane with a discontinuous, punctate pattern.

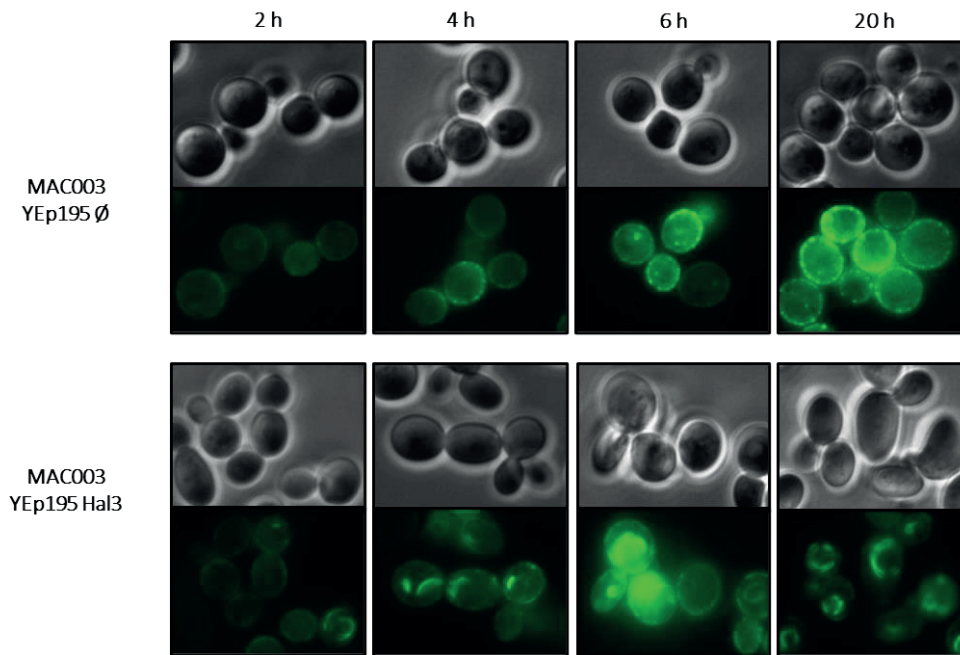**Figure 25. Time-course of Ppz1-GFP localization in the MAC003 strain.** MAC003 cells transformed with a YEp195 empty plasmid (upper panel) and with YEp195 Hal3 (lower panel) were grown until saturation. Cultures were prepared for observation as described in section 4.4.4. Exposition was performed during 3000 ms and 1500 ms for the upper and lower panel images, respectively. For each given time, a representative micrography is shown.

6.3.2.3. Hal3 restores cell growth by altering Ppz1 subcellular distribution in the MAC003 strain

The presence of Ppz1 in internal membranes when Ppz1 and Hal3 are expressed from a multicopy plasmid prompted us to study if this behavior could be also observed when Ppz1 is expressed from the strong *GAL1-10* promoter, which produces Ppz1 levels that actually block cell growth. To this end, the MAC003 strain was transformed with a YEp195 *HAL3* vector and we observed these cells under the fluorescence microscope. Already 2 hours after inducing Ppz1 overexpression, the presence of the phosphatase in some internal structures can be detected (Fig. 25, lower panel). The number of cells showing these structures increase with time, being detectable in almost all cells after 20 hours in galactose. Therefore, when Ppz1 is expressed at toxic levels, the presence of Hal3 also results in a dramatic relocalization of the phosphatase, which appears mostly at internal membranes. Therefore, Hal3 does not only negatively regulate Ppz1 by inhibiting its phosphatase activity, as it was previously described (De Nadal *et al*, 1998), but it also disrupts the normal localization of the phosphatase. This might prevent Ppz1 from interacting with certain substrates on the peripheral membrane. Because the expression of Hal3 normalizes growth of MAC003 cells, it could be postulated that this beneficial effect could be derived, at least in part, from the removal of Ppz1 from the peripheral membranes thus avoiding the action of the phosphatase on targets relevant for Ppz1 toxicity.

6.3.2.4. Ppz1 localizes mainly in vacuolar membranes when cells overexpress Hal3

The possibility that Hal3 could alleviate Ppz1 toxicity by retaining the phosphatase in internal locations prompted us to study which were these internal structures. The shape of the internal membranes seen above, either with the multicopy plasmids or with the MAC003 strain transformed with multicopy Hal3 vector, was reminiscent of vacuolar membranes and prompted us to verify it this was the case. To test our hypothesis, DBY746 cells were transformed with YEp195 Ppz1-GFP and YEp181 Hal3. Cultures were grown in synthetic medium lacking uracil and leucine until saturation and then diluted in fresh media. The fluorescent dye FM4-64, which is widely used to visualize vacuolar membranes, was added to the cultures as described in section 4.4.5. Cells were deposited into a μ-Slide 8 Well (Ibidi) and monitored using a Leica TCS SP5 confocal microscope. As it can be seen in Figure 26 (A and B), Ppz1 colocalizes with the fluorescent dye when Hal3 is expressed at the same time from a multicopy plasmid, thus confirmed the presence of the phosphatase in vacuolar membranes.

Careful observation of the images obtained revealed that, in some cases, the shape of the compartments where Ppz1 could be detected was hard to reconcile with vacuolar membranes. To get further insight, we cotransformed MAC003 cells with YEp195 Hal3 and a pRS315 mCherry-HDEL vector, expressing the DsRed fluorescent protein attached to a signal for retention at the endoplasmic reticulum. This experiment revealed that in a few cases Ppz1 did localize with the ER and/or perinuclear membrane (Figure 26C).
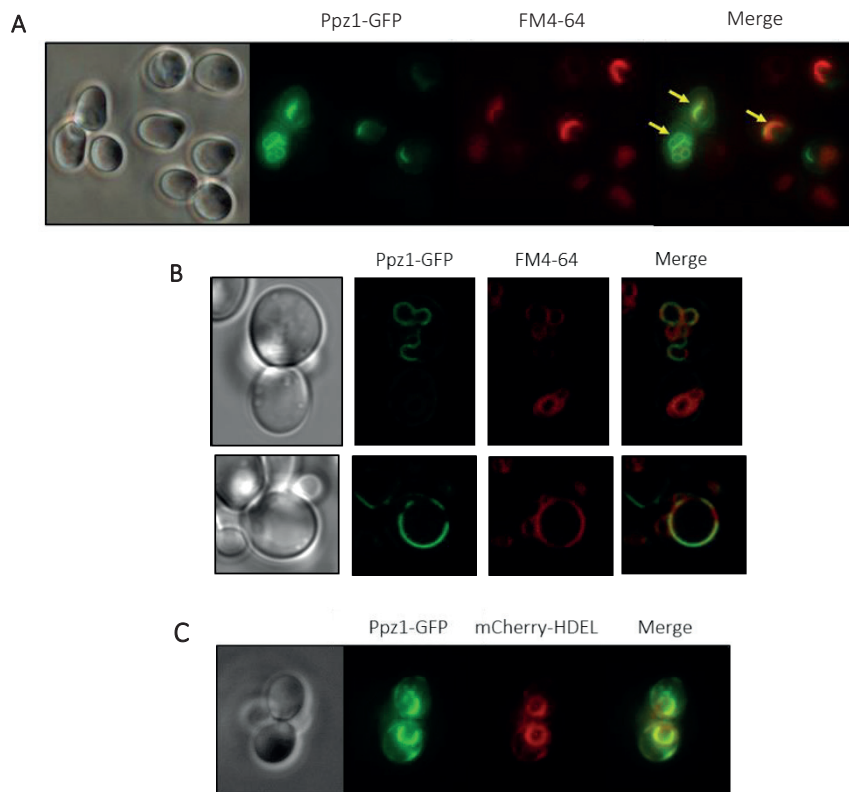
Figure 26. Ppz1 localizes in vacuolar membranes when cells carry a Hal3 multicopy plasmid and in fewer cases in the ER. DBY746 cells carrying the plasmids YEp195 Ppz1-GFP and YEp181 Hal3 were treated with FM4-64 as described in section 4.4.5. Cell were then monitored in **A**) Nikon Eclipse TE2000-E inverted microscope and **B**) confocal microscope (Leica TCS SP5). In **C**) MAC003 cells transformed with YEp195 Hal3 and pRS315 mCherry-HDEL were monitored after 2 hours of galactose addition under the Nikon Eclipse TE2000-E inverted microscope.

6.3.2.5. Mutation of the *VPS27* gene alters Ppz1 distribution inside cells overexpressing Ppz1 and Hal3

Degradation of cell surface proteins depends on the function of the multivesicular body sorting (MVB) pathway (Katzmann *et al*, 2003). The endosomal sorting complexes required for transport (ESCRT) are responsible for the formation of the MVBs. In yeast cells, a complex formed by Vps27 and Hse1 (ESCRT-0) directly binds to transmembrane proteins that have been ubiquitinated and recruits the ESCRT-I complex to the endosomes (Morvan *et al*, 2012). The Vps27 subunit of ESCRT-0 is a key player in this process, as it contains two ubiquitin-interacting motifs (Swanson, 2003) and it is the subunit that actually signals the activation of the MVB sorting (Katzmann *et al*, 2003). Moreover, a *vps27* mutant shows a defect in vacuolar protein sorting (Robinson *et al*, 1988). To test if this mutation could have any effect on Ppz1 subcellular localization, we co-transformed DBY746 wild-type and *vps27* cells with YEp195 Ppz1-GFP plus either YEp181 or YEp181 Hal3. The first difference that can be observed between the two genetic backgrounds is that in the wild-type, as previously observed, not all cells show detectable levels of Ppz1-GFP when combined with the empty vector (Fig. 27A, upper panel), while in the *vps27* strain all cells are detected in the GFP channel (Fig. 27A, lower panel). The second major

difference appears when YEp195 Ppz1-GFP is co-expressed with YEp181 Hal3. While in the wild-type background we see the characteristic internal structures, shown above, (Fig. 27B, upper panel), in the *vps27* background there are almost no cells with Ppz1 localized in internal membranes (Fig. 27, lower panel). It must be noted that in this background Hal3-GFP localizes in the cytosol of cells, either when cells carry an empty vector or a multicopy plasmid containing *PPZ1*, (Figure 27C and 27D).
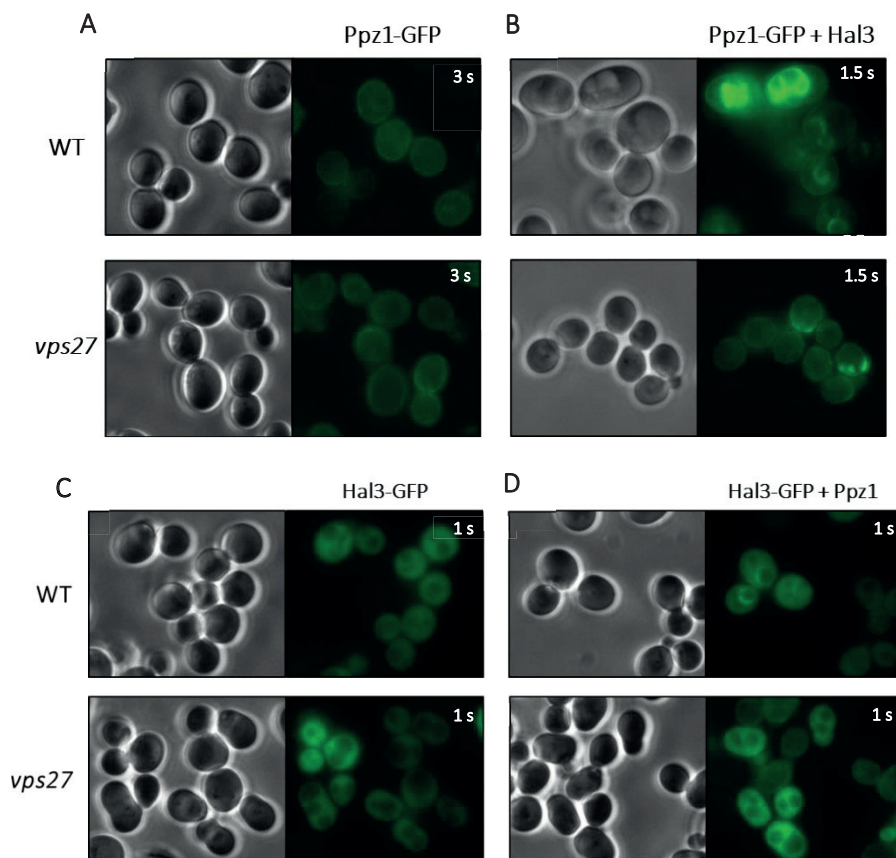
Figure 27. Ppz1 distribution is altered in the *vps27* background. DBY746 (WT) and *vps27* cells carrying the combination **A**) Ppz1-GFP + empty vector, **B**) Ppz1-GFP + Hal3, **C**) empty vector + Hal3-GFP, and **D**) Ppz1 + Hal3-GFP were grown until saturation in the appropriate selective medium. Then a dilution in fresh medium at OD_{600} = 0.2 was prepared. After resuming growth for 4 hours, cells were monitored under a Nikon Eclipse TE2000-E as described in section 4.4.4. For each image the time of exposure is shown.

To confirm this result, we analyzed by flow cytometry cultures carrying each combination of plasmids in both backgrounds. As seen in Figure 28A, the percentage of Ppz1-GFP-positive cells is higher for the *vps27* background expressing only Ppz1-GFP, which agrees with the higher number of cells showing detectable levels of Ppz1-GFP under the microscope. However, when comparing the average GFP intensities of both backgrounds, they are virtually identical (Fig. 28B), which points out that both strains have similar levels of the phosphatase. In fact, in Figure 29C, an immunodetection of Ppz1 (upper panel) shows that protein levels of the phosphatase are indeed very similar in both backgrounds.

RESULTS

As seen in Figure 28A, wild-type and *vps27* cells transformed also with the multicopy Hal3 vector show no significant differences in the percentage of Ppz1-GFP-positive cells. However, when comparing the average intensity values of these cells (Fig. 28B), the wild-type strain doubles the values of the *vps27* mutant. This result could suggest that the wild-type strain presented higher expression levels of the phosphatase than the *vps27* background. However, as it can be seen in Figure 28C, immunodetection of Ppz1 indicates that the expression of Ppz1 (upper panel) barely differs between both backgrounds. The disagreement between the flow-cytometry assay and the western blot analysis are likely due to the difference in the detection principle. The levels of Hal3 protein (lower panel) are indeed very similar between both strains. Therefore, the possible differences in Ppz1 levels between the wild-type and *vps27* backgrounds, if any, could not be attributed to different Hal3 expression levels.
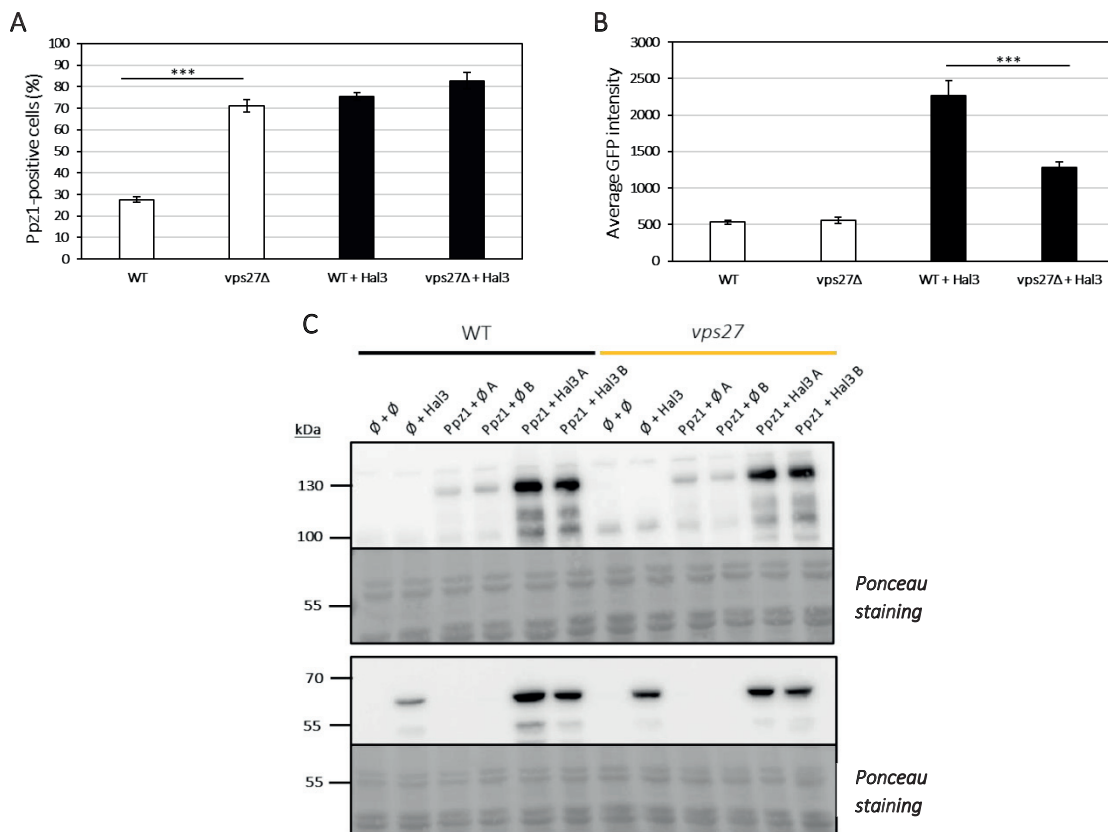
Figure 28. Flow-cytometry and western blot of wild-type and *vps27* backgrounds expressing Ppz1-GFP. DBY746 (WT) and DBY746 *vps27* strains were transformed with Ppz1-GFP plus either an empty (empty bars) or a Hal3 (filled bars) multicopy vector and cultures. The percentage of Ppz1-GFP-positive cell (**A**) and GFP intensity levels (**B**) is shown for each background and combination of plasmids. Six to eleven biological replicates were performed and mean values with SEMs are represented. (***, p< 0.001). **C**) An immunodetection for Ppz1 and Hal3 in DBY746 wild-type and *vps27* genetic backgrounds is shown. Cultures were grown in duplicate for cells carrying Ppz1 + Ø and Ppz1 + Hal3 (A and B). Whole yeast extracts were prepared as described in section 4.6.1. Two gels were loaded in parallel, one was processed for anti-Ppz1 detection (upper panel) and the other for anti-Hal3 detection (lower panel). Staining with Ponceau Red is shown to verify loading and transfer efficiency.

6.3.2.6. Deletion of *VPS27* in Ppz1-overexpresing cells impedes growth recovery caused by Hal3 overexpression.

Because deletion of *VPS27* had a dramatic effect on Ppz1 and Hal3 localization, we decided to examine further the effects that could derive from the inability to retain Ppz1 in vacuolar membranes. To this end, DBY746 and *vps27* cells were transformed with the following combination of multicopy plasmids: a) empty/empty, b) Ppz1-GFP/empty and c) Ppz1-GFP/Hal3 and monitor their growth. The result of this test can be seen in Figure 29. As expected, in wild-type cells expression of Ppz1-GFP alone results in slower growth, and normal cell growth is restored when cells carry the combination Ppz1-GFP/Hal3. Mutation of *VPS27*, by itself, does not significantly affect growth. Notably, *vps27* cells carrying the Ppz1-GFP/empty plasmid combination show a dramatic decrease of cell growth in comparison with wild-type cells with the same combination. Remarkably, the expression of Hal3 barely improves growth of these cells. The fact that Hal3 is unable to alleviate the slow growth phenotype of Ppz1-overexpressing cells in a background with a disturbed vacuolar protein sorting pathway could mean that trafficking to vacuolar membranes is necessary for Hal3 to counteract Ppz1 toxicity.
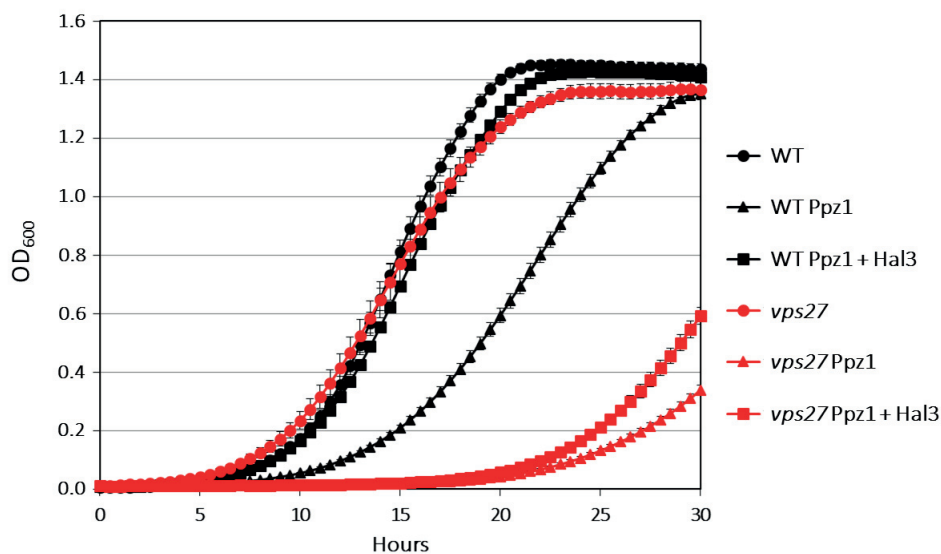
Figure 29. Growth curves of DBY746 wild-type (WT, black) and *vps27* (red) cells. Both strains were transformed with the indicated combination of plasmids: Ø + Ø (circles), Ppz1-GFP/Ø (triangles) and Ppz1-GFP/Hal3 (squares). Cultures were grown until saturation and then diluted in fresh medium to OD_{600} = 0.02. At this point, cells were distributed in the honeycomb plates and these were introduced in the Bioscreen C apparatus. Growth was monitored as described in section 4.3. Represented values are the mean ± SEM of 5 to 12 independent cultures.

7. DISCUSSION

The fact that high levels of Ppz1 could be deleterious for the yeast cell was already hinted in 1996, when our laboratory described that cells carrying a YEp195 Ppz1 plasmid showed a slow growth phenotype (Clotet *et al*, 1996). Recently, our laboratory also showed that the enzymatic activity of Ppz1 is crucial for its toxicity (Calafí *et al*, 2020b). Therefore, an excess of Ppz1 phosphatase activity could be altering the phosphorylation state of diverse cellular targets, which could induce the toxic effects. In the last few years different approaches have been taken to elucidate the molecular basis of the toxicity of this phosphatase.

The data obtained from transcriptomic and phosphoproteomic analysis of cells overexpressing Ppz1 provided a plethora of information regarding what cells undergo when the levels of the phosphatase are high enough to impede normal cell growth. For both transcriptomic and phosphoproteomic analysis, the Ppz1 overexpression system used was the ZCZ01 strain, which has the *PPZ1* ORF under the control of a *GAL1-10* promoter. One of the first results of the transcriptomic assay that caught our attention was the transcriptional induction of many genes responsive to oxidative stress. Using the dihydrorhodamine 123 fluorescent dye, we confirmed the presence of ROS in cells that overexpress Ppz1 (Figure 7A) and, moreover, that these cells undergo DNA damage, as seen by the Rad52 foci formation (Figure 7B). One critical effect of oxidative stress is that it can induce a halt in protein translation at the initiation and post-initiation phases mediated by the phosphorylation of eIF2α by the Gcn2 kinase (Mascarenhas *et al*, 2008). We recently described that Ppz1 overexpression can lead to a halt in protein translation as it causes a hyperphosphorylation of eIF2α at the conserved Ser51, a residue that is the target for the Gcn2 kinase (Calafí *et al*, 2020b). In addition, it was found that deletion of *GCN2* partially alleviated the growth defect caused by Ppz1 overexpression. This suggests that the oxidative stress that suffer Ppz1-overexpressing cells could be contributing to the halt in translation observed in these cells.

Another interesting transcriptomic result was the strong perturbation that suffered the *ADE* pathway in Ppz1-overexpressing cells. This pathway is crucial for the synthesis of purine nucleotides, and every gene of the pathway, except for *ADE16*, were down-regulated. The fact that *ADE16* was the only exception prompted us to study if this was mediated by Bas1-Bas2 transcription factors, as *ADE16* is the only gene in the pathway not regulated by the Bas1-Bas2 complex (Pinson *et al*, 2000a; Denis *et al*, 1998). Pinson and coworkers described how oxidative stress could lead to a down regulation of the *ADE* pathway by blocking the crucial Bas1-Bas2 interaction (Pinson *et al*, 2000a). Our first hypothesis was that Ppz1-overexpressing cells were unable to grow normally due to a depletion of purine nucleotides derived from the repression of the *ADE* pathway, which could explain the cell cycle blockade that these cells suffer (Clotet *et al*,

DISCUSSION

1999). Nevertheless, we found that Ppz1-overexpressing cells carrying a constitutively active fusion of Bas1-Bas2 show no improvement on cell growth (Figure 8), which suggested that inhibition of the *ADE* pathway is not the cause of the cell cycle stop. Moreover, we present further evidence of how Ppz1-overexpressing cells are not suffering from dNTPs scarcity, but they are, instead, accumulating nucleotides to higher levels than the wild-type strain (Figure 9). Thus, the cell cycle arrest in Ppz1-overexpressing cells cannot be attributed to a lack of DNA precursors. On the light of these findings, the observed repression of genes belonging to the ADE pathway could be interpreted as a physiological negative feed-back response to high levels of end products of the pathway. This scenario is supported by the strong decrease in the levels of AICAR monophosphate (ZMP) in Ppz1-overexpresing cells (Velázquez *et al*, 2020). The ZMP intermediate has been shown to be a major activator of the expression of the Bas1-Bas2 dependent genes in the pathway (Pinson *et al*, 2009).

Preliminary results obtained in our laboratory pointed out that cells overexpressing Ppz1 were not responding to a carbon limiting environment at the same level that a wild-type strain did (Figure 10A and 10B). This was interesting because it has been recently described, using a $tetO_7$-based overexpression system, that Ppz1 toxicity increases as the glucose of the medium is reduced (Calafí *et al*, 2020b). Analysis of the phosphoproteomic data revealed that several critical players involved the response to carbon stress were affected in their phosphorylation status when Ppz1 was overexpressed. One of them was Snf1, which was dephosphorylated at T210. This change would lead to Snf1 inhibition, since it has been described that Snf1 activation relies on the phosphorylation of Thr210 by the upstream kinases Sak1, Elm1 and Tos3 (McCartney & Schmidt, 2001). By western blot analysis we could confirm the dephosphorylation of Snf1 and illustrate how cells show a rapid decrease in Snf1-P levels after 1 hour of Ppz1-overexpression (Figure 11), when Ppz1 is not even close to its highest levels. In glucose limiting conditions Snf1 would be phosphorylated, thus active, and it would induce the phosphorylation of Reg1. However, in the phosphoproteomic data Reg1 appears to be dephosphorylated in Ppz1-overexpressing cells at Ser346 and Ser349 (Velázquez *et al*, 2020). These residues are included in the Reg1[1-443], a fragment that has been shown to act as a substrate in vitro for Ppz1 (García-Gimeno *et al*, 2003). Phosphorylation affects the electrophoretic mobility of this polypeptide. Our western blot data shows that in the ZCZ01 strain, upon galactose addition, the Reg1[1-443] fragment shifts to higher mobility species (Figure 12), being after 4 h indistinguishable from the protein found in glucose-grown wild-type cells. This change in mobility could be explained by a dephosphorylation of the protein in the mentioned residues. Dephosphorylation of Reg1 has been usually attributed to Glc7 (Sanz *et al*, 2000). However, our data suggest that Reg1 might also

be an *in vivo* substrate for Ppz1. At present, the possible relevance of the phosphorylation status of Reg1 Ser346 and Ser349 in the function of the protein is not known.

Another protein involved in the adaptation to carbon limiting situations that suffered changes in its phosphorylation state was Mig1. In Ppz1-overexpressing cells this transcription factor was found dephosphorylated at Ser311 and Ser314, which are physiological targets for the Snf1 kinase. In wild-type cells under low glucose conditions, Snf1 phosphorylates Mig1 at Ser311 and Ser314 (Treitel *et al*, 1998), inducing Mig1 eviction from the nucleus and activating the transcription of the glucose-repressed genes. It was shown, using the ZCZ01 strain, that after two hours of Ppz1 induction, Mig1 is retained in the nucleus in a 30-35% of ZCZ01 cells (Velázquez *et al*, 2020), whereas in the wild-type strain roughly 1% of cells displayed Mig1 inside the nucleus. As the ZCZ01 strain cannot be tested in the presence of glucose in the medium, to confirm the anomalous behavior of Mig1 in actual low glucose conditions, we used the MLM04 strain, which carries a *tetO7*-based Ppz1 expression system. Upon shifting wild-type cells to a low glucose medium (0.05% glucose), very few wild-type cells presented Mig1 in the nucleus, whereas in the MLM04 strain, around 30% displayed nuclear Mig1 (Figure 13). The observation that Mig1, in a limiting carbon source situation, is retained in the nucleus of Ppz1-overexpressing cells fits well with an inactive Snf1. Therefore, since retention of Mig1 inside the nucleus likely implies that the expression of those genes needed to adapt to alternative carbon sources is repressed, Ppz1-overexpressing cells are probably impaired in their capacity to properly respond to a carbon stress situation.

Although the Snf1 primary role is the response to diverse stress factors, besides limiting glucose conditions, some recent non-conventional functions have been described for this kinase (Coccetti *et al*, 2018). Among them, an implication in cell cycle progression has been demonstrated. In fact, there is evidence that Snf1 must be active in yeast cells in order to promote a normal G_1/S transition, in contrast to multicellular eukaryotes, where Snf1 activation causes an arrest in G_1 (Igata *et al*, 2005). In this work we have discarded the possibility that Ppz1-mediated blockage of cell cycle progression could be due to lack of DNA biosynthesis precursors. An alternative possibility was that Ppz1-overexpressing cells could not progress through the G_1/S transition due to Snf1 being inactivated because its dephosphorylation at T210. However, a constitutively active version of Snf1 (T210E) for the cell cycle function was unable to restore the growth of the ZCZ01 strain growing in the presence of galactose (Figure 14). This suggests that the cell cycle blockade seen in Ppz1-overexpressing cells must be caused by other factors rather than Snf1 inactivation. The phosphoproteomic analyses highlighted a number of additional protein kinases suffering alterations in their phosphorylation (and likely activation) state. One of

these is Hog1, which becomes phosphorylated at Thr174 and Tyr176 residues (crucial for its activation). It has been shown that Hog1 activation induces a delay in the G_1/S transition. Remarkably, deletion of this kinase improves growth in Ppz1-overexpressing cells (Velázquez *et al*, 2020). Therefore, while changes in Snf1 phosphorylation could be irrelevant, activation of Hog1 might mediate, at least in part, the effect on cell growth caused by high levels of Ppz1.

As our experiments with the ZCZ01 strain indicated that different proteins involved in the adaptation to alternative carbon sources or carbon limiting conditions were affected by Ppz1-overexpression, we decided to construct a new strain that could overexpress Ppz1 independently of the carbon source of the medium. Although the existing MLM04 strain met this requirement, its Ppz1 expression kinetics is very slow compared to that of strain ZCZ01 and, furthermore, the Ppz1 levels obtained are only moderate and far lower than those obtained with the ZCZ01 strain. To avoid these problems, we constructed the MAC001 strain. It is a ZCZ01-based strain in which Ppz1 is induced by the addition of β-estradiol in the medium. After 4 hours of induction, and from 5 nM β-estradiol onward, Ppz1 levels in MAC001 are very close to the ones observed in strain ZCZ01 (Figure 15B), and result in blockage of cell growth in both solid and liquid tests (Figures 16A and 16B). This growth defect is in agreement with the accumulation of unbudded MAC001 cells (Figure 16C). It must be noted that in ZCZ01 cells, after 4 hours of Ppz1 overexpression the percentage of unbudded cells was ≈85% (Zhang, 2019), while in the MAC001 strain, after 6 hours the percentage was somewhat lower (55-60%, Figure 16C). Therefore, although similarly to ZCZ01 cells, MAC001 cells are unable to proliferate in the long term, these results might indicate a delay in the toxic effects, due either to differences in the potency of the expression system and/or to the presence of glucose as carbon source. Cells with very high levels of Ppz1 are unable to grow even when the medium contains 2% of glucose, this fact indicates that the carbon adaptation is not crucial to explain the toxic effects of Ppz1 overexpression. This scenario is in agreement with the finding that overexpressing Ppz1 using a tetO_7-based system in a *mig1 mig2* double mutant had deleterious effects (Calafí, 2020).

From the results of this work (ROS accumulation, DNA damage and inability to adapt to alternative carbon source or low glucose conditions) plus other recent findings from our laboratory like the halt of protein translation initiation (Calafí *et al*, 2020b), it is clear that Ppz1-overexpressing cells have multiple problems that could jeopardize cell proliferation. So, it is conceivable that the toxicity of an excess of Ppz1 phosphatase activity relies in the alteration of many cellular targets rather than a unique cause.

Ppz1 plays a key role in cationic homeostasis as it: a) negatively regulates the activity of the main potassium import system Trk1,2 and b) represses the expression of the *ENA1* gene, encoding a P-type ATPase Na$^+$ pump (Yenush *et al*, 2002; Ruiz *et al*, 2003). It seemed reasonable that the overexpression of Ppz1 could lead to a very strong inhibition of the K$^+$ import, which has been described to negatively impact on cell growth. However, supplementation of the media with KCl, to a point that permitted a *trk1 trk2* double mutant to grow normally, did not allow growth of ZCZ01 cells in Ppz1-overexpressing conditions (Figure 17A). This suggests that the toxicity of Ppz1 is not due to an exacerbated inhibition of the Trk1,2 transporters. Nevertheless, the finding that deletion of the *NHA1* in the ZCZ01 strain does ameliorate cell growth in Ppz1-overexpressing conditions pointed again the focus on the role Ppz1 on monovalent cation homeostasis. Nha1 is a constitutively expressed protein that actively exports Na$^+$ and K$^+$ in exchange for protons (Bañuelos *et al*, 1998), so it plays a crucial role in regulating intracellular pH (Sychrová *et al*, 1999) and membrane potential (Kinclova-Zimmermannova *et al*, 2006).

In collaboration with the Laboratory of Membrane Transport, Institute of Physiology of the Czech Academy of Sciences from Prague, we have described how an excess of Ppz1 induces a sharp decrease in the intracellular concentration of K$^+$ and a fast acidification of the cytosol, confirming that high Ppz1 levels have an impact in cation homeostasis (Albacar *et al*, 2021). Interestingly, it has been described that cells suffering short-term potassium deprivation display some traits that are reminiscent of those observed upon Ppz1 overexpression (Barreto *et al*, 2012), including ROS accumulation, down-regulation of genes required for ribosome biogenesis and translation, and a decrease in the expression of components needed to progress through cell cycle.

The fact that deleting *NHA1* partially restores both K$^+$ and H$^+$ intracellular levels points out that Nha1 function is contributing to the observed alterations. Therefore, we hypothesized that an increment in Ppz1 levels could lead to the hyperactivation of Nha1, resulting in an exacerbated influx of H$^+$ in exchange for K$^+$ ions. This idea is supported by two observations. On one hand, decreasing the intra-extracellular pH gradient abolished the beneficial effect of deleting the *NHA1* gene (Figure 18), since in this situation the antiporter would have a lesser role in K$^+$/H$^+$ exchange. On the other hand, recent results from our collaborators showed that transforming ZCZ06 cells with a plasmid carrying native Nha1 restore the poor growth of a ZCZ01 strain, while expression of a non-functional version of Nha1 does not. Therefore, it can be assumed that the toxicity of an excess of Ppz1, which is followed by a rapid loss of K$^+$ and a drop in intracellular pH, depends on the presence of Nha1 in the plasma membrane and its function as cation transporter.

DISCUSSION

Although Nha1 expression is constitutive, its activity has been described to be controlled by phospho-dephosphorylation reactions affecting its long C-terminal tail. Specifically, it was proposed that phosphorylation of Thr-765 and Thr-876 by the Hog1 kinase was important for short-term activation of Nha1 in a salt stress situation (Proft & Struhl, 2004). Besides, Ser-481 is responsible for binding to yeast 14-3-3 proteins when phosphorylated by an unknown kinase (Smidova et al, 2019; Zahrádka et al, 2012). Interestingly, mutation of Ser-481 to Ala, preventing the phosphorylation of the residue, significantly boosted the cation efflux activity via Nha1 (Smidova et al, 2019). Remarkably, phosphoproteomic results of our laboratory, performed under the same experimental conditions used in this work, described that Nha1 was significantly dephosphorylated at Ser-481 already after one h of Ppz1 induction (Velázquez et al, 2020). In this context, the fact that ZCZ06 cells carrying the S481A version grow worse than strain ZCZ01, as expected from a hyperactive Nha1 antiporter, provides further support to our proposal. Moreover, Tarassov and coworkers detected an interaction between Ppz1 and Nha1 using a protein-fragment complementation assay (Tarassov et al, 2008). This result could be a hint for a direct Ppz1-mediated dephosphorylation of Nha1.

The fact that the deletion of $NHA1$ in a Ppz1-overexpressing strain results in only a partial normalization of growth rate and of K$^+$ and H$^+$ intracellular content suggests that other targets important for monovalent cation homeostasis are affected by an excess of Ppz1 activity. One crucial determinant for this homeostasis is the Na$^+$-ATPase encoded by $ENA1$. However, this option could be discarded since Ppz1 acts as a repressor of its expression instead of as an activator. In yeast cells, the plasma membrane ATPase Pma1 is the major determinant of plasma membrane potential, because of its electrogenic transport of H$^+$ and it is believed to play a crucial influence in cytosolic pH (Kane, 2016). We described that Ppz1-overexpressing cells fail to properly acidify the medium, a limitation partially restored when the $NHA1$ gene is deleted (Figure 19A). This result prompted us to study if an excess of Ppz1 activity could be negatively affecting normal Pma1 function. The activity of this H$^+$-ATPase is controlled by reversible phosphorylation and by transcriptional modulation, for instance in response to glucose (see (Kane, 2016) for further references). Since Ppz1 overexpression has been described to impair protein translation (Calafí et al, 2020b), we needed to monitor the levels of Pma1 during the overexpression of the phosphatase, because a decrease of Pma1 levels could explain the loss in acidification capacity. Nevertheless, our result indicates that the levels of the ATPase are higher in cells that overexpress Ppz1 than in wild-type cells (Figure 19B). Pma1 can be phosphorylated in the cell at least at 20 sites, essentially located at its N- and C-terminal moieties (see SGD at http://www.yeastgenome.org/). Among those sites, phosphorylation of Ser-911 and Thr-912

seems to be important for the activation of Pma1, with a minor contribution of Ser-899, a residue highly conserved (Eraso & Portillo, 1994; Lecchi *et al*, 2007). It is worth noting that our reported phosphoproteomic assay showed that the overexpression of Ppz1 affected the phosphorylation state of a few Pma1 residues. Remarkably, these included not only Ser-911 and Thr-912, but also Ser-899 (Velázquez *et al*, 2020). The decrease in the phosphorylation was significant in all three cases, being reduced to one-half of the normal levels, and it was already noticeable after 60 min of Ppz1 induction and was sustained over time. Thus, it seems reasonable that these changes in the phosphorylation state of Pma1 may be behind the reduction of its H$^+$ pumping capacity, hence explaining (at least in part) the Nha1-independent changes in intracellular H$^+$ content. The activity of the Pma1 ATPase is the primary consumer of ATP in yeast cells, employing from 20 to 50% of the cellular ATP (Burgstaller, 1997). Pharmacological inhibition of the Pma1 proton ATPase (Kjellerup *et al*, 2017; Olsen *et al*, 2009) or point mutations in the protein that lead to partial defects in pumping activity (Stevens & Nichols, 2007) have been reported to result in increased ATP levels. Indeed, recent work from our laboratory reported that Ppz1-overexpressing cells accumulate higher than normal (up to two-fold) ATP levels (Velázquez *et al*, 2020). Therefore, it is plausible that the higher levels of ATP found in Ppz1-overexpressing cells are, at least in part, a consequence of the decrease in Pma1 activity.

The intrinsically disordered N-terminal region of Ppz1 has been described to be the determinant for its toxicity (Calafí *et al*, 2020a). One interesting feature of this region is the presence of a myristoylable glycine in position 2 (Clotet *et al*, 1996). This modification is crucial for Ppz1 membrane localization and mutation of the Gly-2 to Ala renders the phosphatase cytosolic. Remarkably, in overexpressing conditions, cells carrying the Ppz1-G2A variant have been described to grow slightly better than those carrying the native phosphatase (Calafí *et al*, 2020a). This result suggested that altering Ppz1 plasma membrane localization could impede that the interaction of the phosphatase with some of its substrates relevant for the toxic effects and led us to investigate more in depth the subcellular localization of Ppz1.

We started by studying the localization of the phosphatase by transforming cells with multicopy vectors carrying tagged versions of Ppz1 controlled by its endogenous promoter, which account for moderate expression levels of the phosphatase. As seen in Figure 20, the Ppz1 localizes mostly in the peripheral membrane (A), its inactive version (Ppz1-R451L) can be roughly equally detected in peripheral and internal membranes (B) and the Ppz1-G2A version is completely cytosolic (C). Therefore, our results confirm the recent report that Gly-2 mutation to Ala results in disappearance of Ppz1 from peripheral membranes (Lee *et al*, 2019). However, upon transforming cells with the mentioned plasmids plus a YEp181 vector carrying the *HAL3* gene,

most of the native Ppz1 localizes in internal structures rather than the plasma membrane (Figure 21A). In the case of Ppz1-R451L, even though it is a more subtle change, it can be also detected in internal structures (Figure 21B). Lastly, Ppz1-G2A shows no alteration in its distribution (Figure 21C), since it is still cytosolic. Therefore, the ability to interact with membranes it is essential for the internalization of the phosphatase.

Hal3, as a negative regulatory subunit of Ppz1, is able to regulate most of Ppz1 functions in the cell. Our tagged version of Hal3 localizes in the cytosol (Figure 22A) as it was previously described by Ferrando and coworkers (Ferrando *et al*, 1995). However, when cells overexpress Hal3-GFP and Ppz1, Hal3 can be detected in internal structures, in addition to the cytosol (Figure 22B). It could be assumed that this translocation to the internal structures would be related to its function as Ppz1 regulatory subunit. The observation that only a fraction of Hal3 changes its localization to internal structures could be explained by its moonlighting function. Thus, part of the Hal3 molecules would be retained in the cytosol as part of the PPCDC complex (Ruiz *et al*, 2009).

When cells carry tagged versions of both Ppz1 and Hal3 (either Ppz1-GFP plus Hal3-mCherry or Ppz1-mCherry plus Hal3-GFP), both proteins can be detected in internal structures and in some regions of the plasma membrane (Figure 23A and B). At this point, we do not know what triggers the internalization of both proteins, but it could be possible that this process was related with the excess of Ppz1 activity. There are many examples of plasma membrane proteins that are internalized, as the uracil permease Fur4 or the high-affinity glucose transporters Hxt6 and Hxt7 (see (Munn, 2001) for further references). These proteins have been shown to undergo endocytic internalization for subsequent vacuolar degradation. It is not clear that this could be the case for Ppz1, since, firstly its interaction with the membrane has been described to be only peripheral since it is not resistant to treatments with detergents (Yenush *et al*, 2005), and second, we do not have a clear evidence of Ppz1 being inside the vacuole.

All the results obtained so far were obtained using the YEp195 Ppz1-GFP vector, which leads to expression of the phosphatase to levels that induce a slow growth phenotype, but are insufficient to block cell growth. Therefore, we decided to also to monitor Ppz1 subcellular localization in strong overexpression systems known to impede cell growth. The ZCZ01 strain has been well characterized in our laboratory and it has been used to obtain transcriptomic and phosphoproteomic data that provides insight to what cells undergo under very high levels of the phosphatase. Because of this, we decided to generate a derivative of strain ZCZ01 containing a GFP-tagged version of Ppz1 (strain MAC003). Given that the GFP tag did not attenuate the

negative impact of Ppz1 overexpression in cell growth (Figure 24A and B), we proceeded to monitor the subcellular localization of the phosphatase. In this strain Ppz1 can be detected in the plasma membrane already after 2 hours of galactose addition and, as time increases, very intense spots appear in the cell periphery (Figure 25, upper panel). In comparison to the localization of Ppz1-GFP expressed from a multicopy plasmid, in the MAC003 strain the punctate pattern is much clearer, probably due to the much higher expression levels. It can be assumed that the pattern observed in MAC003 faithfully reproduces the situation in ZCZ01 cells upon Ppz1 overexpression. Some of the targets postulated for Ppz1, such as Trk1, Nha1 or Pma1 (the last two proposed in this work), are organized in lipid rafts (see (Mollinedo, 2012) and references therein). Even though Ppz1 has been described as peripheral membrane proteins (Yenush et al., 2005), the phosphatase could be transiently found in lipid rafts as shown for some non-raft proteins in mammalian cells (see (Mollinedo, 2012) for further references).

When MAC003 cells overexpressing Ppz1 carry a multicopy vector that contains the *HAL3* gene the phosphatase progressively disappears from peripheral membrane and appears in internal structures (Figure 25, lower panel). Probably, this internalization of the phosphatase is what contributes to normalize cell growth, since Ppz1 would be unable to interact with Trk1, Nha1 or Pma1. However, cells transformed with a vector containing Ppz1-G2A, the cytosolic version of the phosphatase, display only a modest improvement in growth compared with cells carrying the native version of the phosphatase (Calafí *et al*, 2020a). Such improvement could be attributed to the inability of Ppz1-G2A to interact with relevant plasma membrane targets such as Trk1 (Yenush *et al*, 2002), Nha1 or Pma1 (this work). Nevertheless, the fact that expression of Ppz1-G2A only results in partial improvement of cell growth indicates that further Ppz1 cytosolic targets relevant for toxicity must exist. In this regard, in addition to its capacity to inhibit Ppz1 activity, the ability of Hal3 to remove the phosphatase from the plasma membrane and the cytosol, accumulating Ppz1 in internal structures could largely contribute to block the toxic effects of the excess of the phosphatase.

By staining vacuolar membranes with FM4-64, we could prove that the internal structures where Ppz1 can be detected when cells overexpress Ppz1 and Hal3, correspond to vacuolar membranes (Figure 26A and B). In a few cases Ppz1 and Hal3 also colocalized with the ER or perinuclear membrane (Figure 26C). To gain insights into this internalization process, we decided to employ a *vps27* mutant, a strain that displays a defect in vacuolar protein sorting (Robinson *et al*, 1988). When *vps27* cells carry the Ppz1-GFP multicopy vector, virtually all cells show Ppz1-GFP in their membranes (see Figure 27A, lower panel for a representative micrography), in agreement with the higher number of Ppz1-GFP-positives cells detected by flow cytometry (Figure 28A),

compared to the wild-type. Nevertheless, their intensities are very similar (Figure 28B), in agreement with the expression levels detected by western blot (Figure 28C).

Taken together these results, the deletion of the *VPS27* gene, which has a crucial role in down-regulation of surface proteins (Katzmann *et al*, 2003), renders cells unable to internalize Ppz1 to the vacuolar membrane. Then, we hypothesized that if the growth improvement seen when wild-type cells carry both Ppz1 and Hal3 plasmids was achieved because of the internalization of Ppz1, this effect would not take place in a *vps27* mutant. Indeed, *vps27* cells carrying Ppz1-GFP and Hal3 vectors, show only a slightly improvement in cell growth, very far from that of the *vps27* with empty vectors (Figure 29). Therefore, the ability to internalize the phosphatase seems crucial for cell proliferation.

One might assume that the shift of Ppz1 to vacuolar membranes in the presence of Hal3 could be a cellular strategy to remove Ppz1 from its targets at the plasma membrane and bring the phosphatase to the vacuolar lumen for degradation. However, there are at least two main observation arguing against this hypothesis. On the one hand, even after a long period of Ppz1 overexpression (see figure 25), we detected the phosphatase in the vacuolar membrane, and very rarely in the vacuolar lumen. On the other hand, when cells overexpress both Ppz1 and Hal3, the amount of immunodetected phosphatase does not decrease with time (Calafí *et al*, 2020b). Therefore, it is unlikely that Ppz1 is being internalized for its degradation. There are some examples of yeast proteins that can translocate to the vacuolar membrane as part of their normal function. For instance, *Saccharomyces cerevisiae* Sch9 AGC family protein kinase in log phase is localized throughout the cell, but it is enriched at the vacuolar membrane (Jorgensen *et al*, 2004). Moreover, this localization is dynamic, as the signal from vacuolar membrane localization vanishes upon carbon starvation (Jorgensen *et al*, 2004). Recent work showed that the N-terminal domain of Sch9 is necessary for its recruitment in the vacuolar surface, where the kinase can be phosphorylated by the TORC1 complex, and thus activated (Novarina *et al*, 2021). Another example could be the PpAtg9 protein from *Pichia pastoris*, which localizes in structures near the plasma membrane during methanol growth and, on glucose-induced micropexophagy translocates to perivacuolar structures (Chang *et al*, 2005). In the case of the Ppz1 phosphatase it is not clear at this point how or why it translocates to the vacuolar membrane, and further investigation is needed to unveil the details behind this process.

We show in this work that Ppz1-overexpressing cells display a drop in internal pH, and we postulate that this could be due to the combination of an hyperactivation of Nha1 and the inhibition of the Pma1 proton pump. It has been proposed that the interaction between Ppz1 and

Hal3 could be pH sensitive, based on the observation that an affinity resin containing Ppz1-retained higher levels of Hal3 at pH 6.0 than at pH 7.5 (Yenush *et al*, 2005). A plausible scenario would be that a decrease in intracellular pH would lead to an increased interaction between Hal3 and Ppz1. Such interaction would result in the direct inhibition of the Ppz1 activity and in the sequestering of the phosphatase away from its targets to avoid the negative consequences derived from its excessive dephosphorylation.

8. CONCLUSIONS

1. An excess of Ppz1 activity induces an accumulation of ROS in yeast cells, which in the mid-long term also causes DNA damage.

2. The blockade in cell cycle progression at the G_1/S transition observed in Ppz1-overexpressing cells is not due to the inhibition of the *ADE* pathway nor to limiting levels of DNA biosynthetic precursors.

3. High levels of Ppz1 induce alterations in several proteins associated to the carbon stress response, including: i) a rapid dephosphorylation of Snf1, ii) a decrease in Reg1 phosphorylation, and iii) a retention of Mig1 inside the nucleus. All these changes indicate that cells are not properly responding to a non-favorable carbon source situation.

4. The inactivation of Snf1 in Ppz1-overexpressing cells is not the cause of the cell cycle arrest at the G_1/S transition.

5. The MAC001 strain displays a fast and strong Ppz1 overexpression that is independent of the carbon source of the medium, induces an accumulation of unbudded cells, and is deleterious to yeast cells. Therefore, this strain is an excellent tool to evaluate the effects of strong Ppz1 overexpression in the presence of glucose.

6. The presence of 2% glucose in the medium does not attenuate Ppz1 toxicity in strong overexpression systems.

7. The deleterious effect of Ppz1 overexpression is not attenuated by increasing K^+ in the medium and is likely not attributable to the inhibition of the Trk transporters.

8. Deletion of the *NHA1* gene improves growth of a Ppz1-overexpressing strain, and this effect vanishes as external pH approaches neutrality.

9. ZCZ01 cells overexpressing Ppz1 display a reduced acidification capacity that is not associated to low Pma1 protein levels. Deletion of *NHA1* partially normalizes this acidification defect.

10. We postulate that Ppz1 overexpression induces the hyperactivation of the Nha1 antiporter and likely decrease Pma1 activity. These effects could be explained by the abnormal dephosphorylation of both proteins.

11. Localization experiments expressing a Ppz1-GFP tagged version from a multicopy vector showed that co-expression of Hal3 leads to mobilization of Ppz1 from plasma membrane to internal structures of the cell.

12. When Ppz1 and Hal3 are overexpressed they preferentially colocalize in vacuolar membranes.

13. Deletion of the *VPS27,* which blocks Ppz1 internalization, also avoids normalization of growth rate caused by overexpression of Hal3. Therefore, removal of the excess of Ppz1 from plasma membrane and cytosol would be crucial to counteract its toxicity.

9. REFERENCES

Abrie JA, Molero C, Ariño J & Strauss E (2015) Complex stability and dynamic subunit interchange modulates the disparate activities of the yeast moonlighting proteins Hal3 and Vhs3. *Sci Rep* 5: 1–17

Ádám C, Erdei É, Casado C, Kovács L, González A, Majoros L, Petrényi K, Bagossi P, Farkas I, Molnar M, *et al* (2012) Protein phosphatase CaPpz1 is involved in cation homeostasis, cell wall integrity and virulence of *Candida albicans*. *Microbiology* 158: 1258–1267

Adams A, Gottschling DE, Kaiser CA & Stearns T (1998) Methods In Yeast Genetics: A Cold Spring Harbor Laboratory Course Manual. *Cold Spring Harb Lab Press New York*

Aksenova A, Muñoz I, Volkov K, Ariño J & Mironova L (2007) The HAL3-PPZ1 dependent regulation of nonsense suppression efficiency in yeast and its influence on manifestation of the yeast prion-like determinant [ISP+]. *Genes to Cells* 12: 435–445

Albacar M, Sacka L, Calafí C, Velázquez D, Casamayor A, Ariño J & Zimmermannova O (2021) The Toxic Effects of Ppz1 Overexpression Involve Nha1-Mediated Deregulation of K+ and H+ Homeostasis. *J Fungi* 7: 1010

Alepuz PM, Cunningham KW & Estruch F (1997) Glucose repression affects ion homeostasis in yeast through the regulation of the stress-activated *ENA1* gene. *Mol Microbiol* 26: 91–98

Alvaro D, Sunjevaric I, Reid RJD, Lisby M, Stillman DJ & Rothstein R (2006) Systematic hybrid LOH: a new method to reduce false positives and negatives during screening of yeast gene deletion libraries. *Yeast* 23: 1097–1106

Ariño J (2002) Novel protein phosphatases in yeast: An update. *Eur J Biochem* 269: 1072–1077

Ariño J, Casamayor A & González A (2011) Type 2C protein phosphatases in fungi. *Eukaryot Cell* 10: 21–33

Ariño J, Ramos J & Sychrová H (2010) Alkali metal cation transport and homeostasis in yeasts. *Microbiol Mol Biol Rev* 74: 95–120

Arndt KT, Styles CA & Fink GR (1989) A suppressor of a *HIS4* transcriptional defect encodes a protein with homology to the catalytic subunit of protein phosphatases. *Cell* 56: 527–537

Balcells L, Gómez N, Casamayor A, Clotet J & Ariño J (1997) Regulation of salt tolerance in fission yeast by a protein-phosphatase-2-like Ser/Thr protein phosphatase. *Eur J Biochem* 250: 476–483

Bañuelos MA, Sychrová H, Bleykasten-Grosshans C, Souciet J-L & Potier S (1998) The Nha1 antiporter of *Saccharomyces cerevisiae* mediates sodium and potassium effux. *Microbiology* 144: 2749–2758

Barreto L, Canadell D, Valverde-Saubí D, Casamayor A & Ariño J (2012) The short-term response of yeast to potassium starvation. *Environ Microbiol* 14: 3026–42

Benito B, Quintero FJ & Rodríguez-Navarro A (1997) Overexpression of the sodium ATPase of

REFERENCES

Saccharomyces cerevisiae: conditions for phosphorylation from ATP and Pi. *Biochim Biophys Acta - Biomembr* 1328: 214–225

Böhm S & Buchberger A (2013) The budding yeast Cdc48(Shp1) complex promotes cell cycle progression by positive regulation of protein phosphatase 1 (Glc7). *PLoS One* 8: e56486

Bollen M, Peti W, Ragusa MJ & Beullens M (2010) The extended PP1 toolkit: designed to create specificity. *Trends Biochem Sci* 35: 450–458

Botstein D & Fink GR (2011) Yeast: An experimental organism for 21st century biology. *Genetics* 189: 695–704

Brachmann CB, Davies A, Cost GJ, Caputo E, Li J, Hieter P & Boeke JD (1998) Designer deletion strains derived from *Saccharomyces cerevisiae* S288C: a useful set of strains and plasmids for PCR-mediated gene disruption and other applications. *Yeast* 14: 115–132

Burgstaller W (1997) Transport of small Ions and molecules through the plasma membrane of filamentous fungi. *Crit Rev Microbiol* 23: 1–46

Calafí C (2020) La proteína fosfatasa Ppz1 de levadura: estudios estructurales y funcionales en sobreexpresión. Doctoral Thesis, Universitat Autònoma de Barcelona

Calafí C, López-Malo M, Albacar M, Casamayor A & Ariño J (2020a) The N-terminal region of yeast protein phosphatase Ppz1 is a determinant for its toxicity. *Int J Mol Sci* 21: 1–16

Calafí C, López-Malo M, Velázquez D, Zhang C, Fernández-Fernández J, Rodríguez-Galán O, de la Cruz J, Ariño J & Casamayor A (2020b) Overexpression of budding yeast protein phosphatase Ppz1 impairs translation. *Biochim Biophys Acta - Mol Cell Res* 1867: 118727

Canadell D, González A, Casado C & Ariño J (2015) Functional interactions between potassium and phosphate homeostasis in Saccharomyces cerevisiae. *Mol Microbiol* 95: 555–572

Cannon JF (2010) Function of Protein Phosphatase-1, Glc7, in *Saccharomyces cerevisiae* 1st ed. Elsevier B.V.

Cannon JF, Pringle JR, Fiechter A & Khalil M (1994) Characterization of glycogen-deficient glc mutants of Saccharomyces cerevisiae. *Genetics* 136: 485–503

Ceulemans H & Bollen M (2004) Functional diversity of protein phosphatase-1, a cellular economizer and reset button. *Physiol Rev* 84: 1–39

Chabes A, Georgieva B, Domkin V, Zhao X, Rothstein R & Thelander L (2003) Survival of DNA damage in yeast directly depends on increased dNTP levels allowed by relaxed feedback inhibition of ribonucleotide reductase. *Cell* 112: 391–401

Chang T, Schroder LA, Thomson JM, Klocman AS, Tomasini AJ, Strømhaug PE & Dunn WA (2005) Pp*ATG9*

encodes a novel membrane protein that traffics to vacuolar membranes, which sequester peroxisomes during pexophagy in Pichia pastoris. *Mol Biol Cell* 16: 4941–53

Cheng Y-L & Chen R-H (2015) Assembly and quality control of the protein phosphatase 1 holoenzyme involves the Cdc48-Shp1 chaperone. *J Cell Sci* 128: 1180–92

Clotet J, Garí E, Aldea M & Ariño J (1999) The Yeast Ser/Thr Phosphatases Sit4 and Ppz1 Play Opposite Roles in Regulation of the Cell Cycle. *Mol Cell Biol* 19: 2408–2415

Clotet J, Posas F, Casamayor A, Schaaff-Gerstenschläger I & Arinõ J (1991) The gene *DIS2S1* is essential in *Saccharomyces cerevisiae* and is involved in glycogen phosphorylase activation. *Curr Genet* 19: 339–342

Clotet J, Posas F, De Nadal E & Ariño J (1996) The NH2-terminal extension of protein phosphatase *PPZ1* has an essential functional role. *J Biol Chem* 271: 26349–26355

Coccetti P, Nicastro R & Tripodi F (2018) Conventional and emerging roles of the energy sensor Snf1/AMPK in Saccharomyces cerevisiae. *Microb Cell* 5: 482–494

Cohen P (1989) The structure and regulation of protein phosphatases. *Annu Rev Biochem* 58: 453–508

Cohen P (1991) Classification of Protein- Serine/Threonine Phosphatases: Identification and Quantitation in Cell Extracts. *Methods Enzymol* 201: 389–398

Cohen PTW (2002) Protein phosphatase 1 - Targeted in many directions. *J Cell Sci* 115: 241–256

Di Como CJ, Chang H & Arndt KT (1995) Activation of *CLN1* and *CLN2* G1 cyclin gene expression by *BCK2*. *Mol Cell Biol* 15: 1835–1846

Denis V, Boucherie H, Monribot C & Daignan-Fornier B (1998) Role of the Myb-like protein Bas1p in *Saccharomyces cerevisiae*: a proteome analysis. *Mol Microbiol* 30: 557–566

Egloff MP, Cohen PT, Reinemer P & Barford D (1995) Crystal structure of the catalytic subunit of human protein phosphatase 1 and its complex with tungstate. *J Mol Biol* 254: 942–59

Eraso P & Portillo F (1994) Molecular mechanism of regulation of yeast plasma membrane H(+)-ATPase by glucose. Interaction between domains and identification of new regulatory sites. *J Biol Chem* 269: 10393–9

Farrugia G & Balzan R (2012) Oxidative stress and programmed cell death in yeast. *Front Oncol* 2 JUN: 1–21

Feng Z, Wilson SE, Peng ZY, Schlender KK, Reimann EM & Trumbly RJ (1991) The yeast *GLC7* gene required for glycogen accumulation encodes a type 1 protein phosphatase. *J Biol Chem* 266: 23796–23801

Fernandez-Sarabia MJ, Sutton A, Zhong T & Arndt KT (1992) SIT4 protein phosphatase is required for the

REFERENCES

normal accumulation of SWI4, CLN1, CLN2, and HCS26 RNAs during late G1. *Genes Dev* 6: 2417–2428

Ferrando A, Kron SJ, Rios G, Fink GR & Serrano R (1995) Regulation of cation transport in *Saccharomyces cerevisiae* by the salt tolerance gene *HAL3*. *Mol Cell Biol* 15: 5470–5481

Ferrer-Dalmau J, González A, Platara M, Navarrete C, Martínez JL, Barreto L, Ramos J, Ariño J & Casamayor A (2010) Ref2, a regulatory subunit of the yeast protein phosphatase 1, is a novel component of cation homoeostasis. *Biochem J* 426: 355–64

Ferrer-Dalmau J, Randez-Gil F, Marquina M, Prieto JA & Casamayor A (2015) Protein kinase Snf1 is involved in the proper regulation of the unfolded protein response in *Saccharomyces cerevisiae*. *Biochem J* 468: 33–47

Francisco L, Wang W & Chan CS (1994) Type 1 protein phosphatase acts in opposition to IpL1 protein kinase in regulating yeast chromosome segregation. *Mol Cell Biol* 14: 4731–40

Fulgenzi FR, Peralta ML, Mangano S, Danna CH, Vallejo AJ, Puigdomenech P & Santa-María GE (2008) The Ionic Environment Controls the Contribution of the Barley HvHAK1 Transporter to Potassium Acquisition. *Plant Physiol* 147: 252–262

Gaber RF, Styles CA & Fink GR (1988) TRK1 encodes a plasma membrane protein required for high-affinity potassium transport in *Saccharomyces cerevisiae*. *Mol Cell Biol* 8: 2848–2859

García-Gimeno MA, Muñoz I, Ariño J & Sanz P (2003) Molecular Characterization of Ypi1, a Novel *Saccharomyces cerevisiae* Type 1 Protein Phosphatase Inhibitor. *J Biol Chem* 278: 47744–47752

Ghosh A & Cannon JF (2013) Analysis of protein phosphatase-1 and aurora protein kinase suppressors reveals new aspects of regulatory protein function in *Saccharomyces cerevisiae*. *PLoS One* 8: e69133

Gibbons JA, Kozubowski L, Tatchell K & Shenolikar S (2007) Expression of human protein phosphatase-1 in *Saccharomyces cerevisiae* highlights the role of phosphatase isoforms in regulating eukaryotic functions. *J Biol Chem* 282: 21838–47

Goffeau A, Barrell BG, Bussey H, Davis RW, Dujon B, Feldmann H, Galibert F, Hoheisel JD, Jacq C, Johnston M, *et al* (1996) Life with 6000 Genes. *Science (80-)* 274: 546–567

González-Vioque E, Torres-Torronteras J, Andreu AL & Martí R (2011) Limited dCTP availability accounts for mitochondrial DNA depletion in mitochondrial neurogastrointestinal encephalomyopathy (MNGIE). *PLoS Genet* 7

González A, Ruiz A, Serrano R, Ariño J & Casamayor A (2006) Transcriptional profiling of the protein phosphatase 2C family in yeast provides insights into the unique functional roles of Ptc1. *J Biol Chem* 281: 35057–35069

Haro R, Garciadeblas B & Rodriguez-Navarro A (1991) A novel P-type ATPase from yeast involved in sodium transport. *FEBS Lett* 291: 189–191

He X & Moore C (2005) Regulation of yeast mRNA 3' end processing by phosphorylation. *Mol Cell* 19: 619–29

Hedbacker K & Carlson M (2006) Regulation of the nucleocytoplasmic distribution of Snf1-Gal83 protein kinase. *Eukaryot Cell* 5: 1950–6

Hedbacker K, Hong S-P & Carlson M (2004) Pak1 protein kinase regulates activation and nuclear localization of Snf1-Gal83 protein kinase. *Mol Cell Biol* 24: 8255–63

Hisamoto N, Sugimoto K & Matsumoto K (1994) The Glc7 type 1 protein phosphatase of *Saccharomyces cerevisiae* is required for cell cycle progression in G2/M. *Mol Cell Biol* 14: 3158–3165

Igata M, Motoshima H, Tsuruzoe K, Kojima K, Matsumura T, Kondo T, Taguchi T, Nakamaru K, Yano M, Kukidome D, *et al* (2005) Adenosine monophosphate-activated protein kinase suppresses vascular smooth muscle cell proliferation through the inhibition of cell cycle progression. *Circ Res* 97: 837–44

Ingebritsen TS & Cohen P (1983) Protein phosphatases: Properties and role in cellular regulation. *Science (80-)* 221: 331–338

Ito H, Fukuda Y, Murata K & Kimura A (1983) Transformation of intact yeast cells treated with alkali cations. *J Bacteriol* 153: 163–168

Janke C, Magiera MM, Rathfelder N, Taxis C, Reber S, Maekawa H, Moreno-Borchart A, Doenges G, Schwob E, Schiebel E, *et al* (2004) A versatile toolbox for PCR-based tagging of yeast genes: New fluorescent proteins, more markers and promoter substitution cassettes. *Yeast* 21: 947–962

Johnson DR, Cok SJ, Feldmann H & Gordon JI (1994) Suppressors of nmt1-181, a conditional lethal allele of the *Saccharomyces cerevisiae* myristoyl-CoA:protein N-myristoyltransferase gene, reveal proteins involved in regulating protein N-myristoylation. *Proc Natl Acad Sci* 91: 10158–10162

Johnson SA & Hunter T (2005) Kinomics: Methods for deciphering the kinome. *Nat Methods* 2: 17–25

Jorgensen P, Rupeš I, Sharom JR, Schneper L, Broach JR & Tyers M (2004) A dynamic transcriptional network communicates growth potential to ribosome synthesis and critical cell size. *Genes Dev* 18: 2491–2505

Kane PM (2016) Proton Transport and pH Control in Fungi. *Adv Exp Med Biol* 892: 33–68

Katzmann DJ, Stefan CJ, Babst M & Emr SD (2003) Vps27 recruits ESCRT machinery to endosomes during MVB sorting. *J Cell Biol* 162: 413–423

Kinclova-Zimmermannova O, Gaskova D & Sychrova H (2006) The Na+,K+/H+ -antiporter Nha1 influences

REFERENCES

the plasma membrane potential of *Saccharomyces cerevisiae*. *FEMS Yeast Res* 6: 792–800

Kinclová O, Ramos J, Potier S & Sychrová H (2001) Functional study of the *Saccharomyces cerevisiae* Nha1p C-terminus. *Mol Microbiol* 40: 656–668

Kjellerup L, Gordon S, Cohrt KO, Brown WD, Fuglsang AT & Winther A-ML (2017) Identification of Antifungal H+-ATPase Inhibitors with Effect on Plasma Membrane Potential. *Antimicrob Agents Chemother* 61

Ko CH, Buckley AM & Gaber RF (1990) *TRK2* is required for low affinity K+ transport in *Saccharomyces cerevisiae*. *Genetics* 125: 305–312

Ko CH & Gaber RF (1991) *TRK1* and *TRK2* encode structurally related K+ transporters in Saccharomyces cerevisiae. *Mol Cell Biol* 11: 4266–4273

Koch C, Schleiffer A, Ammerer G & Nasmyth K (1996) Switching transcription on and off during the yeast cell cycle: Cln/Cdc28 kinases activate bound transcription factor SBF (Swi4/Swi6) at start, whereas Clb/Cdc28 kinases displace it from the promoter in G2. *Genes Dev* 10: 129–141

Lecchi S, Nelson CJ, Allen KE, Swaney DL, Thompson KL, Coon JJ, Sussman MR & Slayman CW (2007) Tandem phosphorylation of Ser-911 and Thr-912 at the C terminus of yeast plasma membrane H+-ATPase leads to glucose-dependent activation. *J Biol Chem* 282: 35471–81

Lee KS, Hines LK & Levin DE (1993) A pair of functionally redundant yeast genes (*PPZ1* and *PPZ2*) encoding type 1-related protein phosphatases function within the PKC1-mediated pathway. *Mol Cell Biol* 13: 5843–5853

Lee S, Ho H-C, Tumolo JM, Hsu P-C & MacGurn JA (2019) Methionine triggers Ppz-mediated dephosphorylation of Art1 to promote cargo-specific endocytosis. *J Cell Biol* 218: 977–992

Lee S, Tumolo JM, Ehlinger AC, Jernigan KK, Qualls-Histed SJ, Hsu P-C, McDonald WH, Chazin WJ & MacGurn JA (2017) Ubiquitin turnover and endocytic trafficking in yeast are regulated by Ser57 phosphorylation of ubiquitin. *Elife* 6

Leiter É, González A, Erdei É, Casado C, Kovács L, Ádám C, Oláh J, Miskei M, Molnar M, Farkas I, *et al* (2012) Protein phosphatase Z modulates oxidative stress response in fungi. *Fungal Genet Biol* 49: 708–16

Liu H, Krizek J & Bretscher A (1992) Construction of a *GAL1*-regulated yeast cDNA expression library and its application to the identification of genes whose overexpression causes lethality in yeast. *Genetics* 132: 665–73

Liu H & Naismith JH (2008) An efficient one-step site-directed deletion, insertion, single and multiple-site plasmid mutagenesis protocol. *BMC Biotechnol* 8: 91

Maicas S (2020) The role of yeasts in fermentation processes. *Microorganisms* 8: 1–8

Makanae K, Kintaka R, Makino T, Kitano H & Moriya H (2013) Identification of dosage-sensitive genes in *Saccharomyces cerevisiae* using the genetic tug-of-war method. *Genome Res* 23: 300–311

Manning G, Plowman GD, Hunter T & Sudarsanam S (2002) Evolution of protein kinase signaling from yeast to man. *Trends Biochem Sci* 27: 514–20

Marquina M, Queralt E, Casamayor A & Ariño J (2012) Lack of the Glc7 phosphatase regulatory subunit Ypi1 activates the morphogenetic checkpoint. *Int J Biochem Cell Biol* 44: 1862–71

Mascarenhas C, Edwards-Ingram LC, Zeef L, Shenton D, Ashe MP & Grant CM (2008) Gcn4 is required for the response to peroxide stress in the yeast *Saccharomyces cerevisiae*. *Mol Biol Cell* 19: 2995–3007

Maziarz M, Shevade A, Barrett L & Kuchin S (2016) Springing into Action: Reg2 Negatively Regulates Snf1 Protein Kinase and Facilitates Recovery from Prolonged Glucose Starvation in *Saccharomyces cerevisiae*. *Appl Environ Microbiol* 82: 3875–3885

McCartney RR & Schmidt MC (2001) Regulation of Snf1 Kinase. Activation requires phosphorylation of threonine 210 by an upstream kinase as well as a distinct step mediated by the Snf4 subunit. *J Biol Chem* 276: 36460–36466

Mendenhall MD & Hodge AE (1998) Regulation of Cdc28 Cyclin-Dependent Protein Kinase Activity during the Cell Cycle of the Yeast *Saccharomyces cerevisiae*. *Microbiol Mol Biol Rev* 62: 1191–1243

Merchan S, Bernal D, Serrano R & Yenush L (2004) Response of the *Saccharomyces cerevisiae* Mpk1 Mitogen-Activated Protein Kinase Pathway to Increases in Internal Turgor Pressure Caused by Loss of Ppz Protein Phosphatases. *Eukaryot Cell* 3: 100–107

Miller ME & Cross FR (2001) Cyclin specificity: how many wheels do you need on a unicycle? *J Cell Sci* 114: 1811–20

Minhas A, Sharma A, Kaur H, Rawal Y, Ganesan K & Mondal AK (2012) Conserved Ser/Arg-rich motif in PPZ orthologs from fungi is important for its role in cation tolerance. *J Biol Chem* 287: 7301–7312

Mollinedo F (2012) Lipid raft involvement in yeast cell growth and death. *Front Oncol* 2

Moorhead GBG, Trinkle-Mulcahy L & Ulke-Lemée A (2007) Emerging roles of nuclear protein phosphatases. *Nat Rev Mol Cell Biol* 8: 234–44

Moorhead GBG, De Wever V, Templeton G & Kerk D (2009) Evolution of protein phosphatases in plants and animals. *Biochem J* 417: 401–409

Morvan J, Rinaldi B & Friant S (2012) Pkh1/2-dependent phosphorylation of Vps27 regulates ESCRT-I recruitment to endosomes. *Mol Biol Cell* 23: 4054–4064

Munn AL (2001) Molecular requirements for the internalisation step of endocytosis: insights from yeast.

REFERENCES

Biochim Biophys Acta 1535: 236–57

Muñoz I, Ruiz A, Marquina M, Barceló A, Albert A & Ariño J (2004) Functional characterization of the yeast Ppz1 phosphatase inhibitory subunit Hal3: A mutagenesis study. *J Biol Chem* 279: 42619–42627

Muñoz I, Simón E, Casals N, Clotet J & Ariño J (2003) Identification of multicopy suppressors of cell cycle arrest at the G1 - S transition in *Saccharomyces cerevisiae*. *Yeast* 20: 157–169

De Nadal E, Clotet J, Posas F, Serrano R, Gomez N & Ariño J (1998) The yeast halotolerance determinant Hal3p is an inhibitory subunit of the Ppz1p Ser/Thr protein phosphatase. *Proc Natl Acad Sci U S A* 95: 7357–7362

De Nadal E, Fadden RP, Ruiz A, Haystead T & Ariño J (2001) A Role for the Ppz Ser/Thr Protein Phosphatases in the Regulation of Translation Elongation Factor 1Bα. *J Biol Chem* 276: 14829–14834

Nasmyth K (1993) Control of the yeast cell cycle by the Cdc28 protein kinase. *Curr Opin Cell Biol* 5: 166–79

Navarrete C, Petrezsélyová S, Barreto L, Martínez JL, Zahrádka J, Ariño J, Sychrová H & Ramos J (2010) Lack of main K+ uptake systems in *Saccharomyces cerevisiae* cells affects yeast performance in both potassium-sufficient and potassium-limiting conditions. *FEMS Yeast Res* 10: 508–517

Novarina D, Guerra P & Milias-Argeitis A (2021) Vacuolar Localization via the N-terminal Domain of Sch9 is Required for TORC1-dependent Phosphorylation and Downstream Signal Transduction. *J Mol Biol* 433: 167326

Offley SR & Schmidt MC (2019) Protein phosphatases of *Saccharomyces cerevisiae*. *Curr Genet* 65: 41–55

Ohgaki R, Nakamura N, Mitsui K & Kanazawa H (2005) Characterization of the ion transport activity of the budding yeast Na+/H+ antiporter, Nha1p, using isolated secretory vesicles. *Biochim Biophys Acta* 1712: 185–96

Ohkura H, Kinoshita N, Miyatani S, Toda T & Yanagida M (1989) The fission yeast dis2+ gene required for chromosome disjoining encodes one of two putative type 1 protein phosphatases. *Cell* 57: 997–1007

Olsen LF, Andersen AZ, Lunding A, Brasen JC & Poulsen AK (2009) Regulation of glycolytic oscillations by mitochondrial and plasma membrane H+-ATPases. *Biophys J* 96: 3850–61

Orii M, Kono K, Wen H-I & Nakanishi M (2016) PP1-Dependent Formin Bnr1 Dephosphorylation and Delocalization from a Cell Division Site. *PLoS One* 11: e0146941

Orlova M, Barrett L & Kuchin S (2008) Detection of endogenous Snf1 and its activation state: application to Saccharomyces and Candida species. *Yeast* 25: 745–754

Oughtred R, Stark C, Breitkreutz BJ, Rust J, Boucher L, Chang C, Kolas N, O'Donnell L, Leung G, McAdam R,

et al (2019) The BioGRID interaction database: 2019 update. *Nucleic Acids Res* 47: D529–D541

Papouskova K, Moravcova M, Masrati G, Ben-Tal N, Sychrova H & Zimmermannova O (2021) C5 conserved region of hydrophilic C-terminal part of *Saccharomyces cerevisiae* Nha1 antiporter determines its requirement of Erv14 COPII cargo receptor for plasma-membrane targeting. *Mol Microbiol* 115: 41–57

Pedelini L, Marquina M, Ariño J, Casamayor A, Sanz L, Bollen M, Sanz P & Garcia-Gimeno MA (2007) YPI1 and SDS22 proteins regulate the nuclear localization and function of yeast type 1 phosphatase Glc7. *J Biol Chem* 282: 3282–92

Pessina S, Tsiarentsyeva V, Busnelli S, Vanoni M, Alberghina L & Coccetti P (2010) Snf1/AMPK promotes S-phase entrance by controlling *CLB5* transcription in budding yeast. *Cell Cycle* 9: 2189–2200

Pinson B, Gabrielsen OS & Dalgnan-Fornier B (2000a) Redox regulation of AMP synthesis in yeast: A role of the Bas1p and Bas2p transcription factors. *Mol Microbiol* 36: 1460–1469

Pinson B, Kongsrud TL, Ording E, Johansen L, Daignan-Fornier B & Gabrielsen OS (2000b) Signaling through regulated transcription factor interaction: mapping of a regulatory interaction domain in the Myb-related Bas1p. *Nucleic Acids Res* 28: 4665–73

Pinson B, Vaur S, Sagot I, Coulpier F, Lemoine S & Daignan-Fornier B (2009) Metabolic intermediates selectively stimulate transcription factor interaction and modulate phosphate and purine pathways. *Genes Dev* 23: 1399–1407

Posas F, Camps M & Arino J (1995) The PPZ protein phosphatases are important determinants of salt tolerance in yeast cells. *J Biol Chem* 270: 13036–13041

Posas F, Casamayor A & Ariño J (1993) The PPZ protein phosphatases are involved in the maintenance of osmotic stability of yeast cells. *FEBS Lett* 318: 282–286

Posas F, Casamayor A, Morral N & Arino J (1992) Molecular cloning and analysis of a yeast protein phosphatase with an unusual amino-terminal region. *J Biol Chem* 267: 11734–11740

Prior C, Potier S, Souciet J-L & Sychrova H (1996) Characterization of the NHA1 gene encoding a Na + /H + -antiporter of the yeast *Saccharomyces cerevisiae*. *FEBS Lett* 387: 89–93

Proft M & Struhl K (2004) MAP Kinase-Mediated Stress Relief that Precedes and Regulates the Timing of Transcriptional Induction. *Cell* 118: 351–361

Robinson JS, Klionsky DJ, Banta LM & Emr SD (1988) Protein sorting in *Saccharomyces cerevisiae*: isolation of mutants defective in the delivery and processing of multiple vacuolar hydrolases. *Mol Cell Biol* 8: 4936–48

Rodríguez-Navarro A & Ramos J (1984) Dual system for potassium transport in *Saccharomyces cerevisiae*.

REFERENCES

J Bacteriol 159: 940–5

Rojas M, Gingras A-C & Dever TE (2014) Protein phosphatase PP1/GLC7 interaction domain in yeast eIF2γ bypasses targeting subunit requirement for eIF2α dephosphorylation. *Proc Natl Acad Sci U S A* 111: E1344-53

Ruiz A & Ariño J (2007) Function and regulation of the *Saccharomyces cerevisiae* ENA sodium ATPase system. *Eukaryot Cell* 6: 2175–2183

Ruiz A, González A, Muñoz I, Serrano R, Abrie JA, Strauss E & Ariño J (2009) Moonlighting proteins Hal3 and Vhs3 form a heteromeric PPCDC with Ykl088w in yeast CoA biosynthesis. *Nat Chem Biol* 5: 920–928

Ruiz A, Muñoz I, Serrano R, González A, Simón E & Ariño J (2004) Functional characterization of the *Saccharomyces cerevisiae VHS3* gene: A regulatory subunit of the Ppz1 protein phosphatase with novel, phosphatase-unrelated functions. *J Biol Chem* 279: 34421–34430

Ruiz A, Xu X & Carlson M (2011) Roles of two protein phosphatases, Reg1-Glc7 and Sit4, and glycogen synthesis in regulation of SNF1 protein kinase. *Proc Natl Acad Sci U S A* 108: 6349–54

Ruiz A, Xu X & Carlson M (2013) Ptc1 protein phosphatase 2C contributes to glucose regulation of SNF1/AMP-activated protein kinase (AMPK) in Saccharomyces cerevisiae. *J Biol Chem* 288: 31052–8

Ruiz A, Yenush L & Ariño J (2003) Regulation of *ENA1* Na+-ATPase gene expression by the Ppz1 protein phosphatase is mediated by the calcineurin pathway. *Eukaryot Cell* 2: 937–948

Sambrook J, Fritsch EF & Maniatis T (1989) Molecular Cloning: A Laboratory Manual Cold Spring Harbor Laboratory

Sanz P, Alms GR, Haystead TAJ & Carlson M (2000) Regulatory Interactions between the Reg1-Glc7 Protein Phosphatase and the Snf1 Protein Kinase. *Mol Cell Biol* 20: 1321–1328

Schüller HJ (2003) Transcriptional control of nonfermentative metabolism in the yeast *Saccharomyces cerevisiae*. *Curr Genet* 43: 139–160

Serrano R (1996) Salt tolerance in plants and microorganisms: toxicity targets and defense responses. *Int Rev Cytol* 165: 1–52

Shi Y (2009a) Serine/Threonine Phosphatases: Mechanism through Structure. *Cell* 139: 468–484

Shi Y (2009b) Assembly and structure of protein phosphatase 2A. *Sci China Ser C, Life Sci* 52: 135–46

Smidova A, Stankova K, Petrvalska O, Lazar J, Sychrova H, Obsil T, Zimmermannova O & Obsilova V (2019) The activity of *Saccharomyces cerevisiae* Na+, K+/H+ antiporter Nha1 is negatively regulated by 14-3-3 protein binding at serine 481. *Biochim Biophys acta Mol cell Res* 1866: 118534

Stark MJR (1996) Yeast protein serine/threonine phosphatases: Multiple roles and diverse regulation.

Yeast 12: 1647–1675

Stevens HC & Nichols JW (2007) The proton electrochemical gradient across the plasma membrane of yeast is necessary for phospholipid flip. *J Biol Chem* 282: 17563–7

Sutton A, Immanuel D & Arndt KT (1991) The SIT4 protein phosphatase functions in late G1 for progression into S phase. *Mol Cell Biol* 11: 2133–2148

Swanson KA (2003) Solution structure of Vps27 UIM-ubiquitin complex important for endosomal sorting and receptor downregulation. *EMBO J* 22: 4597–4606

Sychrová H, Ramírez J & Peña A (1999) Involvement of Nha1 antiporter in regulation of intracellular pH in *Saccharomyces cerevisiae*. *FEMS Microbiol Lett* 171: 167–72

Takahashi S & Pryciak PM (2008) Membrane Localization of Scaffold Proteins Promotes Graded Signaling in the Yeast MAP Kinase Cascade. *Curr Biol* 18: 1184–1191

Tarassov K, Messier V, Landry CR, Radinovic S, Serna Molina MM, Shames I, Malitskaya Y, Vogel J, Bussey H & Michnick SW (2008) An in vivo map of the yeast protein interactome. *Science (80-)* 320: 1465–1470

Treitel MA, Kuchin S & Carlson M (1998) Snf1 protein kinase regulates phosphorylation of the Mig1 repressor in *Saccharomyces cerevisiae*. *Mol Cell Biol* 18: 6273–80

Tyson JJ, Csikasz-Nagy A & Novak B (2002) The dynamics of cell cycle regulation. *BioEssays* 24: 1095–1109

Velázquez D (2019) Exploring the regulatory mechanisms of the *S. cerevisiae* Ppz1 protein phosphatase and the molecular basis for its toxicity. Doctoral Thesis, Universitat Autònoma de Barcelona

Velázquez D, Albacar M, Zhang C, Calafí C, López-Malo M, Torres-Torronteras J, Martí R, Kovalchuk SI, Pinson B, Jensen ON, *et al* (2020) Yeast Ppz1 protein phosphatase toxicity involves the alteration of multiple cellular targets. *Sci Rep* 10: 15613

Venturi GM, Bloecher A, Williams-Hart T & Tatchell K (2000) Genetic interactions between *GLC7*, *PPZ1* and *PPZ2* in Saccharomyces cerevisiae. *Genetics* 155: 69–83

Verbinnen I, Ferreira M & Bollen M (2017) Biogenesis and activity regulation of protein phosphatase 1. *Biochem Soc Trans* 45 2: 583–584

Vincent O, Townley R, Kuchin S & Carlson M (2001) Subcellular localization of the Snf1 kinase is regulated by specific beta subunits and a novel glucose signaling mechanism. *Genes Dev* 15: 1104–14

Vissi E, Clotet J, de Nadal E, Barceló A, Bakó E, Gergely P, Dombrádi V & Ariño J (2001) Functional analysis of the *Neurospora crassa* PZL-1 protein phosphatase by expression in budding and fission yeast. *Yeast* 18: 115–24

Vlastaridis P, Kyriakidou P, Chaliotis A, Van de Peer Y, Oliver SG & Amoutzias GD (2017) Estimating the

REFERENCES

total number of phosphoproteins and phosphorylation sites in eukaryotic proteomes. *Gigascience* 6: 1–11

Westholm JO, Nordberg N, Murén E, Ameur A, Komorowski J & Ronne H (2008) Combinatorial control of gene expression by the three yeast repressors Mig1, Mig2 and Mig3. *BMC Genomics* 9: 1–15

Williams-Hart T, Wu X & Tatchell K (2002) Protein phosphatase type 1 regulates ion homeostasis in *Saccharomyces cerevisiae*. *Genetics* 160: 1423–37

Wu X & Tatchell K (2001) Mutations in Yeast Protein Phosphatase Type 1 that Affect Targeting Subunit Binding. *Biochemistry* 40: 7410–7420

Yenush L, Merchan S, Holmes J & Serrano R (2005) pH-Responsive, Posttranslational Regulation of the Trk1 Potassium Transporter by the Type 1-Related Ppz1 Phosphatase. *Mol Cell Biol* 25: 8683–8692

Yenush L, Mulet JM, Ariño J & Serrano R (2002) The Ppz protein phosphatases are key regulators of K+ and pH homeostasis: implications for salt tolerance, cell wall integrity and cell cycle progression. *EMBO J* 21: 920–9

Yonemoto W, McGlone ML & Taylor SS (1993) N-myristylation of the catalytic subunit of cAMP-dependent protein kinase conveys structural stability. *J Biol Chem* 268: 2348–2352

Zahrádka J, van Heusden GPH & Sychrová H (2012) Yeast 14-3-3 proteins participate in the regulation of cell cation homeostasis via interaction with Nha1 alkali-metal-cation/proton antiporter. *Biochim Biophys Acta* 1820: 849–58

Zhang C (2019) The Ppz1 protein phosphatase as a potential novel antifungal target. Doctoral Thesis, Universitat Autònoma de Barcelona

Zhang C, García-Rodas R, Molero C, de Oliveira HC, Tabernero L, Reverter D, Zaragoza O & Ariño J (2019a) Characterization of the atypical Ppz/Hal3 phosphatase system from the pathogenic fungus *Cryptococcus neoformans*. *Mol Microbiol* 111: 898–917

Zhang C, de la Torre A, Pérez-Martín J & Ariño J (2019b) Protein Phosphatase Ppz1 Is Not Regulated by a Hal3-Like Protein in Plant Pathogen Ustilago maydis. *Int J Mol Sci* 20: 3817

Zou J, Friesen H, Larson J, Huang D, Cox M, Tatchell K & Andrews B (2009) Regulation of cell polarity through phosphorylation of Bni4 by Pho85 G1 cyclin-dependent kinases in *Saccharomyces cerevisiae*. *Mol Biol Cell* 20: 3239–50